EVALUATION OF IMAGE TUBES FOR USE IN DIRECT PHOTOGRAPHY OF ASTRONOMICAL SOURCES

by

Richard Hayden Cromwell

A Dissertation Submitted to the Faculty of the

DEPARTMENT OF ASTRONOMY

In Partial Fulfillment of the Requirements
For the Degree of

DOCTOR OF PHILOSOPHY

In the Graduate College

THE UNIVERSITY OF ARIZONA

1 9 6 9

THE UNIVERSITY OF ARIZONA

GRADUATE COLLEGE

I hereby recommend that this dissertation prepared under my direction by Richard H. Cromwell

entitled Evaluation of Image Tubes for Use in Direct Photography of Astronomical Sources

be accepted as fulfilling the dissertation requirement of the degree of Doctor of Philosophy

Dissertation Director — Date: 25 March 1969

After inspection of the final copy of the dissertation, the following members of the Final Examination Committee concur in its approval and recommend its acceptance:*

	25 March 1969
W. S. Fitch	25 March 1969
R. Tousey	25 March 1969
	March 25, 1969
Donald J. Taylor	March 25, 1969

*This approval and acceptance is contingent on the candidate's adequate performance and defense of this dissertation at the final oral examination. The inclusion of this sheet bound into the library copy of the dissertation is evidence of satisfactory performance at the final examination.

STATEMENT BY AUTHOR

This dissertation has been submitted in partial fulfillment of requirements for an advanced degree at The University of Arizona and is deposited in the University Library to be made available to borrowers under rules of the Library.

Brief quotations from this dissertation are allowable without special permission, provided that accurate acknowledgment of source is made. Requests for permission for extended quotation from or reproduction of this manuscript in whole or in part may be granted by the head of the major department or the Dean of the Graduate College when in his judgment the proposed use of the material is in the interests of scholarship. In all other instances, however, permission must be obtained from the author.

SIGNED: Richard H. Cromwell

ACKNOWLEDGMENTS

I wish to extend my appreciation to the following persons: Dr. A. B. Meinel for serving as dissertation director and for continual support and encouragement; Drs. W. K. Ford, W. C. Livingston, and C. R. Lynds for their informative discussions during this investigation; Drs. B. J. Bok, W. S. Fitch, D. J. Taylor, and B. E. Westerlund for their many helpful suggestions and assistance on the drafts of this paper; and my wife, Dawn, for her willingness and assistance in typing the several drafts.

Acknowledgment is gratefully extended to the Department of Terrestrial Magnetism, Carnegie Institution of Washington, for the loan of a Carnegie image tube and some of the laboratory equipment used in this investigation.

This work has been supported in part under USAF Contract No. F04695-67-C-0197.

TABLE OF CONTENTS

TABLE OF CONTENTS--Continued

TABLE OF CONTENTS--Continued

LIST OF ILLUSTRATIONS

LIST OF ILLUSTRATIONS--Continued

LIST OF ILLUSTRATIONS--Continued

LIST OF TABLES

ABSTRACT

A brief description is given of the various types of image tubes presently used in astronomical research and a review is presented of the past applications of image tubes to direct astronomical photography. A detailed laboratory evaluation of the Carnegie image tube is summarized and photographs at the telescope are presented to confirm and extend the results obtained in the laboratory.

Iris photometry of stellar images can be carried out on Carnegie tube photographs with about the same accuracy as is obtained by normal photographic techniques. Compared to unaided plates the image tube typically requires about 1/15 the exposure time to record stellar images of a specified threshold magnitude. When exposures are made to near the sky limit, however, the Carnegie tube cannot record stars as faint as can be recorded with an unaided plate. When exposed at a given focal length telescope, the limiting magnitude of an image tube record is about 1 magnitude brighter than that of an unaided photograph.

Primarily two characteristics of the Carnegie tube, an over-all mottled sensitivity pattern and a light-induced background, are found to be responsible for the loss in limiting magnitude of a Carnegie tube record. The mottle pattern is characterized by an rms variation in sensitivity of ±1.3 percent. It modulates the photographic record of the night-sky radiation and seriously affects the signal-to-noise ratio of the

threshold images. The additional background produced by the light-induced background of the image tube generally amounts to 25 percent of the night-sky radiation on a sky-limited photograph.

In order to record the same sky-limited magnitude on a Carnegie tube plate and an unaided plate, the image tube record must be exposed at a longer focal length telescope. The exposure time required by the image tube is then about 1/2 to 1/3 that of the unaided plate. Because of the higher scale of the image tube photograph in such a case, however, the effective gain provided by the image tube over the unaided plate is generally somewhat larger than the relative exposure time.

The photography of extended objects is found to be particularly affected by the nonuniformities of the image tube. Besides reducing the over-all signal-to-noise ratio of the image tube record, the general mottle pattern and additional discrete patches and ripples in sensitivity of the image tube tend to mimic low contrast features of galaxies and nebulae. The rather subjective effects of the nonuniformities can be significantly reduced by using telescopes with moderately long focal lengths, so that the seeing image is then large in comparison to the nonuniformities.

The photography of astronomical sources through narrowband interference filters has been found to be a particularly promising application of the Carnegie image tube. Preliminary tests reported in the present study include the photography of supernova remnants, planetary nebulae, galaxies, and reflection nebulae.

The basic quality criterion for comparing the image tube to unaided photographic emulsions is argued to be the detective quantum efficiency. Typical values of the gain over unaided emulsions provided by

the Carnegie tube are calculated to be in the range 10 to 20. It is emphasized, however, that because of the variety of requirements in specific research areas and because of the several unique characteristics of a given image tube, no single figure of merit may be defined that will predict the usefulness of an image tube in all applications. It is suggested that the resolution of a detector should not generally be combined into the calculation of a single figure of merit but should be considered as a separate quality criterion.

Certain problems with the Carnegie tube (and other image tubes as well) potentially limit its usefulness in specific research areas. Besides the problems already mentioned, other problems include low resolution, geometrical distortion, the complexities of analyzing the final record (as compared to an unaided photograph), and the limited field of the image tube. Each of these characteristics can be highly significant or entirely inconsequential in different applications.

CHAPTER I

INTRODUCTION

The importance of image tubes for astronomical observations is based primarily on one outstanding fact: photoemissive surfaces (photocathodes) have a significantly higher quantum efficiency than photographic emulsions. The quantum efficiencies of various photographic emulsions have been measured to be between 0.1 and 1 percent (Webb 1948; Fellgett 1953, 1958a; Argyle 1955; Baum 1955; Jones 1958; Zweig, Higgins, and MacAdam 1958), while photocathodes are being produced with quantum efficiencies of from 10 to greater than 20 percent in the blue spectral region. The efficiency with which an ideal image tube detects radiation may thus be 10 to 200 times that of a photographic emulsion--based on the relative quantum efficiencies.

General Types of Image Tubes

Several methods have been developed for amplifying and recording the photoelectrons emitted from the photocathode of an image tube. The designs which have proved most successful and which have been applied to astronomical observations of low light level phenomena will be briefly described in the following paragraphs. For a more complete discussion of the various types of image tubes--their theory of operation, technological development, and applications--the reader is

referred to the book by Soule (1968), *Electro-Optical Photography at Low Illumination Levels*. For image tubes used in astronomy, the most general references are those by Baum et al. (1955-1968), Hiltner (1962), McGee (1962), and Livingston (1967a).

In the simplest image tube configuration, the electrons liberated from the photocathode are accelerated by an electrostatic field to energies sufficient to expose electron-sensitive nuclear track emulsions directly. As in other image tubes, electrostatic or magnetic lenses serve to focus the electronic image. The original version of this type of image tube was developed by Lallemand and has been successfully used for astronomical observations. However, the coexistence of the electronographic emulsion and the photocathode in the same vacuum environment poses several problems that have led to the development of other types of electronographic tubes. Principal among these are a tube developed by Kron utilizing a valve to facilitate changing of plates and a tube developed by McGee in which the high energy electrons pass through a thin mica window to expose an emulsion held in contact with the window. To withstand atmospheric pressure, the window configuration of McGee's tube is long and narrow (about 30 × 7 mm). This tends to restrict the device to spectrographic applications.

Another type of image tube configuration uses a phosphor for detecting the accelerated electrons. Each photoelectron gives rise to a discrete scintillation of light at the phosphor which may be recorded photographically. The optical coupling may be by relay lens or by direct contact for tubes having thin output windows. To obtain

efficient recording of the original photoelectrons it is generally necessary to increase the brightness of the phosphor scintillations more than is possible in a single-stage tube. This can be accomplished by providing electron amplification within the tube.

One technique for internal amplification has been to directly couple the phosphor output of one image tube stage with the photocathode input of another. This type of multistage image tube is referred to as a cascade design. Another technique has been to use a series of plane-parallel, secondary-emitter dynodes. The first dynode is placed at the focus of the photocathode electron image. For each primary electron incident on the dynode several secondary electrons are emitted. The secondaries are focused at the next element of the image tube. This element may be either another dynode of the series or the output phosphor. The particular dynode assembly is generally referred to as a transmission secondary emission (TSE) design. For both the transmission secondary emission and cascade image tubes the amplification required can in principal be obtained by selecting the appropriate number of stages.

The final type of image tube to be considered here is the signal generating, or television-type, image tube. The various designs of such tubes all provide two-dimensional storage of an electrical charge image that is proportional to the radiation incident on the photocathode. The charge image is changed into an electrical output signal by one of several techniques involving scanning of the electron image by an electron beam. It is beyond the scope of this investigation

to consider in more detail the complex nature of signal generating tubes. Except for summarizing the work of other investigators, the present paper will not be concerned with this particular type of image tube.

Basic Advantages of Image Tube Photography

More than 30 years ago Lallemand (1936) suggested the advantages an image tube would have over conventional photography and photoelectric photometry. These advantages have been further expanded by Baum et al. (1955-1968) in the "Annual Reports of the Committee on Image Tubes for Telescopes", as well as by others (Fellgett 1958b, Hiltner 1958, McGee 1958, and Baum 1962a). The basic point in all these papers is that image tubes not only have the panoramic capability of photographic plates but also have the high quantum efficiency of photomultipliers. It thus becomes possible to record a given object with greatly reduced exposure times. Perhaps even more important, it is possible to detect fainter objects than can be detected with a photographic plate in the same total exposure time.

In addition to higher efficiency, another advantage of the photoemissive surface over a photographic emulsion is the strict linearity between the incident light flux and the resulting number of photoelectrons. The degree to which this advantage is realized in an actual image tube, however, is a function of the design and operation of the particular device under consideration.

Carnegie Image Tube, Present Investigation

An image tube which has been of particular interest to astronomers is the "Carnegie image tube", so named because its development has been largely guided by the Carnegie Committee on Image Tubes for Telescopes. In many spectrographic applications, the Carnegie image tube system has been simple and straightforward to use and has provided a significant gain over the photographic plate. Further, due to the efforts of the Carnegie Committee, this system is generally available to the interested astronomer. The present investigation was made possible by the loan of a Carnegie image tube system to the Steward Observatory of The University of Arizona.

In view of the great interest in image tubes in general, and this tube in particular, it was decided that a full evaluation of the Carnegie image tube for use in direct photography of astronomical objects was desirable. Such an evaluation is the basic purpose of the present investigation. The basic point of view is to consider the image tube as an alternative to the photographic emulsion, and therefore the discussions are generally presented in photographic terminology. It is felt that this terminology provides the most immediately useful understanding of the capabilities of the image tube for astronomers unfamiliar with such a device.

For the present study, tests of the Carnegie tube have been made both in the laboratory and at the telescope. The conditions necessary for optimum operation of the entire Carnegie system were determined early in the laboratory investigation. The laboratory

investigation included measurements of properties which are generally important in any image detector: resolution, geometrical distortion, dark-emission background, light-induced background, spectral sensitivity, photometric uniformity, and limiting detectable signal (limiting magnitude capability). When applicable, astronomical plates and the image tube have been directly compared by testing both detectors with the same apparatus.

The detailed measurements carried out in the laboratory, and the results, are presented in Chapter II. Chapter III is devoted to a development and discussion of appropriate figures of merit for comparing the image tube with normal photographic plates. In the final sections of Chapter III the results of the laboratory investigation are discussed in terms of these figures of merit.

In Chapter IV the telescopic observations are discussed. Exposures at the telescope were typical of those usually encountered in direct astronomical photography. Advantages and limitations of the image tube are graphically presented by comparing direct photographs taken with normal astronomical emulsions and with the image tube. General starfields, globular clusters, diffuse nebulae, and galaxies have been photographed. The telescopic observations provide a check on the capabilities predicted from the laboratory investigation and provide additional tests supplementing those made in the laboratory. More important, the telescopic observations demonstrate in practice, not theory, the unique advantages of using the Carnegie image tube in astronomical direct photography.

Chapter V summarizes the most important results of the investigation. The performance to be expected from other image tubes is discussed in the light of the results of this investigation.

Direct Photography; Comparison to Spectroscopy

By far the greatest emphasis in utilizing image tubes in astronomy has involved applications to astronomical spectroscopy. From an astronomer's point of view the reasons for this are clear. Spectroscopy is a very powerful tool in determining the physical conditions of the objects studied in astronomy; with a proper spectrogram of such an object, more information can be derived about that object than from nearly any other single type of observation. The introduction of image tube cameras on spectrographs has significantly aided the study of faint objects. This has been particularly true for observations of galaxies, quasars, and short period variable stars.

One might assume that an image tube can be applied to full-field, direct photography with as much success as in spectrographic applications. However, there is a problem in image tubes that can potentially limit their usefulness in direct photography applications. The problem referred to here is the light-induced background. Whenever light is incident on the photocathode, there is an additional final output from the image tube that is more or less uniformly distributed throughout the field. This background may generally be caused by several phenomena within the tube. The amount of light-induced background is roughly independent of the image detail and depends mostly on the net radiation received by the photocathode.

When an image tube is being used with a slit spectrograph, only a small portion of the photocathode is illuminated. The light-induced background recorded at any one given image element is correspondingly less than if the entire photocathode were being illuminated--as is usually the case in direct photography. Thus, for direct photography applications, it is necessary to consider the capabilities of an image tube when its entire photocathode area is illuminated. This is particularly true for photography of faint objects because in such photography there is a great deal of radiation from the comparatively bright foreground night sky.

The low resolution of many image tubes compared to photographic emulsions is often pointed out as a limitation of such devices in photography. However, the importance of resolution has often been misunderstood or overstated, as will be discussed in more detail in Chapter III.

Image Tubes in Direct Photography, Past Experiences

In spite of the several difficulties encountered in the use of image tubes, certain types have nevertheless been shown to be effective research tools. The successful application of image tubes to direct astronomical photography will be summarized in this section. Note that no discussion will be made of the excellent spectrographic applications of image tubes that have been reported by Ford, Livingston, Lynds, Rubin, Walker, and others.

Electronographic Tubes--Short Exposure

Perhaps the earliest published results which actually contributed new knowledge to a particular field of application (and not just to the image tube technology alone) are those of Rösch, Wlérick, and Dupré (1961). These investigators made use of the short exposure times, high resolution, and freedom from the Eberhard effect of the Lallemand electronographic camera in the measurement of close double stars. More recently, Laques (1966) has reported additional measurements of close double stars with a Lallemand tube. Short exposure photography of Jupiter and Saturn with the same device has also been reported (Bellier et al. 1963).

Electronographic Tubes--Long Exposure

Only one paper has been published concerning the use of the Lallemand camera in long exposure stellar photometry (Lallemand, Canavaggia, and Amiot 1966). However, this particular application has been more thoroughly studied with a similar electronographic device developed by Kron (Walker and Kron 1967). This paper clearly points out the potential of electronography in stellar photometry. The authors present convincing evidence for the linear relationship between plate density and incident intensity. Observing the globular cluster M13, they found that the linearity extends over a range of 4.6 magnitudes, beginning at the plate limit. This linearity provides, among other things, the possibility of precisely accounting for background nonuniformities such as occur in nebular regions, and the possibility of calibrating

the plates with only the brighter stars in the field, with assurance that a linear extrapolation to the faintest stars is accurate.

Ables and Kron (1967) have calculated that the information gain of Kron's tube when applied to star photography is better than 30, relative to IIa-O and 103a-O plates. Earlier papers, which had not taken into full account the superior signal-to-noise ratio of the electronographic images, had given more conservative estimates of the information gain (Breckinridge, Kron, and Papiashvili 1964; Kron, Breckinridge, and Papiashvili 1965). Due to the superior storage capacity of the electronographic emulsion, stars fainter than those possible to observe with direct plates have recently been recorded with this tube (Kron 1967, unpublished). In another study using the Kron image tube, measurements were made of the brightness distribution of the globular clusters M13 and M15 (Kron and Papiashvili 1967). The authors state that more information was collected at the telescope in a 30 minute exposure than had been gathered in a similar study using photoelectric techniques requiring about 2 hours per cluster (Kron and Mayall 1960).

A prime criticism of Kron's tube, as well as Lallemand's, is the complexity of the preparation for observing. Although Kron has minimized the preparation procedures, there are still several technical skills required of the observer. In Lallemand's device, a slow deterioration of the photocathode is experienced due to gas evolved from the electronographic emulsion. Further, removal of the exposed plates from the tube results in the destruction of the photocathode. In Kron's tube, a valve between the photocathode and plateholder preserves the

photocathode and prevents its destruction during plate changing. It is important to note that the plates cannot be examined immediately after exposure, and this therefore requires very careful control of all focus adjustments. The field that is well corrected is relatively small in these electrostatically-focused tubes (diameter near 15 mm for Kron's). However, it is hoped that with a complete redesign, an electronographic tube can be built in the future with a useful photocathode diameter of around 10 cm (Walker and Kron 1967). The uniformity of these tubes in sensitivity and spectral response has not been thoroughly discussed, nor has the problem of light-induced background been quantitatively reported for Kron's tube. Kron feels, however, that light-induced background is a significant problem in his device (Kron 1967, unpublished). Loss of contrast by scattered light in Lallemand's tube has been reported, and investigations by Wlérick and Grosse (1966) have resulted in design changes in the tube to reduce this problem considerably.

Another present limitation of electronographic tubes appears to be in the threshold detection of images on lightly exposed plates. The individual grains are so small (around 1 μm in diameter) that, when only a few such grains have been recorded in an image, their detection with present measuring equipment is difficult. Furthermore, these nuclear track emulsions are fogged quickly by cosmic rays and natural radioactivity, making threshold images even more difficult to identify.

High Gain Tubes (Transmission Secondary Emission)

For the very high gain image tubes, such as the English Electric Valve TSE (transmission secondary emission) type, the ability to record single photoelectric events is very good. No reports of using high gain tubes in direct astronomical photography have recently been made. However, application appears limited because of the generally high light-induced background in these tubes and because the recording emulsion is quickly saturated by only a few photon events per unit area. Early tests of this type of tube (Baum et al. 1960) indicated these limitations in a preliminary fashion.

Signal Generating Tubes (Television-Type)

The signal generating tubes, such as the photoemissive image orthicon and the photoconductive vidicon, have the unique feature of supplying directly an electrical output signal. This signal can be used to display an image on a closed circuit television system, can be stored for later data processing, and can be transmitted over large distances. In a series of tests carried out by the Carnegie Committee (Baum et al. 1960), it was concluded that the signal generating tubes--limited primarily by their storage and noise characteristics, and the vidicon also by its sensitivity--were less promising for most low light level work than the intensifier type tubes. However, it was pointed out that in certain applications, such tubes might indeed be useful tools.

Livingston (1962) has shown the image orthicon to be useful for low accuracy stellar photometry (probable error of ±0.1 magnitude). However, Livingston states that for the image orthicon to become a tool for scientific measurement, a more thorough description of the internal operation must be made available. In another study using an image orthicon system, Bakos and Rymer (1964) have successfully searched for variable stars in galactic clusters. Other investigators (Hynek and Dunlap 1964; Hynek, Bakos, Dunlap, and Powers 1966) have pointed out that, although the image orthicon does not have the photometric and geometrical accuracies required for most astronomical investigations, there are certain applications where the significant property of a detector is the speed of observing. Examples of such applications are sky surveillance for faint, fast moving objects, and surveys of galaxies for supernovae. Still another field of application that benefits from the unique properties of signal generating tubes is space astronomy. The electronic recording and telemetering of information are highly requisite capabilities in this field. Thus signal generating tubes may be considered as valuable supplements, rather than replacements, of the photographic plate.

New signal generating tubes are now being developed that may overcome several of the disadvantages of the vidicon and image orthicon. One such tube that looks most promising is the SEC (secondary electron conduction) camera, for which experimental photographs at the telescope have been made (Beardsley and Hansen 1968; Green 1968a, 1968b). Advantages of this tube include extremely short rise and decay times, high

storage capacity, very low charge loss or spread during long integrations, and no black border effects with overexposure.

Cascade Tubes

In a study involving direct photography of galaxies with a cascade image tube (Butslov et al. 1962), Russian observers reported a "gain in speed" of 200 over unaided photography. Fifty-eight galaxies were photographed with four filters: Hα and 6100 A interference filters as well as B and V passband filters. The limitations of this particular tube have not been discussed, and one can only guess that they are the same as the other tubes of this type (e.g., the Carnegie tube).

Tuve et al. (1958) have reported on a Carnegie Committee study of direct photography applications with an electrostatically-focused RCA cascade tube. Though the results obtained with this early device were encouraging, they left much to be desired. The main shortcomings of the design were nonuniformity and graininess of the phosphor screens, a useful field diameter of only about 6 mm, and insufficient gain to utilize fully the available quantum efficiency of the photocathode. Technological advances related to these shortcomings, as well as others, have been reported in later reports of the Carnegie Committee. The present Carnegie image tube has evolved from the above-mentioned cascade design. However, as the image tube was improved, the emphasis of application turned to spectrography. Consequently, many details needed for considering direct photography applications were not fully investigated. The investigation of these details is the subject of this paper.

CHAPTER II

LABORATORY INVESTIGATION

It is the purpose of this chapter to summarize the individual studies of the Carnegie image tube system which were carried out in the laboratory. Before the laboratory data is presented, however, it is appropriate to first describe this image tube system in some detail.

Description of Carnegie Image Tube System

Fig. 1 shows the individual pieces of the entire Carnegie image tube assembly when dismantled. The image tube proper is shown encapsulated in a permanent silicone rubber cylinder. The tube is a two-stage cascade, magnetically-focused design built by RCA and identified as RCA-Developmental Type C33011. The photocathode is 38 mm in diameter and is of the S-20 type (extended red sensitivity). Photoelectrons from the photocathode are accelerated in an electric field of 10 kV and strike a phosphor-photocathode sandwich. This amplification element (dynode) multiplies the number of original photoelectrons some 30 to 50 times. The amplified electrons from the second photocathode are again accelerated in a 10 kV field, and are brought to focus on the final output screen--a fine-grained P11 (blue) phosphor. Focus of the electrons is provided by a uniform magnetic field of 220 Gauss. This field is supplied by a permanent magnet array shown directly above the image tube

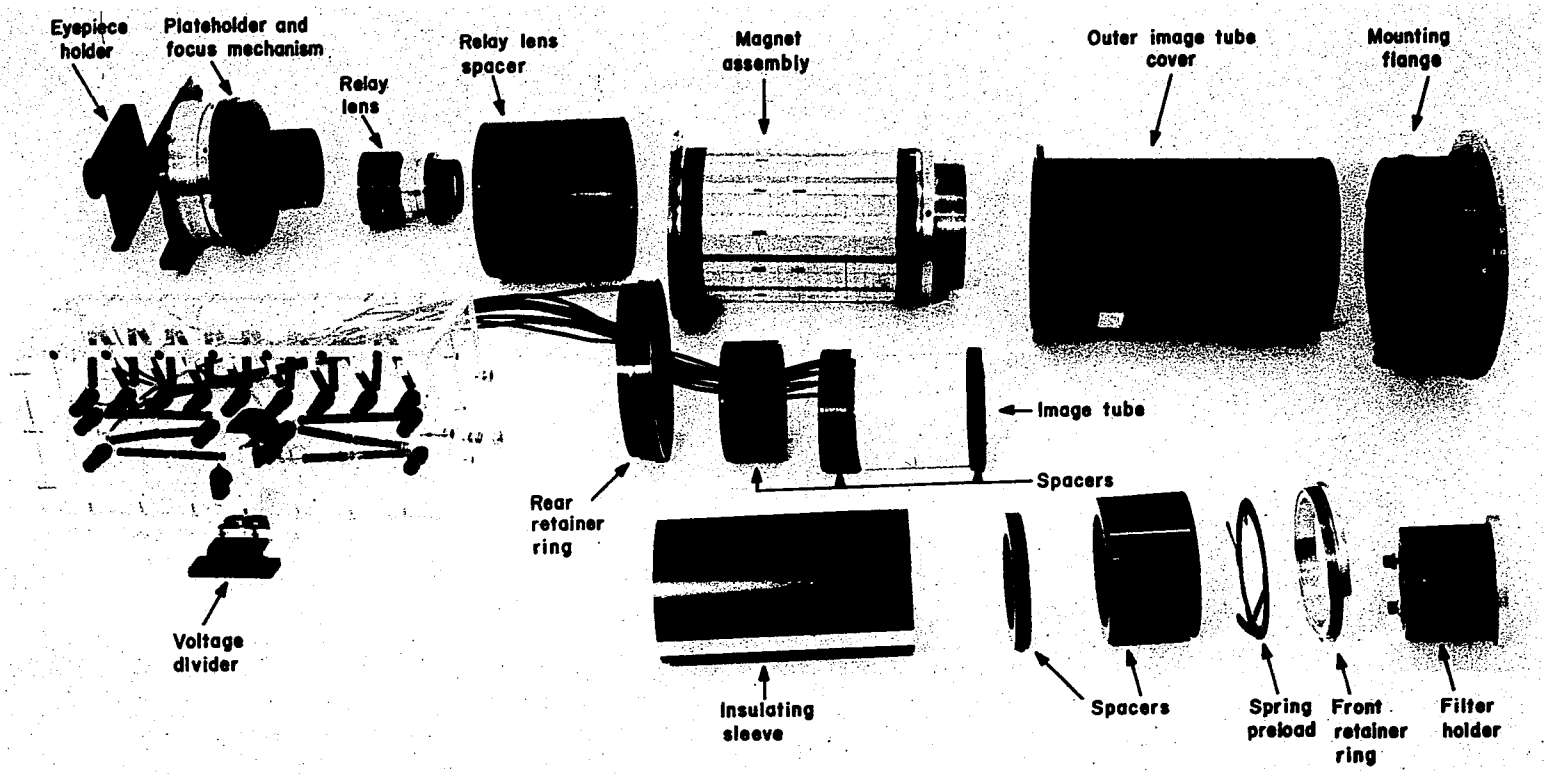

Fig. 1. Dismantled Carnegie Image Tube System.

in Fig. 1. Behind this magnet is shown the relay lens, which is an Elgeet f/1.2 lens designed for one-to-one magnification. This lens transfers the phosphor output to the recording photographic plate. The plateholder assembly is shown directly behind the lens. The entire image tube assembly, when put together and mounted at the telescope, is shown in Fig. 16, Chapter IV.

Certain parameters of the Steward Observatory tube have been measured by the Carnegie Committee or the manufacturer (Ford 1968, private communication). These values are a photocathode sensitivity of 160 μA/lumen[1] to 2,870°K tungsten radiation, a blue sensitivity as measured through a one-half stock thickness Corning 5113 filter of 11 μA/lumen, a radiant power gain (ratio of total output power from phosphor to input radiant power at wavelength of maximum sensitivity) of 4,600, and an equivalent screen background input of 1.6×10^{-16} W/cm^2. When these numbers are compared to those for an average tube as reported by the Carnegie Image Tube Committee (Baum et al. 1965), one concludes that this is a somewhat better than average tube in all figures quoted above.

Resolution

The resolution of image tubes, normally expressed in number of line pairs (one black and one white line) per millimeter is given in almost any description of a particular tube. Unfortunately, such data

---

1. The Radiometry and Photometry Technical Group of the Optical Society of America and the International Commission on Optics disapproves of continued use of the lumen; however, at present, most photosensitive devices are still rated in terms of the lumen (a unit of luminous flux) instead of in terms of a unit of radiant power.

commonly refer only to the central area of the image tube. If a fair comparison to other methods of image detection is to be made, the resolution across the entire field of the image tube must be known.

To investigate the resolution capabilities of the Carnegie image tube a high resolution projector, developed and described by Baum (1962b), was used to image a high contrast resolution pattern onto the photocathode of the image tube. This "microprojector" was loaned by the Department of Terrestrial Magnetism, Carnegie Institution of Washington, and its use is most gratefully acknowledged. A very useful feature of the microprojector is the ability to precisely focus on a partially reflective surface by direct viewing through the projector, thus eliminating the need for focus plates.

Resolution at the Phosphor Output Screen

The resolution measurements. The resolution of the image tube alone was determined by directly viewing the phosphor output screen with a 15-30 power microscope. The numerical results were expressed as the limiting number of line pairs per millimeter (lp/mm) that could be resolved by visual inspection. The resolution test pattern appeared as a uniformly illuminated surface at spatial frequencies higher than the limiting value, and appeared clearly resolved into lines at lower spatial frequencies.

The results of measuring the resolution in this manner across the full field of the image tube are shown in the two upper curves of Fig. 2. The curves represent the resolution for two different settings

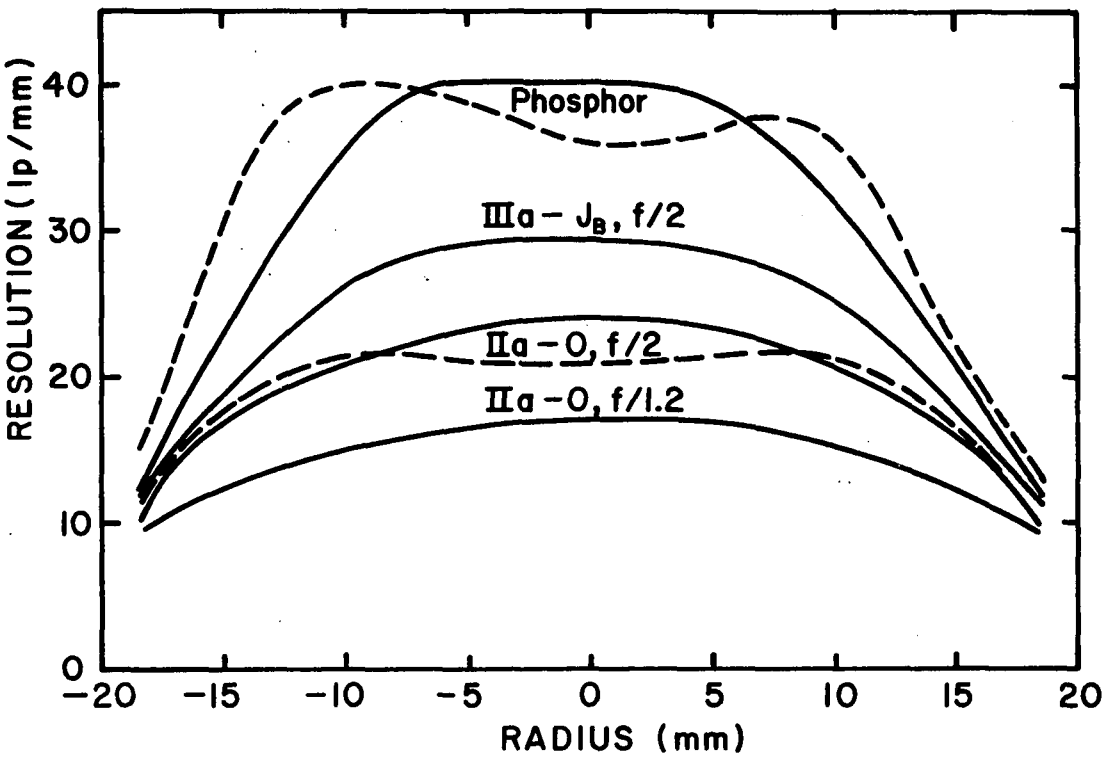

Fig. 2. Resolution Across Image Tube Face.

Shown is the resolution of the phosphor output with two settings of the high voltage supply--providing maximum resolution at the center (solid line) and at a point halfway to the edge (dashed line). The transduced resolution for these two settings are shown for a IIa-0 recording emulsion with the relay lens at f/2. The increased resolution, by using a baked IIIa-J recording emulsion, is clearly demonstrated. The loss in resolution caused by opening the relay lens to f/1.2 is also seen. Though 24 lp/mm resolution is observed at the center for the IIa-0, a more representative value over the useful area of the image tube is around 22 lp/mm--one third that of direct plates. The need for an improved high-speed relay lens is clear.

of the high voltage supply; one setting provides maximum resolution at the center of the image tube field and the other at a point halfway to the edge. The voltage setting is 21.5 kV for maximum central resolution and is 21.2 kV for the 50 percent zone maximum. For the former setting, a resolution of 40 lp/mm is obtained over about a 5 mm radius. The resolution falls off smoothly to 20 lp/mm at a 15 mm radius and to 14 lp/mm at an 18 mm radius. For the lower voltage setting, the edge resolution is improved somewhat, but only at the expense of reduced central resolution. It is interesting to note that with more reduction in over-all voltage, a resolution of 30 lp/mm can be obtained at an 18 mm radius. However, the central resolution is then severely reduced.

Optimum electronic settings, anomalies. Regarding the optimum focus voltage for the image tube, it is clear that only a little extension of the useful field can be obtained by optimizing the focus off center. This is particularly true when one considers the final recorded resolution on a photographic emulsion, which will be discussed shortly. Generally, it is felt that for most objects photographed at the telescope, the maximum resolution ought to occur over the central half of the field.

It should be pointed out that before a stable electronic focus can be achieved, the high voltage must be applied for at least 2 hours. When the power supply is first turned on, maximum resolution is obtained with a voltage of 20.0 kV; when 2 or more hours have passed, the voltage must be readjusted to 21.5 kV. Tests were not made to determine whether it is the image tube or the voltage divider that causes this effect.

The optimum interstage voltage setting was found to be that which produced best resolution in the center of the field. A setting that improved the resolution for an area near one edge of the field would slightly degrade the resolution at a point diametrically opposite that area. Small asymmetries have also been found in other tube characteristics. These results indicate that there are nonuniform magnetic and/or electric fields in the image tube system. Nonuniformities in the fields of image tubes are common problems, however, and the degree appears quite normal for the present device (Livingston 1967b, private communication).

Effects of Relay Lens on Resolution

Field curvature in a relay lens might easily require that the lens be focused on an off-center field point in order to provide optimum resolution over the full image tube field. Tests were carried out to check for this effect, but the results indicate that the field curvature is small for the Elgeet relay lens and that optimum resolution for the entire field is obtained by critically focusing the field center.

The improvement in image quality by stopping down the lens aperture was also investigated. With the lens used at full aperture there is an extended faint distribution of light surrounding the image. This distribution, referred to here as "flare", is presumably caused mostly by spherical aberration. As the lens is stopped from the wide-open aperture of f/1.2 to f/2, there is a particular reduction in the flare,

and a significant increase in resolution. (Note all lens apertures are given for infinity focus and not for 1:1 magnification.) Stopping down the lens further decreases flare and increases resolution very little. The numerical values of resolution for various lens apertures are given in Table 1. A photograph comparing the relay lens at f/2 and f/1.2 is given in Fig. 3. It is concluded from data presented in Figs. 2 and 3 and Table 1 that the f/2 aperture is the optimum setting for the relay lens--balancing resolution and freedom from flare against the reduced speed.

Table 1

Image Characteristics for Two
Recording Emulsions vs. Relay Lens Aperture

	Resolution (lp/mm)		
Aperture	IIa-O	IIIa-J_B	Notes
f/1.2	17	24	Surrounded with flare
f/1.5	20	26	Somewhat less flare
f/2.0	24	29	Flare essentially gone
f/2.4	25	--	Flare essentially gone
f/2.8	26	--	Flare essentially gone

An argument can be made for the need of a high resolution relay lens with an aperture of f/1, and perhaps with a magnification of around 1.5. This need has been pointed out earlier by Ford (Livingston 1967a). The magnification is recommended so that the finite resolving power of the photographic recording emulsion does not limit the net

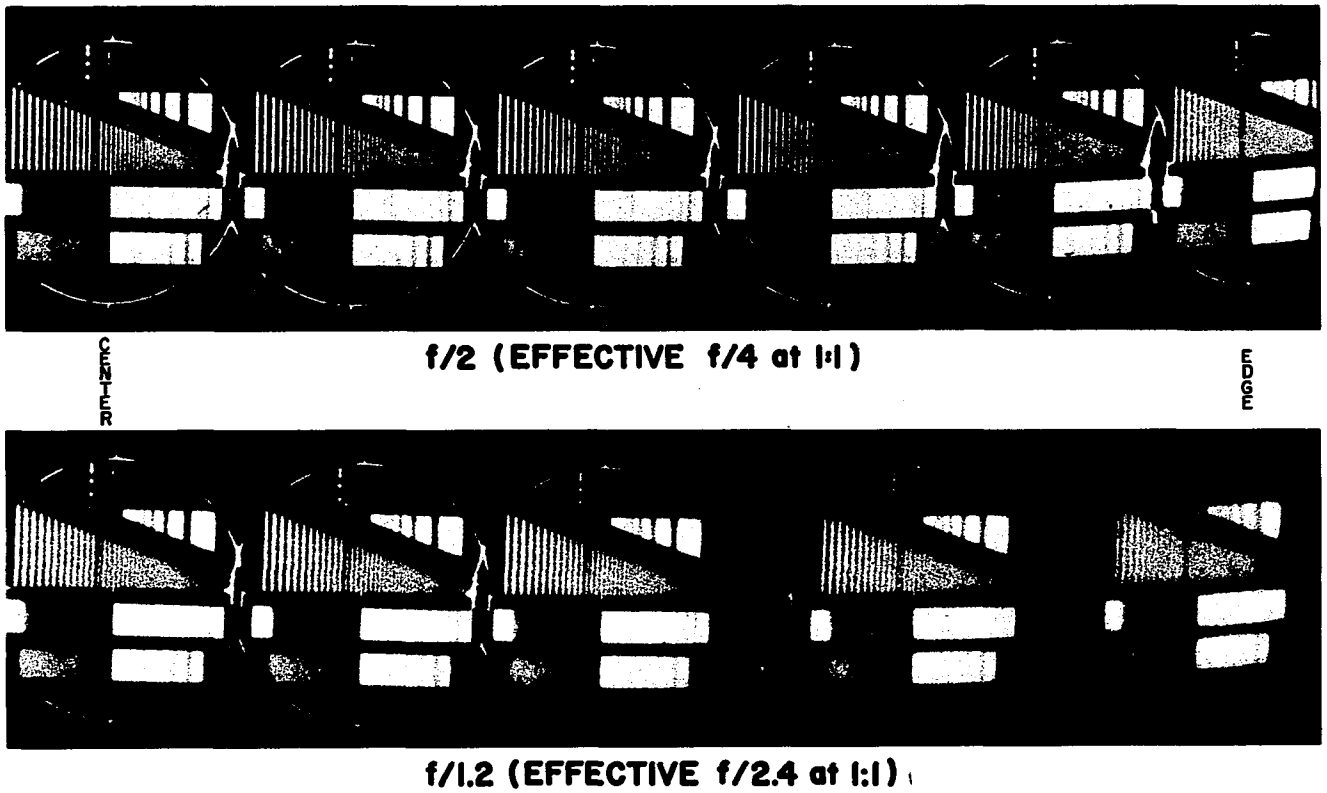

Fig. 3. Image Detail Across Image Tube Face for Two Lens Apertures.

The photographs, recorded on IIa-O emulsions, show the imaging properties of the Carnegie system from the center to the edge of the field. The resolution is seen to increase when the relay lens is stopped down from f/1.2 to f/2. The lens flare is decreased at f/2, but this effect cannot be adequately demonstrated on the reproductions here. Note that the faint "stars" against the "sky background" in the lower left rectangle of the test pattern are essentially lost at f/1.2. The distortion at the edge is caused by the image tube proper.

resolving power of the system. A design that may meet these requirements has recently been described by Bowen (1967).

Effects of Recording Emulsion on Resolution

That resolution of the final image tube record is not entirely limited by the phosphor image and relay lens but is also affected by the recording emulsion, is demonstrated in tests carried out with two photographic materials. A comparison of the final recorded resolution on both IIa-O and baked IIIa-J emulsions is made in Fig. 2 and Table 1. (Note that a subscript B after an emulsion type indicates the emulsion has been baked to increase its sensitivity.) The baked IIIa-J emulsion is seen to provide increased resolution over the IIa-O. Other characteristics of the baked IIIa-J emulsion will be discussed later.

It is seen from Fig. 2 that the present Carnegie tube, when used with a IIa-O recording emulsion and an f/2 relay lens setting, has an average resolution of 22 lp/mm. This figure applies to essentially half the photocathode diameter, or about 20 mm. Using a baked IIIa-J recording emulsion, the average resolution is increased to about 27 lp/mm. Ford (1967, private communication) feels the resolutions found in the present investigation may be a little low compared to the average Carnegie tube system. Naturally, individual differences among image tubes, focusing magnets, and relay lenses are to be expected. Typical resolutions reported by Baum et al. (1965) using IIa-O recording emulsions are 25-30 lp/mm.

Direct Plate Resolution Measurements

The resolutions of several astronomical emulsions were also determined using the same Baum microprojector as was used for the image tube. The 103a series of plates were measured to resolve, on the average, 67 lp/mm, the IIa series 73 lp/mm, and the I-N plates 81 lp/mm. The significantly higher resolution obtained from the I-N emulsion seems to be caused primarily by the higher contrast of this plate, rather than a finer grain structure.

Resolution: Concluding Remarks

It is clear that the Carnegie image tube system will resolve only 1/3 to possibly 1/2 of the detail that can be resolved with the common astronomical emulsions. In certain applications this reduced resolution will limit the usefulness of the image tube. However, in many applications, the focal length of the telescope may be increased until the object observed is equally resolved with the image tube. It should of course be remembered that in direct astronomical photography with moderately long focus telescopes, the resolution on the plate is often "seeing-limited". If the seeing disc is substantially larger than the present measured resolution limit of 40 to 50 μm for the image tube, there should exist essentially no difference in the image resolution of direct or image tube photographs.

Geometrical Properties

It is generally recognized that no image tube in use today has enough freedom from geometrical aberrations to compete with photographic plates in applications of critical positional measurement, and the Carnegie system is no exception. Judging from the qualitative information that is available on other tubes, however, this tube compares favorably.

Fixed Geometrical Distortions

The over-all character of the geometrical distortion present in the Carnegie tube is shown in the photograph of a rectangular grid reproduced in Fig. 4. The most obvious distortions are "S-distortion" and barrel distortion. The former produces a slightly S-shaped image of a straight line. S-distortion is apparent in many magnetically-focused tubes and is created by nonuniformities in the electric and magnetic fields within the image tube. Barrel distortion is caused by a decrease in magnification toward the edge of the field. Quantitative measurements of these distortions are given in Table 2. The linear

Table 2

Magnification; S-Distortion for Carnegie Tube

Radius (mm)	Magnification	Δy (mm)
0	1.015	0.000
4	1.015	0.000
15	0.952	0.104
18	0.878	0.180

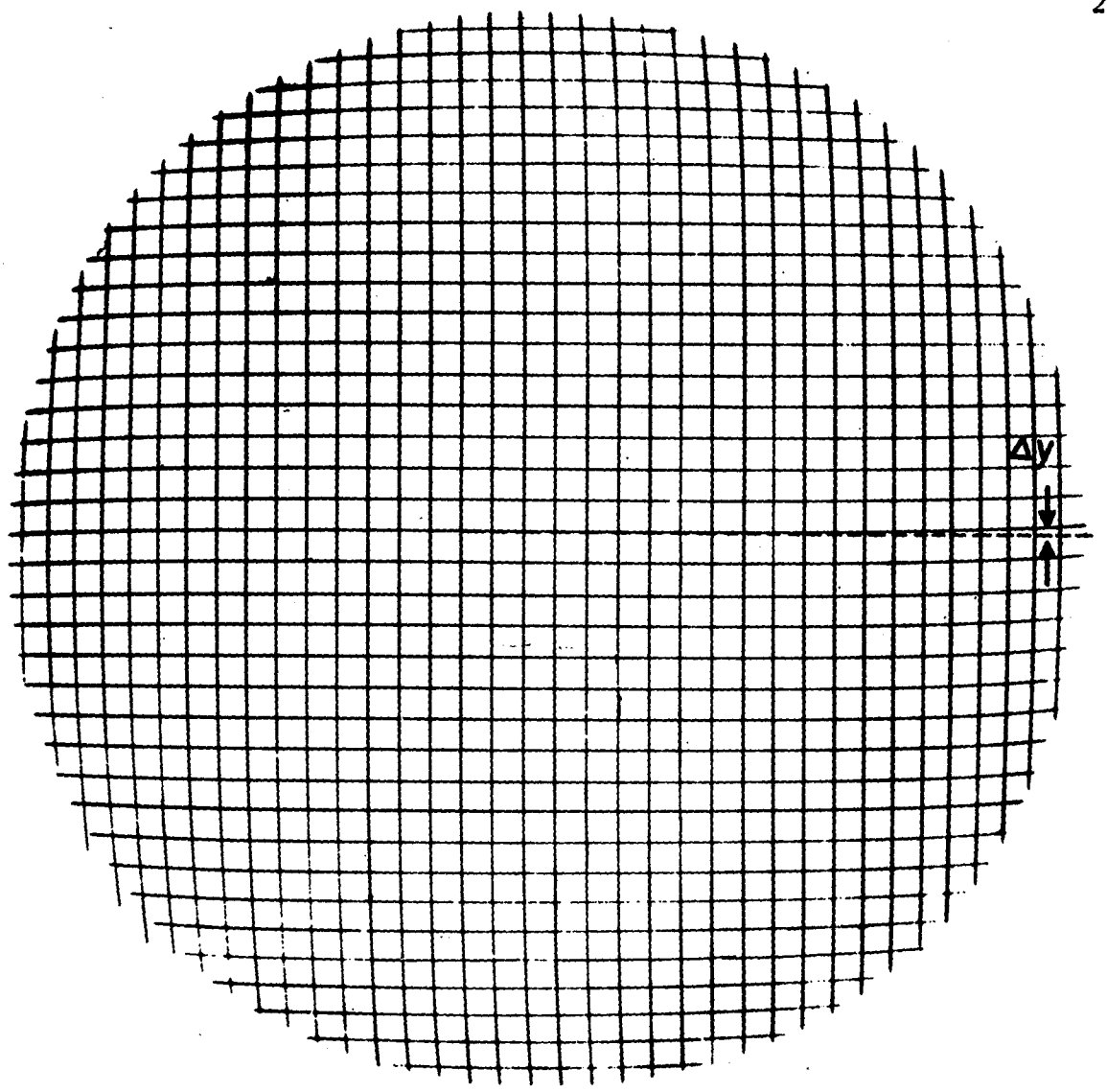

Fig. 4. Geometrical Distortion of Carnegie Image Tube.

The distortions are very apparent when this print is viewed at an angle. Most obvious are S-distortion, indicated by Δy, and barrel distortion, causing demagnification near the edges. For the image tube to compete favorably with the positional accuracy of direct plates, a detailed "map" of geometry would be required, with computer data reduction.

magnification and the deviation from a straight line (indicated as Δy in Fig. 4) are listed for selected field radii. The values for a given radius are averages of measurements taken at several position angles. The amount of local deviation from these average values is significant. For example, values of Δy at an 18 mm radius range from 0.200 mm to 0.149 mm. Clearly, accurate corrections for the field distortions will require a detailed "map" of the image tube field, and such corrections will be troublesome unless computer reduction procedures are used. It is likely that if such an elaborate scheme were applied, however, the positional accuracy of Carnegie tube photographs would compare favorably with that of unaided photographic plates. A recent example of this type of data correction, successfully applied to accurate radial velocity studies obtained with a Carnegie tube spectrograph, has been published by Ford and Rubin (Baum et al. 1968). These authors concluded that, with the particular correction scheme used by them, a single measurement of a point on a spectral line was accurate to within ± 2 μm.

Geometrical Stability

Besides geometrical distortion per se, an additional problem with image tubes is geometrical instability; the electronic image is displaced due to variations in electrostatic and magnetic fields. The variations can either occur in the image tube apparatus or arise from external sources. Laboratory tests for image motion due to instabilities of the image tube and its associated electronics have been

negative. Resolution patterns exposed as long as 6 hours were as well resolved as ones exposed only a few seconds.

Regarding image motion due to external sources (such as the changing magnetic field of the earth or the proximity of ferro-magnetic objects) it is noted from actual telescope experiences that such an effect has never been detected. Based on the apparent lack of degredation of image quality on exposures of up to 3 hours, the image motion must never have exceeded 50 μm.

Dark Background

The noise arising from background emission in image tubes often limits the application of such devices in low light level investigations. Several tests were made in the laboratory in order to determine the severity of the background emission for the present Carnegie tube, but only an upper limit to this emission can be set from the available tests. This is because, even with a 4 hour exposure with the relay lens at f/1.2, no background emission was photographically recorded. Using reasonable assumptions of photographic plate sensitivity, image tube light gain, etc., the laboratory data indicate that the background emission is equivalent to less than 4×10^{-16} W/cm^2 at 4200 A radiation incident on the photocathode. This agrees well with the RCA-determined figure of 1.6×10^{-16} W/cm^2 given earlier.

Spectral Sensitivity

The basic spectral sensitivity of the Carnegie image tube is that of an S-20 photocathode. The average response for such a surface, given in Fig. 5, is characterized by a peak around 4200 A and a red sensitivity extending to 8000 A. Sensitivity in the red varies a great deal from photocathode to photocathode, but essentially no useful response exists beyond 8500 A.

It is the purpose of this section to compare the relative sensitivities of the image tube and the photographic emulsions which would otherwise be used in low light level photography. The quantity determined here is the "blackening rate" of the image tube plates, relative to the direct plate. This may be defined simply as the ratio of exposure times required to obtain a specified density above fog for the comparison plate and the image tube plate.

The photographic plates which have been chosen for comparison are those which would normally be used at the particular wavelength in question and which in practice have been found to be best suited for astronomical applications. Recent improvement in the sensitivity of the IIa-0 emulsion has resulted in its general acceptance as equal to or superior to the 103a-0 in low light level astronomical photography (Miller et al. 1966). For radiation redward of 5000 A, however, the general higher sensitivity of the 103a series of plates is still considered an advantage for most direct photography, and therefore tests in the appropriate wavelength regions were made with 103a-D, 103a-E and 103a-F plates. For the near infrared, comparison of the image tube and unhypersensitized I-N plates was also made.

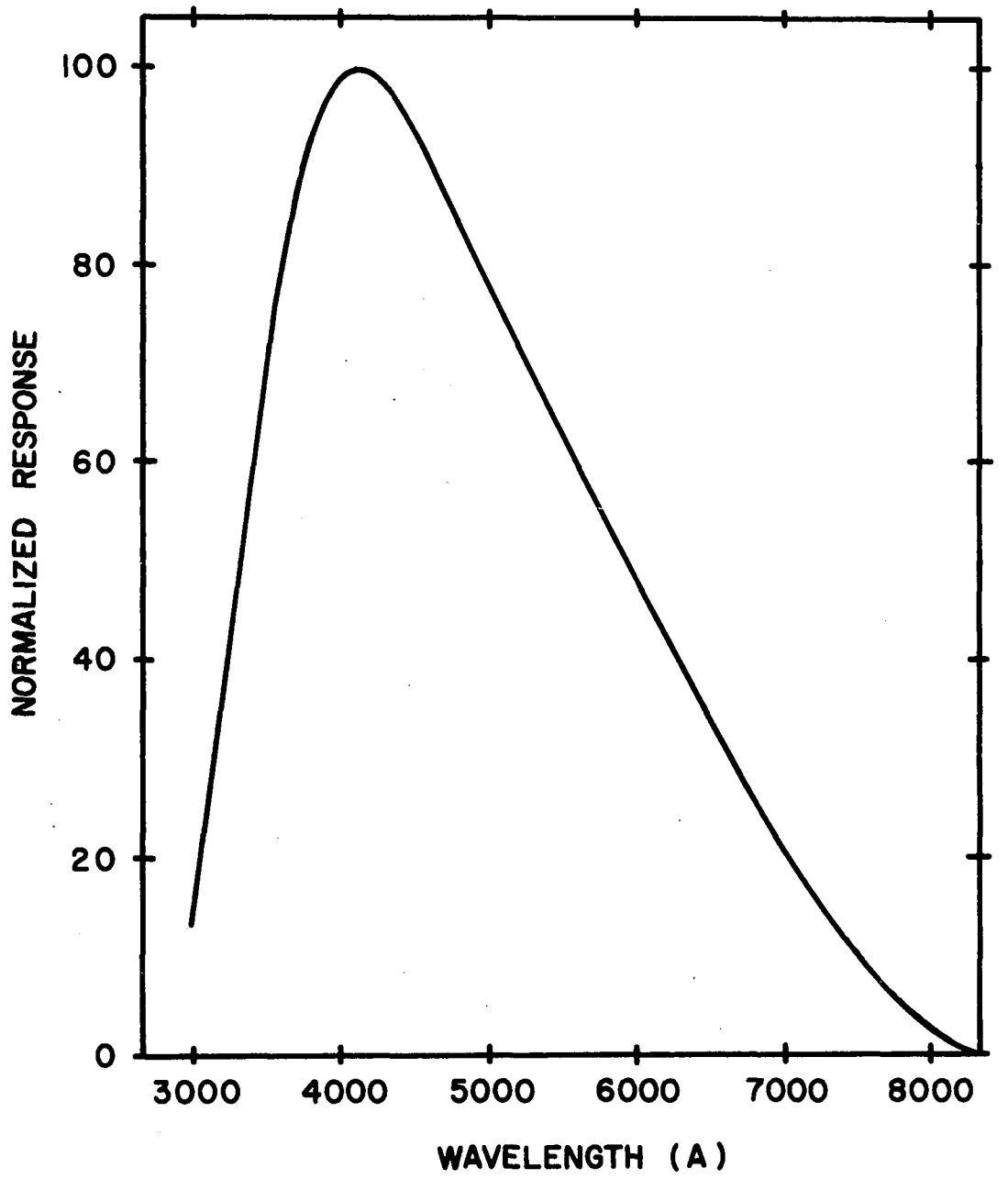

Fig. 5. Wavelength Response of Typical S-20 Photocathode of Carnegie Image Tube.

Sensitometric Test Apparatus, Procedure

For the spectral sensitivity tests a projector was built that projected, with uniform illumination and low scattering, a "neutral density" step wedge formed by layers of evaporated rhodium. Although it is often assumed that the relative transmissions of the various wedges of such a filter are quite independent of wavelength, tests for wavelength dependence made in the laboratory showed a definite dependence, indicating differences in the relative transmissions of greater than 20 percent. These measurements were made by normalizing the "clear" portions of the wedge to 100 percent transmission and covered the wavelength region from 3500 A to 7500 A. The wedge was illuminated by a Bausch and Lomb monochromator which was measured to have a passband at any one wavelength of less than 120 A. The steps of the wedge were further measured when projected in the entire projector system using a photomultiplier cell. The nonuniformities discovered in the relative intensities were corrected for in the final data.

The sensitometric exposures were made at numerous wavelengths by first exposing a IIa-0 recording emulsion through the image tube, then a comparison plate, and finally a second exposure with the image tube. The relay lens was set at f/2 for these blackening rate tests of the image tube. The exposure times were selected so that the resulting densities on both the image tube and the unaided plates were as equal as possible. The times averaged 40 minutes for the unaided plates and 80 seconds for the image tube plates although there were variations in both to account for wavelength sensitivity peaks and dips in the

photographic emulsions. One long-exposure pair of plates was taken to test for the effects of reciprocity failure. A IIa-O emulsion was exposed 30 minutes and 12½ hours, respectively, for the image tube and unaided exposures. The image tube and unaided plate pairs for all the above tests were always developed together in D-19 at 68°F for 4 minutes, with careful control of temperature, time, and agitation during the tray development. In the case of the IIa-O plates, the image tube exposures and the direct plate exposures were on the same plate. Because the sensitivity of a IIa-O emulsion is greater when developed in D-76, compared to D-19, an appropriate correction was made in calculating the final relative blackening rates.

The plates were all measured with Steward Observatory's Jarrell-Ash microdensitometer, and characteristic curves were plotted for each set of plates. Each set consisted of two image tube exposures and one direct plate exposure. To calculate the relative rates at which the direct plate and image tube plate acquired a specified density, the relative exposure times were used along with the intensity scale of the characteristic curve for whatever interpolation was required.

Results, Blackening Rate

Two values of the relative blackening rate were determined for each set of plates at a given wavelength. One value was calculated for the low plate density of 0.3 and another for the appreciably higher density of 1.0. The low-density tests are representative of a class of astronomical problems involving the detection of weak signals in the

absence of background radiation. The high-density tests, on the other hand, are representative of those problems where it is desired to detect and measure very low-contrast images against a strong background. The relative blackening rates of the image tube compared to the various photographic plates are plotted as a function of wavelength in Figs. 6 and 7, for the low and high densities, respectively. The average deviation in a measured value of the blackening rate is ± 3 percent.

It should be noted that for all wavelengths longward of 4500 A the relative blackening rate is lower at high densities than at low densities. This is because the direct plates show higher contrast than do the image tube plates. Shortward of about 4300 A the situation is reversed because of the wavelength dependence of contrast for the IIa-0 emulsion. The contrast is constant for the image tube plates because in the image tube the emulsion is always receiving the same spectral distribution of light from the phosphor. However, the contrast in the corresponding direct plate changes as the wavelength of the incident radiation is changed. For the IIa-0 emulsion, the contrast becomes less than that of the image tube when the wavelength is shorter than 4300 A. There is of course a color dependence for the red-sensitive plates as well, but they always show higher contrast than the image tube plates over their respective wavelength regions. Thus, the relative blackening rate for the image tube is always lower at high densities when compared with red-sensitive plates.

When a baked IIIa-J emulsion is used as the recording emulsion in the image tube, there are some changes in the relative blackening

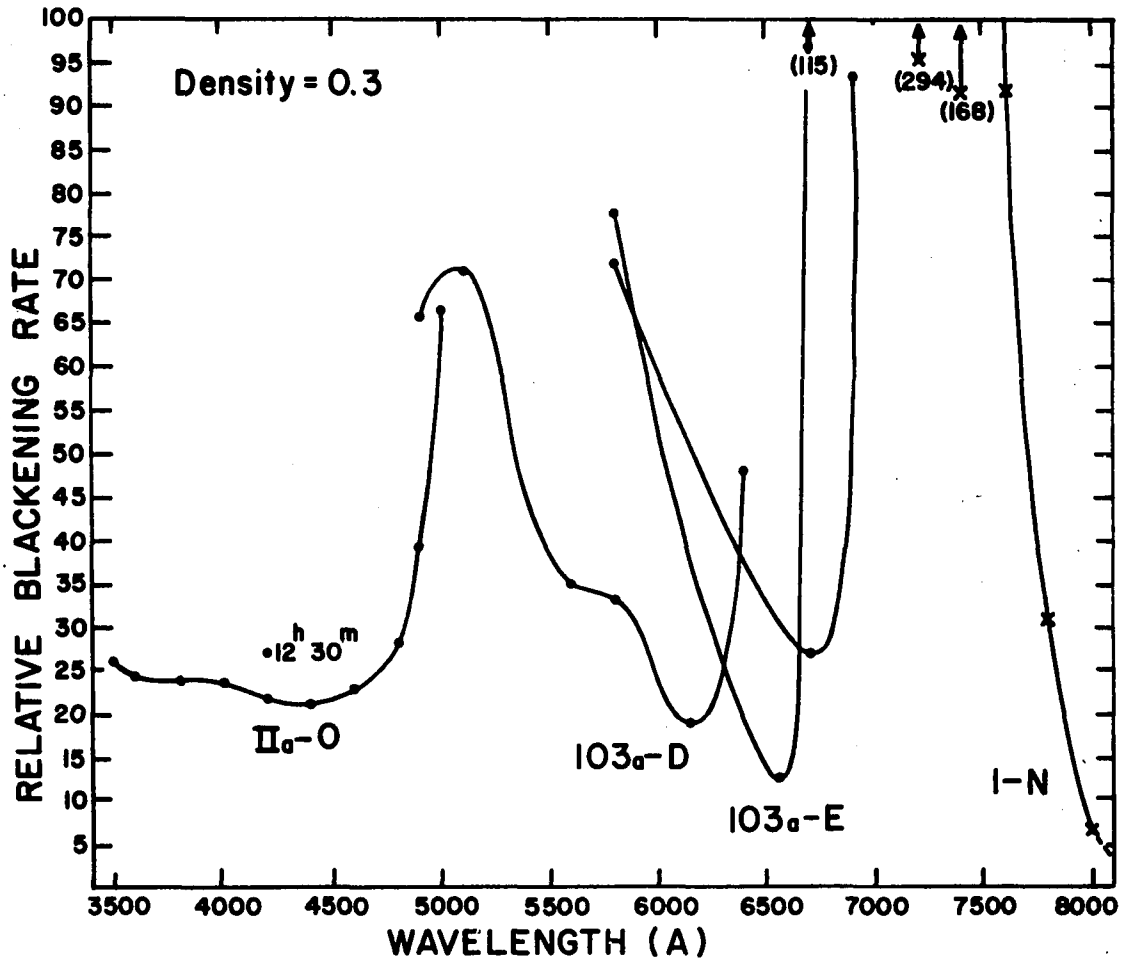

Fig. 6. Relative Blackening Rate, Density = 0.3.

The rate at which an image tube plate obtains a specified density is expressed relative to that of several astronomical emulsions in the above plots. The recording emulsion used for the image tube was a IIa-O and the relay lens setting was f/2. The exposure times for the direct plates were approximately 40 minutes. A single long-exposure test was made with a IIa-O plate by exposing the direct emulsion for 12^h30^m. The density of 0.3 is representative of a plate that has been minimally exposed to detect high contrast objects against a weak background. In certain applications the figure of merit of the Carnegie tube is nearly equal to the relative blackening rate.

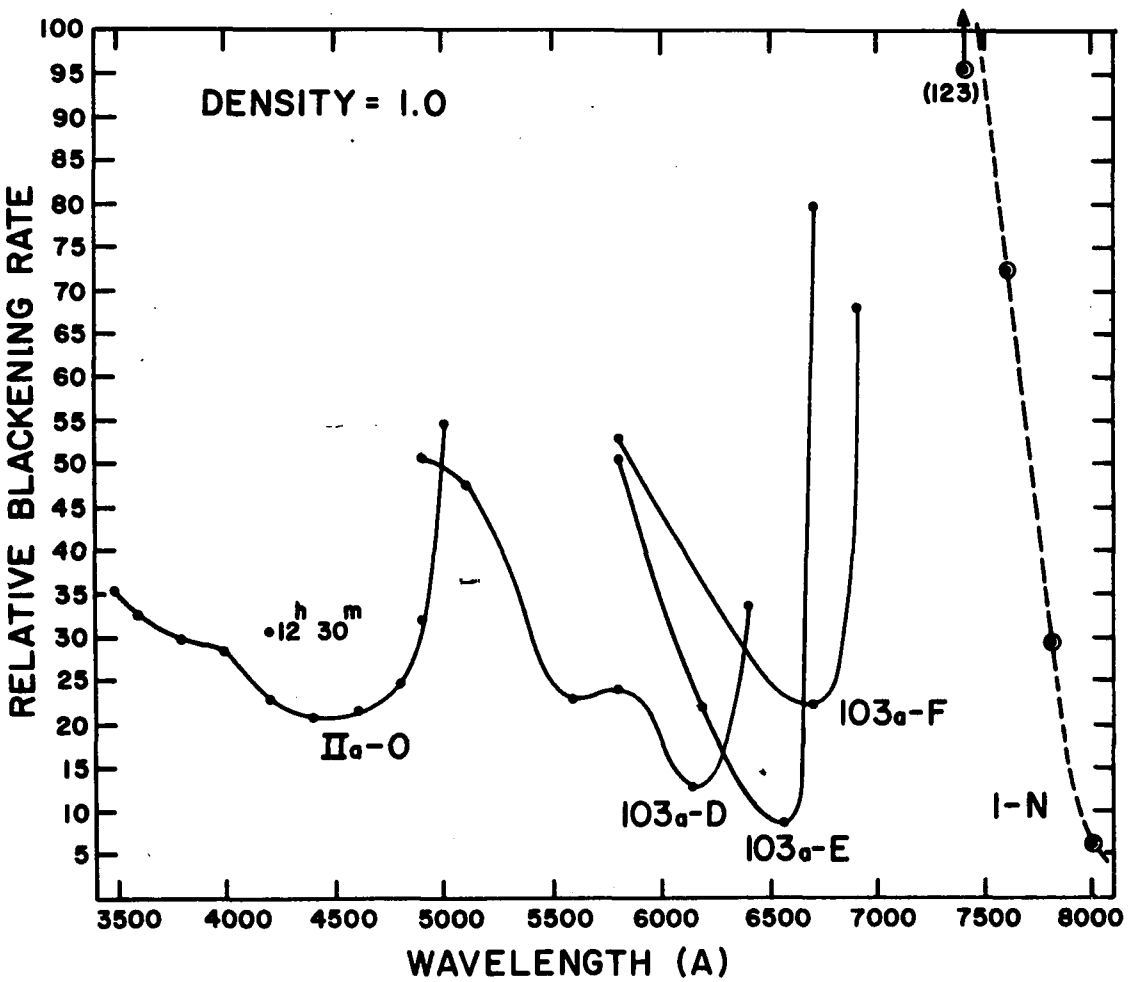

Fig. 7. Relative Blackening Rate, Density = 1.0.

The difference between this figure and Fig. 6 is the higher plate density specified. This high density is typical of a sky-limited exposure, where low contrast objects are to be detected against the night-sky background. Data for the I-N plates were interpolated somewhat because the highest plate densities were less than 1.0.

rate characteristics. The rate of blackening is decreased by the factor 0.54 for the low densities and by the factor 0.76 for the high densities. This makes the relative blackening rates fairly comparable for both densities, as the contrast of the image tube plus baked IIIa-J is roughly equal to that of the direct plates.

Contrast Measurements (Gradient)

Measurements of the slopes of the characteristic curves were made for the image tube and unaided plates. A "mean" value for each emulsion was determined by finding the slope of a straight line drawn through the characteristic curve where it intersects the density values of 1.0 and 0.3. This contrast figure is commonly called the "gradient" for the emulsion. In the present case, the gradient values refer to the most appropriate wavelength region for each particular emulsion. The determined values of gradient are presented in Table 3.

Table 3

Gradient Values

Direct plate	Gradient
IIa-O	1.12
103a-D	1.26
103a-E	1.49
103a-F	1.24
1-N	1.50
Image tube	
IIa-O	1.12
$IIIa\text{-}J_B$	1.35

Spectral Sensitivity: Concluding Remarks

The results of this investigation on the relative sensitivity of the image tube compared to astronomical emulsions may be summarized by stating that the image tube is about 25 times faster than unaided plates over most wavelength ranges. This figure applies to the image tube when the relay lens is set at f/2 and a IIa-O recording emulsion is used. Further, this speed gain is for a typical unaided plate exposure of 40 minutes--and the image tube correspondingly 25 times shorter. If the image tube is exposed for 30 minutes, an unaided plate would have to be exposed not only 25 times longer to obtain the same density, but an additional exposure factor would be required because of reciprocity failure. For the long-exposure test with a IIa-O emulsion carried out in the laboratory, this factor was found to be 1.3. It should be noted that from Eastman Kodak data on reciprocity characteristics for their plates (Eastman Kodak 1967), this exposure factor may be calculated to be greater than 5. The discrepancy between these two values indicates that for the IIa-O emulsion, at least, the reciprocity characteristics have been improved since the last reciprocity curves were determined by Eastman Kodak.

In one important region of the spectrum, the 6563 A Hα region, the sharply peaked sensitivity of the 103a-E emulsion reduces the relative blackening rate of the image tube to approximately 10. In the spectral region of 6800-7400 A the image tube is several hundred times more sensitive than any existing photographic plate, but as the wavelength is further increased to 8000 A the image tube is only some 6

times faster than the I-N emulsion. The I-N can in general be hypersensitized enough to match the speed of the image tube at 8000 A and beyond. As was suggested earlier, however, it is suspected that this particular image tube is somewhat less sensitive in the red and infrared than an average Carnegie tube. In any event, lack of sensitivity, as well as a further lack of uniformity, limit the usefulness of this tube for most applications beyond 7500 A.

It should be pointed out that the blackening rate of the image tube can be increased by nearly a factor of 2 by using the relay lens at f/1.5 instead of f/2. If the particular application will allow the reduced resolution and increased lens flare accompanying this faster lens setting, then it should by all means be used. An example of such an application might be the search for objects with peculiar emission features, using interference filters to isolate spectral regions just off, and on, the emission wavelength. Provided the contrast of the images is sufficiently high compared to the surrounding background, the increased lens flare would not seriously affect such an application, and the increased speed would be significant.

Uniformity

A qualitative estimate of the photometric uniformity of the Carnegie tube can be obtained by visually studying Figs. 8, 9, and 10. For these photographs, the entire field of the photocathode was uniformly illuminated by a distant point source of light. The wavelength of the illuminating radiation was 5500 A for Figs. 8 and 9 and was 8000 A for

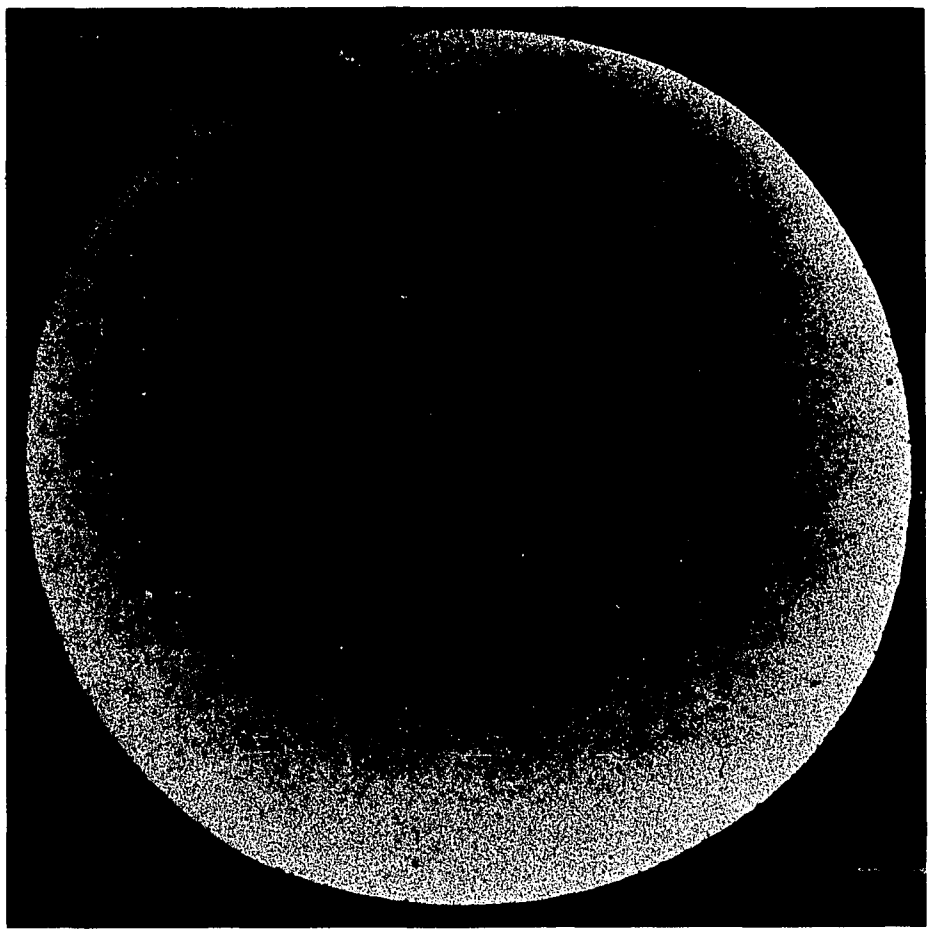

Fig. 8. Photograph of Uniformly-Illuminated Photocathode at 5500 A, IIa-O Recording Emulsion (Positive Print).

The large-scale uniformity appears quite good although some increase in sensitivity at the edges is detectable. The small-scale sensitivity variations, forming patches and ripples, are just discernible above the grain noise of the IIa-O. However, the pinholes are clearly seen. (See Fig. 9.)

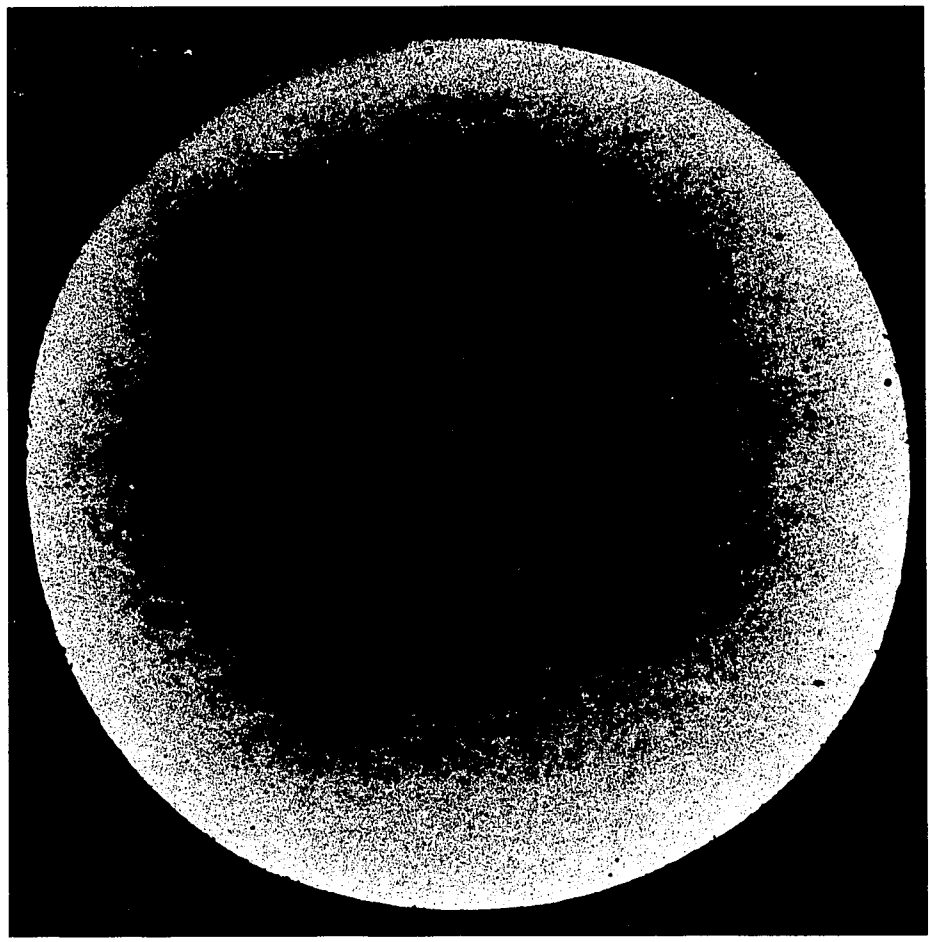

Fig. 9. High Contrast Photograph of Uniformly-Illuminated Photocathode at 5500 A, IIIa-J Recording Emulsion (Positive Print).

This IIIa-J record shows more clearly the large-scale sensitivity increase at the image tube edges than is shown on the IIa-O photograph in Fig. 8, and clearly reveals the individual sensitivity patches and ripples of the image tube. The most obvious patches are characteristically under 1 mm in size and deviate in sensitivity some 3 to 5%. Their effect on photometry is statistically small, but they may often mimic faint objects and reduce detection. The general mottled pattern over the entire image tube surface affects the photometry of 175 μm star images by adding only a 0.7% rms error. However, threshold images may often be adversely affected because the characteristic size of an element of the mottle pattern may be that of a star image.

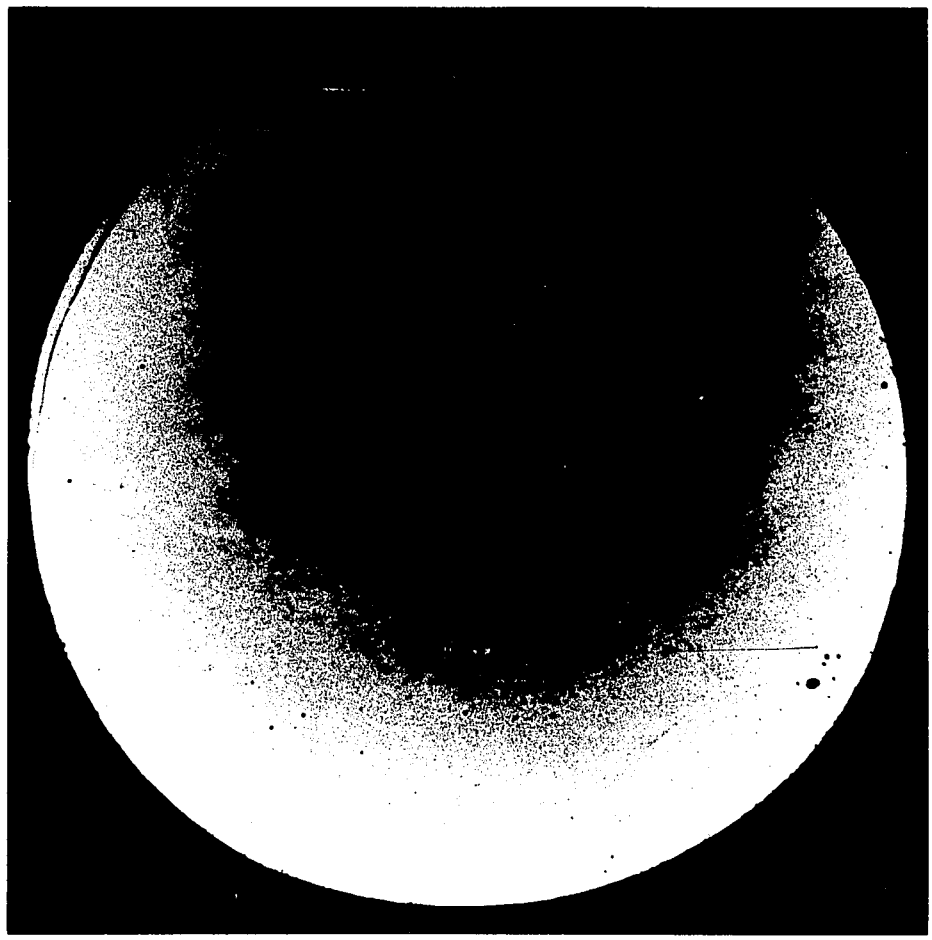

Fig. 10. High Contrast Photograph of Uniformly-Illuminated Photocathode at 8000 A, IIIa-J Recording Emulsion (Positive Print).

The nonuniform large-scale sensitivity in the infrared is very apparent here; the edge sensitivity is increasing rapidly compared to the center and there is an anomalous "hole" in the middle of the photocathode. Comparing this photograph to the 5500 A plate of Fig. 9, it is seen that the small-scale nonuniformities are unchanged with wavelength and must be caused by the phosphors. The pinholes are enlarged, and are clearly on the photocathode. This particular sample of the Carnegie tube may have less sensitivity and more anomalies in the infrared than average. No severe anomalies exist in this tube for radiation wavelengths shortward of 7000 A.

Fig. 10. The recording emulsion in Fig. 8 was IIa-O and, for this commonly used emulsion, the response of the image tube appears moderately uniform. However, in Fig. 9, the nonuniformities of the image tube response become quite apparent to the eye. The increased prominence of the nonuniformities in this figure results from using a fine-grained, high-contrast, IIIa-J recording emulsion. By comparing the IIIa-J photographs in Figs. 9 and 10, the wavelength dependence of the nonuniformities can be seen.

The nonuniformities of the image tube may be divided into four basically different types according to their morphological structure. First, there is a general "sensitivity profile", by which is meant the smooth, large-scale change in sensitivity. From the figures, the sensitivity profile is seen to increase toward the edges of the field. Second, there are several individual bright and dark "patches" and "ripples" within the field. Third, there are many small, dark "pinholes". Fourth, there is an over-all "mottle pattern" of small-scale deviations that exists throughout the field of the image tube. In addition to these four main types of nonuniformities, there is a small area in the center of the field that exhibits an anomalous decrease in sensitivity to infrared radiation (Fig. 10). A detailed description of each of the above nonuniformities will be presented in the following paragraphs. For all the following measurements, the relay lens was set at f/2.

Sensitivity Profile

Determination for 4800 A radiation (small area illumination by step wedge). To determine the sensitivity profile of the Carnegie tube at a typical wavelength, several step wedge patterns--illuminated by 4800 A radiation--were exposed throughout the field on a single image tube plate. As a control, direct plates were also exposed and processed in an identical fashion. Measurement of these direct plates showed that the uniformity determinations were accurate to within ±2 percent.

The sensitivity of the image tube across its face, as obtained by the reduction of this step wedge data, is shown in Fig. 11. The sensitivity is seen to increase with increasing radius from the center. It should be pointed out that this increase in sensitivity toward the edge of the field is not caused by higher effective quantum efficiency but is caused by the decrease in magnification toward the outer portion of the field.

Color dependence of sensitivity profile (full area illumination). To investigate the color dependence of the sensitivity profile, image tube (and unaided control) plates were taken under conditions of uniform, full area illumination. The wavelength of the illuminating light was varied from 3500 to 8000 A. Examples of these plates have already been given in Figs. 8, 9, and 10. The sensitivity profile determined by scanning one such plate with a microphotometer is compared in Fig. 11 to that determined from the step wedge data. The difference in the wavelength of the illuminating radiation is insignificant for the two determinations.

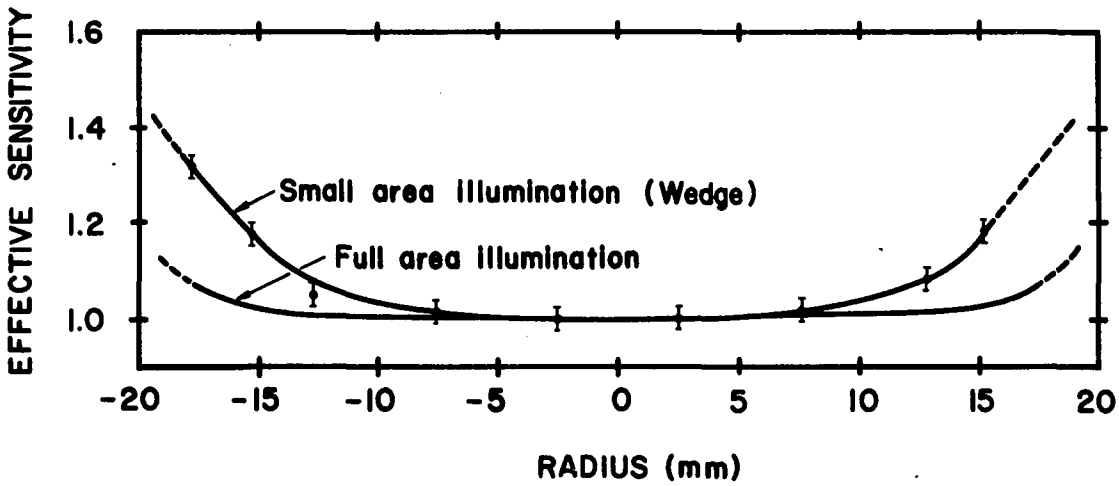

Fig. 11. Full-Area vs. Small-Area Illumination Measurements of Uniformity.

The "sensitivity profile" determined by projecting small-area step wedges at several points across the image tube field is the correct determination. The error bars for these data have been determined from control exposures on direct plates. The apparent increase in sensitivity at the edges is caused by the image demagnification due to geometrical distortion. The measured sensitivity profile is different when the photocathode is uniformly illuminated, and this is caused by light-induced background.

Fig. 11 clearly shows a discrepancy between the two methods of determining the sensitivity profile of the image tube. This apparent discrepancy may be explained by using the results obtained in the investigation of the light-induced background presented in a later section. The sense of the effect is that, when the photocathode is uniformly illuminated, the center of the field receives proportionately more background than the edge. When the effects of the background are allowed for, the apparent discrepancy in Fig. 11 is largely eliminated. Thus, the sensitivity profile determined by the small area (step wedge) illumination is the correct one.

Keeping in mind that the light-induced background prevents the determination of the true sensitivity profile from the full-area illumination plates, these photographs can still be used to determine the relative changes as a function of wavelength. The data thus obtained are presented in Table 4. Note that the 5500 A data in this table are the same as are plotted in Fig. 11. It is seen from Table 4 that over the spectral region of 3500 to 6700 A the relative sensitivity profile changes very little. In fact, the small differences indicated in the profiles up to 6700 A can be shown to be caused by a color dependence of the light-induced background. Thus, the true sensitivity profile remains essentially unchanged over this spectral region. Changes do occur, however, in the sensitivity profile beyond about 7000 A. This is shown by the 8000 A data of Table 4, where the edge of the field tends to increase in sensitivity relative to the center.

Table 4

Relative Sensitivity Profile Measured for Fully-Illuminated Photocathode at Several Wavelengths[a]

Radius (mm)	Measured sensitivity normalized to center			
	3500 A	5500 A	6700 A	8000 A
0.0	1.00	1.00	1.00	1.00[b]
4.4	1.00	1.00	1.00	1.08
5.9	1.00	1.00	1.00	1.10
8.8	1.00	1.00	1.00	1.15
11.8	1.01	1.01	0.99	1.22
14.8	1.03	1.02	1.02	1.33
17.7	1.10	1.07	1.05	1.45

a. No corrections have been made for the effects of light-induced background in these data.

b. An anomalous small-area decrease in sensitivity in the center at 8000 A was removed by a correction factor.

Origin of color dependence of sensitivity profile. The sensitivity profile color dependence (beyond 7000 A) suggests that the effect is associated with the input photocathode. Apparently there is over the photocathode an appreciable variation in the chemical properties which determine the infrared sensitivity. In addition to the change in the sensitivity profile, the small area in the center of the field that exhibits decreased infrared sensitivity must also be associated with the input photocathode. These particular phenomena of the Steward Observatory Carnegie tube may not be typical.

Significance of sensitivity profile. It is concluded that in order for accurate photometric measurement to be made with the Carnegie

tube, definite corrections for the varying sensitivity will have to be made. These corrections will follow the profile given in Fig. 11, provided observations are not made beyond 7000 A. Such corrections will be straightforward for small objects superimposed on a uniform background, where the background (both natural and light-induced) can be clearly separated from the objects of interest. Photometric measurements under these conditions should be only slightly less accurate when made with the Carnegie tube than when made with unaided plates.

In those applications where the object cannot be unambiguously separated from the background (e.g., surface photometry of faint extended objects) accurate photometry will be difficult. In such cases, little more can be done as a means of correcting for the background than to assume the input background is uniform and that the net recorded background is similar to that given in Table 4. This is probably the best that can be done in practice to allow for the light-induced background. It will be shown in the next section that to attempt a more accurate correction would most likely be futile.

Variation of sensitivity profile with position angle. It should be pointed out that the data presented above concerning the sensitivity profile refer to average values, taken over several position angles at given radii. There are smooth variations of 2 to 3 percent with position angle that may be compared to the random variations of 1 to 2 percent that are inherent in carefully processed photographic plates (Latham 1966). However, to properly correct for the sensitivity variations of the image tube--making the large-scale

photometric properties of the image tube in effect as good as those of unaided plates--would require computer reduction of the data.

Patches and Ripples

The bright and dark patches and ripples number about 20 over the field of the image tube and are particularly concentrated to the left of center in Figs. 8, 9, and 10. The longest dimensions of some of the larger ripples and patches are 2 to 4 mm, but the average patch size is less than 1 mm, and the narrow ripples are generally less than 0.1 mm wide. The sensitivity for the most obvious nonuniformities has been measured to deviate ±3 to ±6 percent from that of the surrounding field.

The patches and ripples have been found to be independent of the wavelength of the incident radiation. This suggests that these nonuniformities arise at the dynode and/or output phosphor. Indeed, their "watermark" structure suggests they may be caused by clumping and stretching during the settling process in phosphor manufacture.

The statistical effect of these regions on stellar photometry should be quite small because they occupy very little of the total sensitive area. However, these same patches will make the study of faint nebulosity, or other extended objects, considerably more difficult because the patches will tend to "mimic" some of the expected characteristics of the objects studied. The photometry of either a stellar image or an extended area will of course be affected if the object lies on one of these patches.

Pinholes

The pinholes on an image tube photograph number about 30, are distributed randomly over the field, and are characteristically 20 μm in diameter. The diameters of several, but not all, of the pinholes are significantly larger in the infrared. Such a color dependence indicates that they are probably associated with the dynode and the input photocathode. It seems likely that these pinholes were formed during the evaporation process of photocathode manufacture. Their significance in most photography applications of the Carnegie tube should be very small because of their easily recognizable character and the insignificant fraction of the total sensitive area occupied.

Mottle Pattern

Description. To quantitatively measure the general mottle pattern of the image tube, uniformly exposed plates were scanned with a narrow microdensitometer slit of 5 × 125 μm. The traces revealed an undulating pattern superimposed on the normal fluctuations of the photographic grain of the IIIa-J recording emulsion. Measurements of this pattern show it to be characterized by a mean spatial period of 350 μm. The rms sensitivity fluctuation for this mottle pattern is found to be about 1.3 percent. The maximum deviations, however, are found to be about 4 percent, which are not very different from the deviations of the more obvious sensitivity patches discussed earlier.

Just as in the case for the patches and ripples, the mottle pattern has been found to be color independent. Thus it is probable that this pattern is also associated with the phosphors.

Significance of mottle pattern. The effect of the mottled sensitivity pattern should be similar to grain noise. In the limiting case, the contrast of an image against its surroundings will have to be greater than that required for normal photography. The effect may be particularly strong for star images, realizing that the characteristic size of an element making up the mottle pattern may be about that of a typical star image.

A somewhat different problem than the reduced detectability of threshold stellar images is the error introduced in conventional iris photometry of stars. If it is assumed that the size of a star image is 175 μm, the added noise to stellar photometry can be estimated by representing the mottle pattern as a sinusoidal variation. The rms photometry error due to the mottle effect is then calculated to be about ±0.7 percent, or ±0.008 magnitude. The normal photographic errors inherent in stellar photometry will of couse be added to this value. Realizing that typical probable errors in such photometry amount to ±0.03 magnitude, it is clear that the mottle effect will degrade stellar photometry very little (see Chapter IV).

Comparison of mottle pattern and normal emulsion granularity. Microdensitometer traces of direct photographic plates, using a 125 × 15 μm slit, reveal an rms granularity of about 3.4 percent for the 103a series of plates and 3.0 percent for the IIa-O plates. The granularity expressed here is in terms of intensity fluctuations, not density fluctuations. The values were determined for a density above fog of about 0.65.

The mottle effect of the image tube is almost hidden in the plate grain noise when a IIa-O recording emulsion is used; the granularity for the image tube plus IIa-O has been measured to be 3.4 percent, only some 11 percent greater than the IIa-O alone. For the image tube plus baked IIIa-J, the granularity is about 1.9 percent and the mottle pattern is clearly affecting the value.

Internal Reflections Within Photocathode Faceplate

When initial tests were made of the Carnegie tube under conditions of full-field illumination of the photocathode, an unexpected pattern appeared at the image tube output. A photograph which vividly demonstrates this pattern is reproduced in Fig. 12. In this photograph a mask was placed in front of the image tube so that only an outer portion of the photocathode was illuminated. Studying this phenomenon revealed that the pattern was being caused by reflections from the reflective metallic annulus that surrounds the input photocathode. The light reflected from this annulus was then reflected from the circular wall of the photocathode faceplate and internally reflected again and again between the two faces of the faceplate, producing the pattern observed. The multiple internal reflections of the light initially falling on the metallic annulus are clearly shown in Fig. 12. For this photograph the illuminating light was only slightly divergent at the edge of the photocathode. The distance between the photocathode and the point source of illumination was 2.3 m.

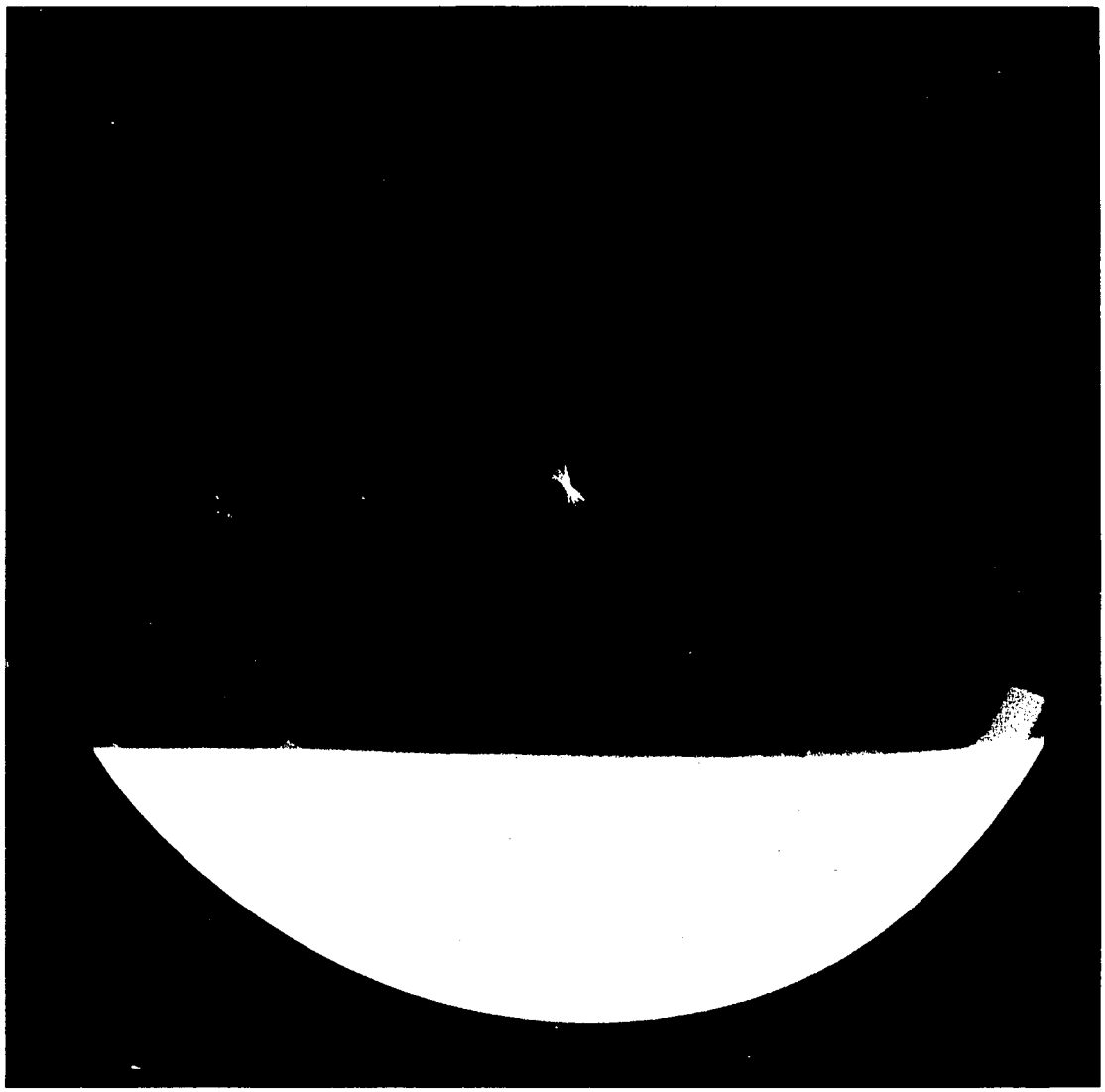

Fig. 12. Internal Reflections from Illuminated Edge of Photocathode.

When initial tests for uniformity of response were made, this unexpected pattern appeared when the photocathode was fully illuminated. In this photograph only a small portion of the photocathode (pure white area) was illuminated; such illumination clearly reveals the nature of the pattern. Caused by reflections at the edge wall of the photocathode faceplate, the pattern was eliminated by adding a paper mask around the entrance window. The importance of internal reflections within the glass faceplates is strikingly pointed out in this photograph. Such internal reflections undoubtedly augment the light-induced background of image tubes--the subject of the next section. Note the faint induced background over the entire photocathode.

Fortunately, the problem caused by these reflections may be successfully eliminated by installing an opaque mask around the entrance window of the image tube. However, the discovery of the effect did serve to point out the importance of internal reflections within the photocathode window. Such reflections are undoubtedly responsible for some of the light-induced background present in the Carnegie image tube and possibly in other image tubes.

Light-Induced Background

It would be well to explain the convention used in this paper for describing all light-induced backgrounds. When such a background component is recorded, it is expressed in terms of an equivalent incident light that would render a similar final record on an ideal image tube (with no induced background). This hypothetical light is always expressed as a percentage of the true incident radiation.

Background from Small Spot

To examine the nature of the light-induced background of the Carnegie tube, a 2.5 mm diameter spot of light was projected onto the photocathode with an f/13 lens system. Plates were exposed long enough to clearly record the faint background surrounding the image of this spot (see Fig. 13). The wavelength of the illuminating radiation was varied from 3500 to 8000 A to investigate the color dependence of the background. Analysis of the plates indicates that the light-induced background consists of two different components and suggests the principal causes of the background in the Carnegie tube.

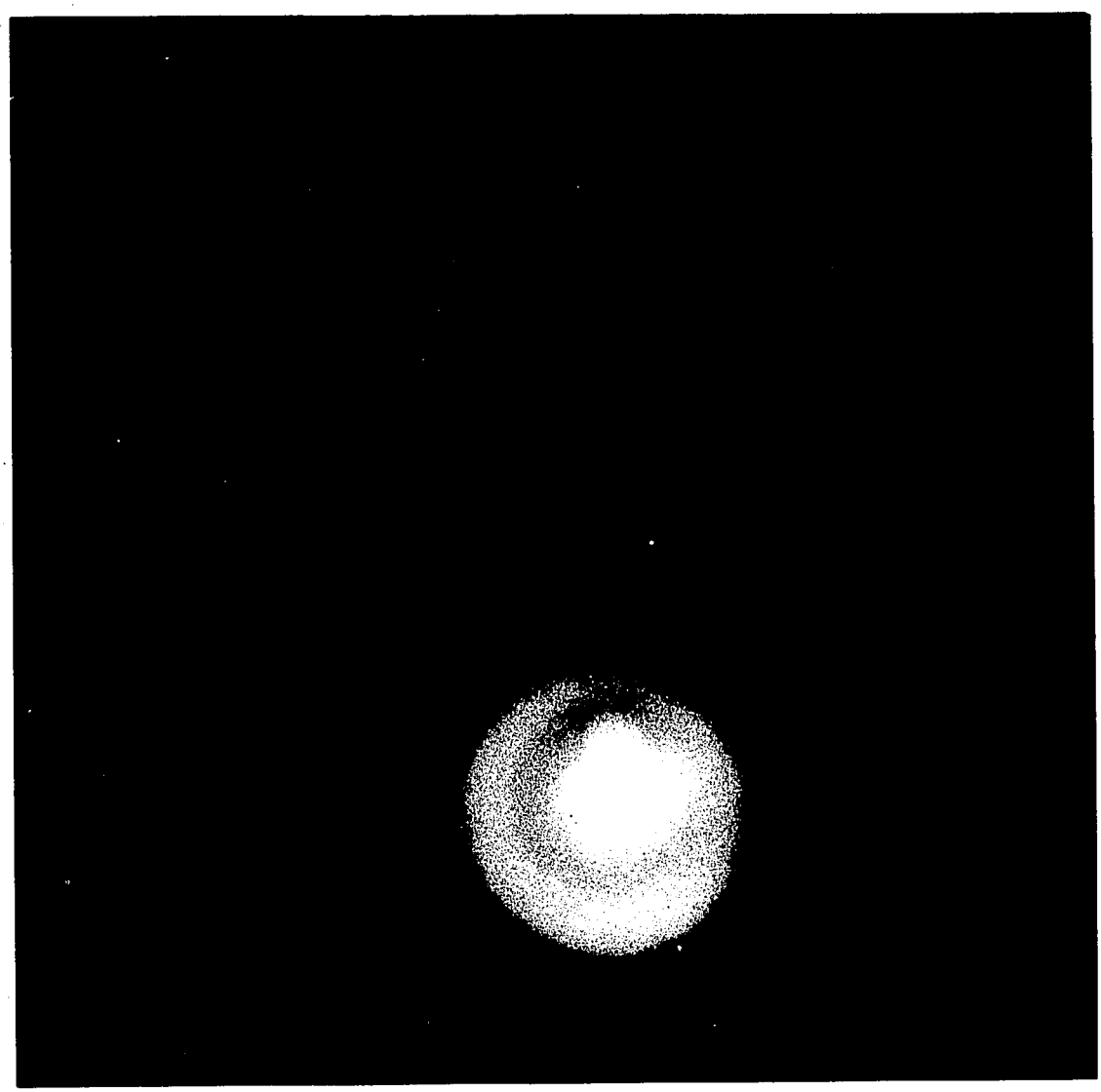

Fig. 13. Photograph Showing Nature of Light-Induced Background.

The rings surrounding the highly overexposed spot are caused by internal reflections in the phosphor output window. The smooth component of the induced background is caused by the light that is transmitted by the photocathode and is subsequently scattered back to it. Measurements of these components are plotted in Fig. 14. The ghost image appearing diametrically opposite the input image is insignificant in contributing to the total induced background.

Color dependent, smooth component. There is a relatively smooth component of background that gradually diminishes in strength with increasing distance from the image. On photographs of this component, certain small defects of the input photocathode are plainly visible. This clearly indicates that the background is caused by emission from the photocathode. In addition, this component is found to be color dependent; the relative amount of background increases as the wavelength of the incident radiation is increased. It is concluded from the above characteristics that this background component is caused by scattering of the incident radiation in the following manner. A certain portion of the incident radiation is transmitted by the semi-transparent photocathode and is subsequently reflected and scattered from the dynode phosphor and possibly the image tube walls. Some of the scattered light is eventually returned to the photocathode.

The distribution of the color dependent induced background is shown for two different wavelengths of the incident radiation in Fig. 14, where the intensity is plotted as a function of distance from the image of the illuminating spot. Straight lines are seen to fit the data points rather well.

Color independent component. Once the background described above is removed from the data, the remaining background is found to be independent of the wavelength of the incident radiation. This component is represented in the photograph of Fig. 13 by the concentric rings surrounding the spot target. The diffuse light immediately surrounding the spot is also part of the color independent component. The

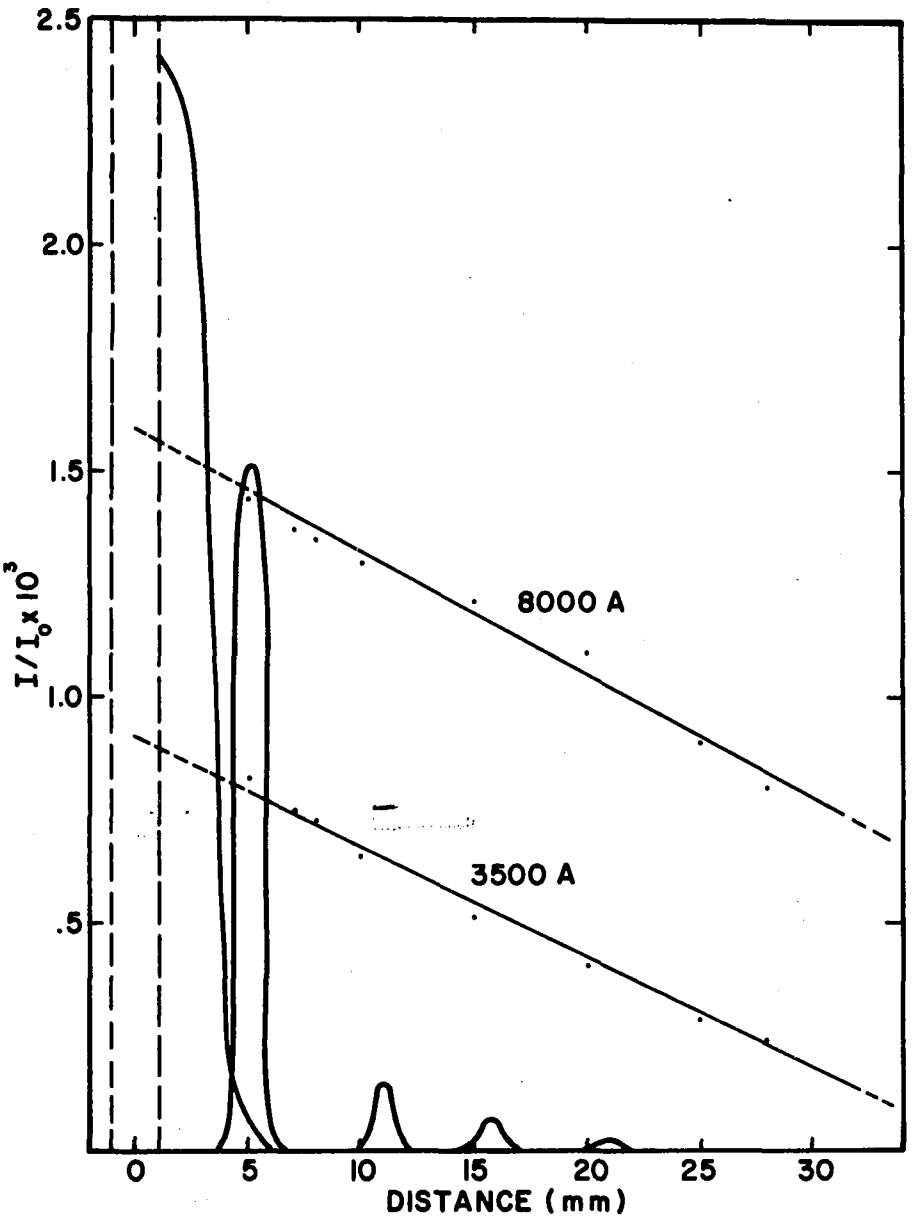

Fig. 14. Plot of Induced Background of 2.5 mm Spot.

The induced background--plotted here as a fraction of the intensity of the 2.5 mm spot--is composed primarily of two parts. One is the color dependent background caused by the transmitted and scattered light originally forming the image on the photocathode. The other is the diffuse scattered light and internal reflections occurring within the output phosphor window.

intensity in the rings and nearby diffuse light is plotted in Fig. 14. The concentric ring structure suggests that this background component is caused primarily by internal reflections within the input or output window, but the color independence and the expected Lambertian radiation law for the phosphor suggests that it is the output window that is mainly involved. A portion of the diffuse light immediately surrounding the spot image may arise within the multiplying dynode of the tube.

Another background component that is independent of wavelength is a "ghost" image occurring diametrically opposite the primary image. (See Fig. 13.) The intensity of this ghost is about 3×10^{-4} that of the primary image. The cause of the ghost image is not presently understood. Its contribution to the total background is insignificant, however.

Calculations from the Background Photographs

Using an appropriate model and the numerical results obtained from the background photography it is possible to predict the amount of light-induced background that will be present when the image tube is uniformly illuminated over its entire field. The model for the scattered incident radiation (color dependent component) follows straightforwardly from the data of Fig. 14. Assume there is a uniform incident radiation, of intensity I_o, falling on the photocathode. Then the incremental intensity, dI, of induced background due to the radiation incident on an incremental area, dA, at a distance, r, from the point under consideration is

$$dI = I_o \, (ar - b) \, dA.$$

The constants, a and b, may be determined from the background data for a given wavelength of incident radiation. For the concentric ring (color independent) component of background, the intensity of the background received from the nth ring may be represented as

$$I_n = a_n I_o (2\pi r_n).$$

Here, $2\pi r_n$ is the circumference and a_n is a constant for the nth ring in the present model.

The above expressions have been integrated (color dependent component) and summed (color independent component) over the appropriate limits to give the background at the center of the image tube. Such calculations are of course possible for any point in the image tube field, but the boundary conditions become rather complex for any point other than the center. These calculations show that the intensity of the color independent background is 4.0 percent of the incident intensity. The color dependent background arising from the scattered incident light is about 14 percent at 3500 A and 29 percent at 8000 A.

Background for the Fully-Illuminated Photocathode: A Test

A second, more direct, method has been used to determine the amount of light-induced background under conditions of a fully-illuminated photocathode. In this test exactly half of the field, a 180^o sector, was illuminated. Measurements of the background were made near the boundary of the illuminated portion, and the resulting values were multiplied by 2 in order to approximate the background for full photocathode illumination. The values thus obtained are presented in

Table 5. A comparison between these values and those predicted from the spot photographs shows the agreement is quite good.

Table 5

Light-Induced Background at Three Wavelengths for Fully-Illuminated Photocathode

Wavelength	Edge (18 mm)	Center	Prediction from spot photographs (center)
3500 A	13 %	21 %	18 %
5500 A	18 %	26 %	--
8000 A	31 %	36 %	33 %

Light-Induced Background: Concluding Remarks

The results of the above study of light-induced background indicate that this particular shortcoming of the image tube can be one of the most severe in certain applications. The facts that the background is color dependent, affects the center more than the edge when the image tube is uniformly illuminated, and is generally dependent on the distribution of light in the incident image make the correction for this background rather difficult. A few numerical examples should indicate the extent of the difficulties.

When photographs of astronomical objects are taken with no bright star in the field, the most important effect of the induced background will be that of effectively increasing the night-sky background by about 25 percent. The actual amount will depend on wavelength

and position in the field according to Table 5. (More accurate values for this background will be difficult to predict because of the complexities involved in the scattered light component. For example, the background should depend on the focal ratio of the input optics to the image tube.)

The additional corrections required by the effects of light-induced background have been discussed in the section concerned with uniformity of the image tube. With such corrections, photometric measurements with the Carnegie tube should be only somewhat less accurate than normal photographic photometry. In addition to the photometric uncertainties, the 25 percent increase in background will undoubtedly affect the signal-to-noise ratio of faint objects.

Whenever a bright object happens to be in the field, the background may seriously compromise the photometric capability of the tube. Using the data of Fig. 14, the following calculation can be made regarding iris photometry of star images: In order to avoid a systematic error of more than 0.01 magnitude caused by the radial variation in induced background from a bright star, the star must be no more than 12 magnitudes brighter than the faintest stars measured. (It is assumed in this calculation that the variation in background has not been corrected for by making individual "sky" measurements around each star.) Thus, if photometry is to be made of twentieth magnitude stars, an eighth magnitude star in the field must either be avoided or at least masked from the photocathode.

Limiting Detectable Signal

It is well known that an object must have sufficient contrast with respect to its background if it is to be detected with a photographic plate. In addition, for a specific photographic emulsion, there is an optimum density to which the background must be exposed in order to record the limiting detectable signal. Thus, two important specifications of a given plate (or plate-image tube combination) are the contrast of the limiting detectable signal and the optimum density required for limiting detection.

To study the limiting detection capability of the image tube and astronomical plates, the Baum microprojector was used to expose its "astronomical test pattern" to the various plates of interest. This test pattern was illustrated earlier in Fig. 3. The portion of interest here is the lower left hand rectangle, which contains a sequence of five simulated star images against a sky background. Each of the stars is 80 μm in diameter and the flux received from each is, respectively, 40, 25, 16, 10, and 6 percent above that received from the background. These figures may be expressed also as equivalent to stars being 1, 1.5, 2, 2.5, and 3 magnitudes fainter than the "sky" background.

For the various emulsions tested, the limiting magnitudes below sky level and the sky densities for the optimum exposures are presented in Table 6. The densities listed here include the fog levels of the plates. Realizing that the optimum density values are significant within only a few tenths, it is seen that they are essentially identical for all the emulsions tested. The limiting magnitudes reported in

Table 6 for direct plates are about one magnitude fainter than those reported by Baum (1962b), and the reason for this is not clear. However, the important figure here is the difference in limiting magnitude between the direct and image tube plates, and only to a lesser degree the actual values.

Table 6

Limiting Magnitude Capability, Optimum Density

Direct plate	Magnitude below sky	Optimum sky density	Fog density
IIa-O	2.5	1.3	0.1
103a-E	2.5	1.4	0.2
I-N	3.0	1.2	0.1
Image tube			
IIa-O	2.0	1.2	0.1
IIIa-J_B	2.5	1.3	0.3

The important conclusions to be drawn from the data in Table 6 are that the image tube suffers about a half-magnitude loss in limiting magnitude, compared to most direct plates, when a IIa-O recording emulsion is used, and this loss apparently is gained back by using a baked IIIa-J recording emulsion.

It should be pointed out that a particular shortcoming of using the Baum microprojector in determining the limiting magnitude capability of an image tube is that only a small portion of the field is illuminated,

and the light-induced background is not as severe as it would be in an actual full-field photography application. The increase in effective sky background due to this phenomenon should reduce the limiting magnitude of the image tube an additional 0.3 magnitude.

Additional Photographic Plate Tests

It has already been mentioned that the IIIa-J emulsion offers certain advantages over a IIa-O emulsion as the recording plate for the image tube. These advantages include higher resolution, higher contrast, lower granularity, and an increased storage capacity. Unfortunately, the IIIa-J is about 9 times slower than the IIa-O when used with the image tube. Baking tests were thus initiated with several different baking times and temperatures in an attempt to increase the speed of the IIIa-J emulsion. The results of these baking tests for the IIIa-J, as well as the IIa-O, are given in Table 7. The relative speeds are given for a density above fog of 1.0, and all speeds are

Table 7

Baking Properties for Plates

		Speed relative to IIa-O		
Plate	Baking conditions	Image tube	4200 A direct	Fog
IIIa-J	Unbaked	0.11	----	.06
IIIa-J	48 hr at 50° C	0.28	----	.12
IIIa-J	18 hr at 65° C	0.60	----	.17
IIIa-J	24 hr at 65° C	0.77	0.56	.25
IIa-O	48 hr at 50° C	1.18	----	.16

normalized to that of an unbaked IIa-O developed in D-76 at 68°F for 15 minutes. The exposure time for all the plates was 30 minutes.

It should be pointed out that the image tube phosphor radiates a significant amount of light at wavelengths beyond 5000 A, where the sensitivity of the IIa-O has been lost, yet where the sensitivity of the IIIa-J is peaking. Therefore, the relative speed of the IIIa-J compared to the IIa-O will generally be more favorable when both are exposed in the image tube than when directly exposed to blue monochromatic light. This effect is confirmed in Table 7 by the one set of exposures made to 4200 A radiation.

In this study it was concluded that the optimum baking conditions for the IIIa-J are to bake the plates for 24 hours at 65° C. Increasing the baking time or temperature much beyond this increases fog drastically. It is not really the fog itself that is the limiting factor, however, but rather the uniformity of the fog. In fact, the baking procedure used produces rather unreliable photometric response for the IIIa-J plates. The variation in fog can affect the photometry by as much as 9 percent according to microdensitometer measurements. In addition to the fog nonuniformity, sensitometric measurements have shown a variation in sensitivity of as much as 10 percent over a 2 × 2 inch plate. Because the variations generally change smoothly, they are seldom apparent when the plates are inspected visually.

In Table 7 note that baking the IIa-O emulsion according to past recommendations results in little speed gain. This is in

agreement with the experience of other observers concerning recent IIa-O plates.

Comparison of D-76 and D-19 Developers

One other test of photographic plates that should be mentioned is the comparison of the relative speeds of IIa-O plates developed in D-76 and D-19 developers. Because of the longer development time of 15 minutes for D-76, as compared with 4 minutes for D-19, many investigators prefer to use D-19 for IIa-O plates. The increase in speed by using D-76 developer, however, more than merits the use of this developer in applications where plate speed is important, according to the present investigation. The relative speed of a IIa-O developed in D-19 and D-76, as well as a baked IIIa-J (24 hr at 65^{o} C) developed in D-19, may be calculated from the set of characteristic curves which are plotted in Fig. 15. These curves apply to the respective plates exposed for 30 minutes in the image tube. There is an obvious difference between the contrast of the baked IIIa-J and IIa-O, as has been previously discussed, and there is also a slight difference in the contrast for the IIa-O plates developed in the two developers. The speed gain obtained by developing a IIa-O in D-76, compared to D-19, is 1.72 at a density of 0.3 and 1.56 at a density of 1.0 above fog. A similar test of developers was made for the baked IIIa-J plate with the result that the speed was decreased about 20 percent when developed in D-76 and the background fog was increased in density by 0.23. Clearly D-19 is the better of the two developers for the IIIa-J emulsion.

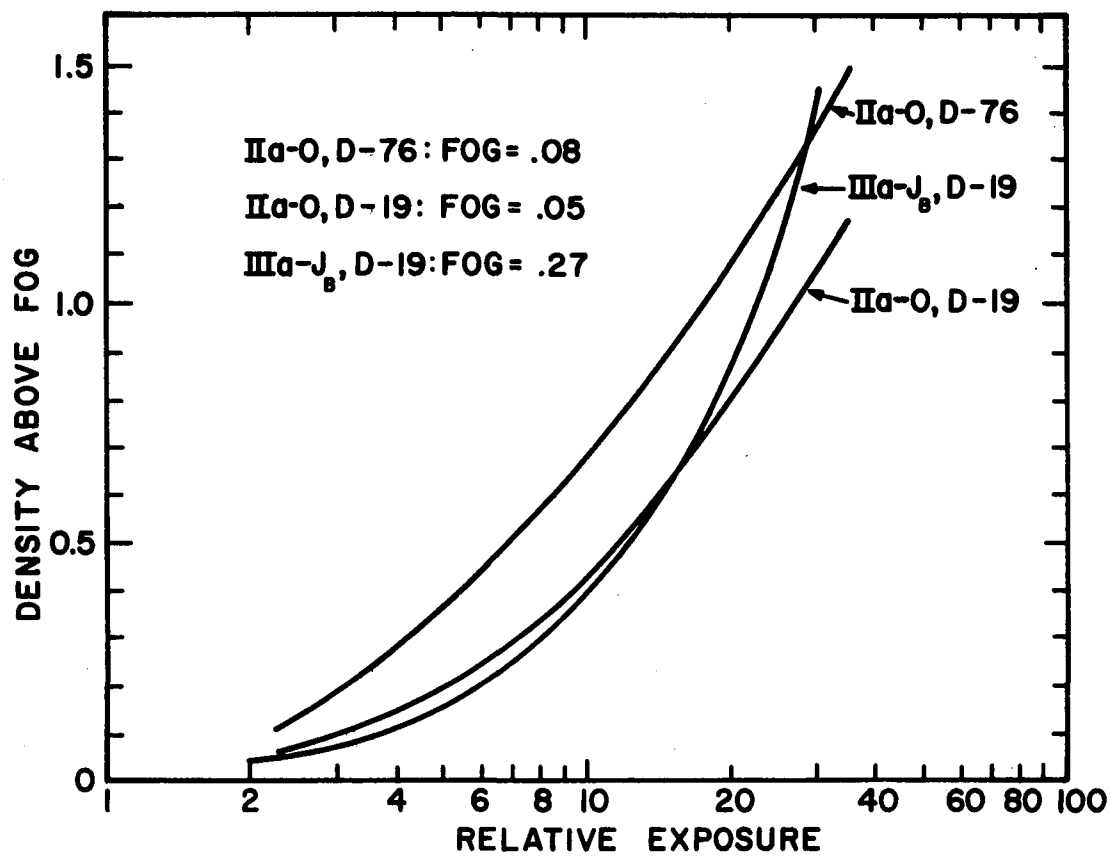

Fig. 15. Characteristic Curve Comparisons for Recording Emulsions.

All three plates were exposed for 30 minutes in the image tube. The increased contrast of the baked IIIa-J over the IIa-O is very apparent. The increased effective speed of the IIa-O, by developing in D-76 instead of D-19, is also very clear. Depending on the research requirement, either the higher-speed, more photometrically-reliable IIa-O, or the higher-resolution, higher-storage capacity baked IIIa-J emulsion may be chosen.

CHAPTER III

QUALITY CRITERIA FOR IMAGE TUBES

The definition of appropriate quality criteria for radiation detectors has been the subject of numerous papers over the past two decades; a great deal of effort has been spent attempting to quantitatively rank such detectors according to some specific merit function. In this chapter we shall discuss the figures of merit which have been most generally useful and by which image tubes can be compared. We shall see that the individual performance characteristics of a particular tube (such as those presented in the last chapter) and the particular requirements of a given application more often determine the usefulness of a tube than any single figure of merit.

Detective Quantum Efficiency

A concept that was introduced by Rose (1946) and has since been expanded by Jones (1959) is the "detective quantum efficiency" (DQE) of a detector. There are earlier papers by Jones, but the reference given above summarizes well this earlier work and includes a survey of the DQE for numerous radiation detectors. The same concept, under the designation "equivalent quantum efficiency", has been discussed by Fellgett (1958a,b).

Definition of Detective Quantum Efficiency

The DQE of a detector may be defined as the square of the output signal-to-noise ratio of the detector divided by the square of the input signal-to-noise ratio of the incident radiation. Symbolically,

$$DQE = \frac{(S/N)^2_{out}}{(S/N)^2_{in}} . \qquad (1)$$

Note that there is a significant difference between the "detective quantum efficiency" defined above and the commonly accepted concept of "quantum efficiency"--designated without the prefix "detective". In the standard concept, quantum efficiency may be defined as the ratio of the number of independent output events (or photoevents) to the number of incident photons. For a certain detector, the detective quantum efficiency is numerically equal to the standard quantum efficiency only if no noise is added by the detector. In most real photodetectors noise is added to the final record. Thus, it is clear that the detective quantum efficiency of a real detector will generally be lower than the actual quantum efficiency of the photosensitive surface.

Detective Quantum Efficiency for a Photographic Emulsion

Jones (1959) has developed an expression for the DQE of a photographic emulsion in terms of quantities measured in the laboratory. The expression may be written as

$$DQE = \frac{(\gamma \log e)^2}{\sigma^2 nAt} . \qquad (2)$$

Here, γ is the slope of the density-log exposure curve and σ is the rms granularity of the photographic emulsion. The rms granularity is expressed in density units and is obtained by scanning the photographic record with a microphotometer slit of area A. The number of photons per unit time per unit area received from the incident radiation is represented by n and the exposure time is represented by t.

Detective Quantum Efficiency of Carnegie Tube Relative to Direct Plates

It is possible to compare the DQE of the Carnegie image tube with the DQE's of the astronomical emulsions tested in the laboratory by using the data presented in the previous chapter. It should be pointed out that in the laboratory no determination was made of the absolute intensity of the incident radiation used to expose the image tube and unaided plates. Thus, no absolute determination of the DQE's can be made. However, the relative DQE's of the Carnegie tube and the unaided plates can be determined.

The expression used to calculate the relative DQE's is derived from Eq. 2 as follows, where the subscripts IT and DP designate values for the image tube and direct plate, respectively:

$$\text{Relative DQE} = \frac{(\overline{\text{DQE}})_{IT}}{(\overline{\text{DQE}})_{DP}} = \frac{\left[\frac{(\gamma \log e)^2}{\sigma^2 t}\right]_{IT}}{\left[\frac{(\gamma \log e)^2}{\sigma^2 t}\right]_{DP}} \quad . \qquad (3)$$

The ratio of exposure times, t_{DP}/t_{IT}, in Eq. 3 has been presented in Chapter II as the relative blackening rate. The values of $\sigma/\gamma \log e$ have been presented in Chapter II in the section dealing with

granularity. (It should be pointed out that $\sigma/\gamma \log e$ is merely expressing σ as a fractional variation in intensity rather than a variation in density.) Note that the terms A and n of Eq. 2 do not appear in Eq. 3. This is because these terms are the same for the image tube and direct plate records and thus cancel in the relative DQE expression.

Table 8 lists the DQE of the Carnegie tube relative to the various direct plates tested in the laboratory. The values apply to a plate density above fog of 0.65--which is considered representative of the plate densities encountered in practical applications. Two sets of relative DQE values are given for the image tube. One set applies to the image tube when a IIa-O is used as the recording emulsion and the other applies when a baked IIIa-J is used. In Table 8 the relative DQE has been calculated near the wavelength of maximum sensitivity for the direct plate being compared. Thus, the relative DQE's listed in Table 8 tend to favor the direct plate.

Table 8 indicates that a typical value of the relative DQE for the image tube used with a IIa-O recording emulsion is around 15. Notable departures from this figure exist for the 6563 A spectral region and the 8000 A spectral region. These departures are basically caused by the peaked sensitivity of the 103a-E emulsion at 6563 A and by the general lack of sensitivity of the Carnegie tube at 8000 A.

Table 8

DQE of Carnegie Tube Relative to Direct Plates
(for a Density Above Fog of 0.65)

Direct plate	λ(A)	Relative DQE of Carnegie tube for two recording emulsions	
		IIa-O	IIIa-J_B
IIa-O	4500	17	36
103a-D	6150	16	34
103a-E	6563	11	23
103a-F	6700	25	52
I-N	8000	6	13

The relative DQE of the image tube is increased essentially by a factor of 2 by going from the IIa-O to the baked IIIa-J recording emulsion. The reasons for the higher performance of the IIIa-J are its higher contrast and lower granularity, coupled with only a slightly reduced sensitivity (when baked) relative to the IIa-O.

Significance of Relative Detective Quantum Efficiency

To provide a clear understanding of the relative DQE a few characteristics of this figure of merit should be mentioned. In the present discussion consideration is given only to images for which the finite resolution of the detector is not important--that is, images that are sufficiently large in comparison to a resolution element. The effects of limited detector resolution will be discussed in a later section.

Consider three photographic plates taken of the same object under the following conditions. One plate is an unaided exposure made at the prime focus of the telescope. A second plate is a Carnegie tube exposure and is also made at the prime focus. The exposure time for the Carnegie tube exposure is such that the plate density is equal to that of the unaided photograph. A third plate is also a Carnegie tube exposure, but it is made at a longer focal length. The exposure time is equal to that of the unaided photograph and the plate density is equal to that of the other two plates. (The telescope focal length for this last plate is clearly specified by the prescribed exposure time and plate density. Such a choice is merely a convenience for purposes of the following discussion.)

The relative DQE presented in Table 8 may now be interpreted in the following manner. For the direct and image tube plates exposed at the same focus, the input signal-to-noise for the Carnegie tube exposure is considerably less than that for the direct plate. (Note that the input signal-to-noise ratio is proportional to the square root of the exposure time.) On the other hand, the output signal-to-noise ratio of the image tube is only somewhat less than that of the direct plate. The somewhat lower signal-to-noise ratio of the image tube record is due to the mottle pattern and other noise sources in the Carnegie tube. The relative output signal-to-noise ratio for the two records may be calculated using the respective exposure times and the appropriate relative DQE value.

For the image tube exposure made at the longer focal length, the exposure time--and therefore the input signal-to-noise ratio--is the same as that for the direct plate. On the other hand, the output signal-to-noise ratio of the image tube is better than that of the direct plate. The factor by which the signal-to-noise ratio has been improved is the square root of the relative DQE (from Eq. 1).

It should be kept in mind that increasing the focal length of a telescope necessarily reduces the field covered by the image tube. This fact will of course be important in certain applications.

The above two examples illustrate the basic significance of the relative DQE as a figure of merit. The "gain" of the image tube over the unaided plate predicted by the relative DQE can be thought of as a reduction in exposure time, an increase in final signal-to-noise ratio, or a combination of both. The manner in which the gain is utilized will depend on the manner in which the image tube is applied to a specific problem.

It is important to point out that the DQE of a photographic emulsion appears to be strongly dependent on the plate density. According to Fellgett (1958a), Jones (1958), and others, the DQE generally reaches a maximum at fairly low densities and then falls off at an increasing rate as the density (or exposure) is increased. Because of the above characteristics, there is an optimum density to which a photographic emulsion must be exposed in order to provide the maximum output signal-to-noise ratio. It is this density to which the sky background is

exposed when the faintest stellar objects are recorded by direct photography (cf. Marchant and Millikan 1965).

In Chapter II evidence was presented that the shape of the characteristic curve of a Carnegie tube photograph is essentially the same as that obtained by exposing the recording emulsion directly to the incident radiation. Further, the optimum background density for recording limiting detectable signals with the Carnegie tube was shown to be essentially the same density as that for the unaided photographic emulsion. An argument may thus be made that for the Carnegie tube the DQE versus density curve is very similar to that of the photographic material being used as the recording emulsion. This hypothesis gives added reason for comparing the DQE's of the Carnegie tube and reference emulsions at the same density.

Note that for other image tubes, particularly the type with very high gain, there may be little correspondence between the DQE-density curve of the final image tube record and that of the original recording emulsion. Evidence presented by Lynds (1968, private communication) indicates that the DQE-density function of the IIa-O emulsion is entirely changed when it is used to record the output of the English Electric Valve image tube.

Information Rate

Another figure of merit for image tubes has been proposed by Baum and is called the "information rate" (Baum et al. 1963). Baum's information rate applies specifically to photographically recorded

information and thus has been used in the past to compare image tubes and conventional photographic emulsions.

Definition of Information Rate

The rate at which information is recorded, according to this concept, is expressed in terms of the resolution, R, in line pairs per millimeter, the exposure time, t, required to obtain a prescribed density above fog by exposure to a given intensity, and the rms granularity, σ, of the photographic record. These values are determined experimentally be exposing the detectors under test to the same optical image. The dependence of the information rate on these parameters is given by Baum as

$$\text{Information Rate} \propto \frac{R^2}{\sigma^2 t} . \tag{4}$$

This figure of merit has generally been used only to compare the relative performance of devices and thus no constants of proportionality have been specified.

Granularity Term of Information Rate Formula

The argument given for the dependence of the information rate on the inverse square of the granularity is based on two assumptions. First, it is assumed that the density of the exposed plate is linearly proportional to the number of exposed grains per unit area in the emulsion. Second, it is assumed that the granularity, a variation in density, is proportional to the square root of the number of grains per unit area. These two assumptions lead to the result that, when different emulsions are exposed to the same density, the relative number

of grains per unit area is given by the inverse square of the relative granularity. In Baum's concept the information collected by a receiver is directly proportional to the number of recorded photoevents (grains) per unit area.

Unfortunately, there is considerable doubt about the validity of the two original assumptions used in deriving the granularity dependence. For example, if the assumptions were strictly true, then the granularity of a given emulsion would vary as the square root of the density. In practice, such a relationship between granularity and density is seldom observed (cf. Jones 1958; Zweig, Higgins, and MacAdam 1958). Every photographic emulsion appears to have a unique granularity-density relationship. Thus, it seems unlikely that a measurement of the relative granularities of two emulsions can accurately provide the relative number of grains per unit area.

An additional argument can be made that the granularity term in Baum's formula does not provide the correct grain number. In certain image tubes the output contains a fixed noise pattern due to nonuniformities. (An example is the mottle pattern of the Carnegie tube.) Clearly the measured granularity in a record from such a tube is caused by more than just the statistical variation in the number of grains.

Resolution Term of Information Rate Formula

The following example has been presented to explain the dependence of information rate on the square of the resolution. Assume that two image tubes differ in resolution by the factor R. In this case it would be possible with the higher resolution tube to reduce the focal

length of the telescope until the original scene was recorded with the same degree of resolution as was previously accomplished with the lower resolution image tube. The reduction in focal length would be the factor 1/R. Correspondingly, the exposure time required to obtain the same density would be reduced by the factor $1/R^2$. To properly take resolution into account in determining the information rate of a detector, Baum thus argues that the granularity and exposure time terms of Eq. 4 must be multiplied by the square of the resolution. (Note that in applications where there is no spatial information in one dimension, such as in the case of a stellar slit spectrograph, Baum states that the dependence of information rate on resolution is to only the first power.)

However, the above argument does not consider an important consequence of decreasing the exposure time and focal length for the higher resolution detector. In the final record of a given area of the scene there will be $1/R^2$ fewer grains because of the reduced area of the image. This in turn suggests that the information recorded of a given area in the scene has been decreased by $1/R^2$.

The amount that the information rate is decreased according to the above argument is exactly the amount that the information rate is increased according to Baum's argument. Clearly, when both arguments are considered, the rate at which a detector gathers information is essentially independent of its inherent resolution. This important point will be further explained in the following section.

Detector Resolution

In discussing the limited resolution of an image tube one fundamental point must be kept in mind. If an image tube is operated so that every photoelectron from the photocathode is recorded with equal significance, then increasing the telescope focal length and exposing for the same time will not change the number of recorded photons of a given element in a scene. Therefore the focal length may be chosen so that the smallest element of interest is clearly resolved. This element may then be recorded with a signal-to-noise ratio that is unaffected by the limited resolution of the detector and that is determined only by the number of photon events that can be recorded.

Note, however, that for the Carnegie tube, the assumption that every photoelectron is recorded with equal significance may not be strictly true. That is, the effective quantum efficiency (or DQE) appears to be a function of the plate density. This effect may change somewhat the signal-to-noise ratio (or information) of a previously resolved spatial detail when the focal length of the telescope is increased and the exposure time is unchanged.

Poor detector resolution can, of course, impose important limitations in certain applications. A practical example is where the telescope focal length cannot be adjusted and where, at the same time, spatial detail finer than the resolution limit of the image tube must be distinguished. In this case, a standard photographic emulsion may prove to be superior because of its higher resolution. On the other hand, there are several applications involving photography with long

focal length telescopes where the final resolution is generally limited by atmospheric seeing. Here the difference in resolution between an image tube and direct plate is completely inconsequential.

There is one additional effect of limited resolution that has not been explicitly discussed. In comparing an image tube to photographic emulsions, the low resolution and small format of the image tube means that it has a relatively small total number of resolution elements. Thus, the image tube simply cannot compete with a photographic emulsion in those applications where a very large number of resolvable elements are to be recorded. Examples of this type of application are large-field direct photography and coudé spectroscopy.

Concluding Remarks

From the discussions presented in this chapter it may be concluded that one significant figure of merit for image tubes and photographic emulsions is the detective quantum efficiency. In many situations the detective quantum efficiency permits predicting the relative output signal-to-noise from two detectors. However, it must be realized that there are several practical limitations to this figure of merit. For example, in the case of the Carnegie tube, the detective quantum efficiency does not adequately take into account the manner in which the discrete nonuniformities (patches, ripples, and mottle pattern) affect records of specific astronomical objects. Also, the light-induced background is not explicitly taken into account. Clearly

the effects of these phenomena will depend on the type of object observed , and the importance of the effects will depend on the requirements of the research problem.

Another significant performance criterion of an image tube is resolution. This characteristic often restricts the types of problems that can be solved with a specific tube. It has been pointed out that resolution should be considered separately from the detective quantum efficiency (and information rate) of a detector.

Besides the specific quality criteria that have been discussed in this chapter, there are many other characteristics of an image tube that can be of importance in certain applications. These phenomena, which have been discussed for the Carnegie tube in Chapter II, include light-induced background, geometrical distortion, sensitivity profile, etc. Each of these characteristics can be highly significant or entirely inconsequential in different applications. Clearly, to predict the success with which an image tube can be applied to a particular research problem, a considerable amount of information is required beyond that which is supplied by any single figure of merit.

CHAPTER IV

OBSERVATIONS AT THE TELESCOPE

In this chapter the results of observations made at the Steward Observatory 36-inch telescope are summarized. Several different types of observations were made in order to cover the wide variety of applications actually encountered in long exposure astronomical photography. The results serve to check the predictions that have been made from the laboratory tests and, at the same time, serve to extend the laboratory evaluation.

Observing Procedure

A photograph of the Carnegie image tube mounted and ready for observing at the Newtonian port of the 36-inch reflector is shown in Fig. 16. The procedure used at the telescope in preparing and operating the Carnegie tube may be described as follows. The image tube and voltage divider are mounted onto the double-slide plateholder with a set of heavy-duty clamps. The wires leading from the image tube are checked to be securely fastened to the voltage divider terminals, and the high voltage cable is connected to the power supply, which is placed on the observing platform. The cable is secured to the telescope tube at appropriate points to prevent it from interfering with the moving portions of the telescope and platform. A resolution target projector is installed at the photocathode end of the image tube. (Entrance to the

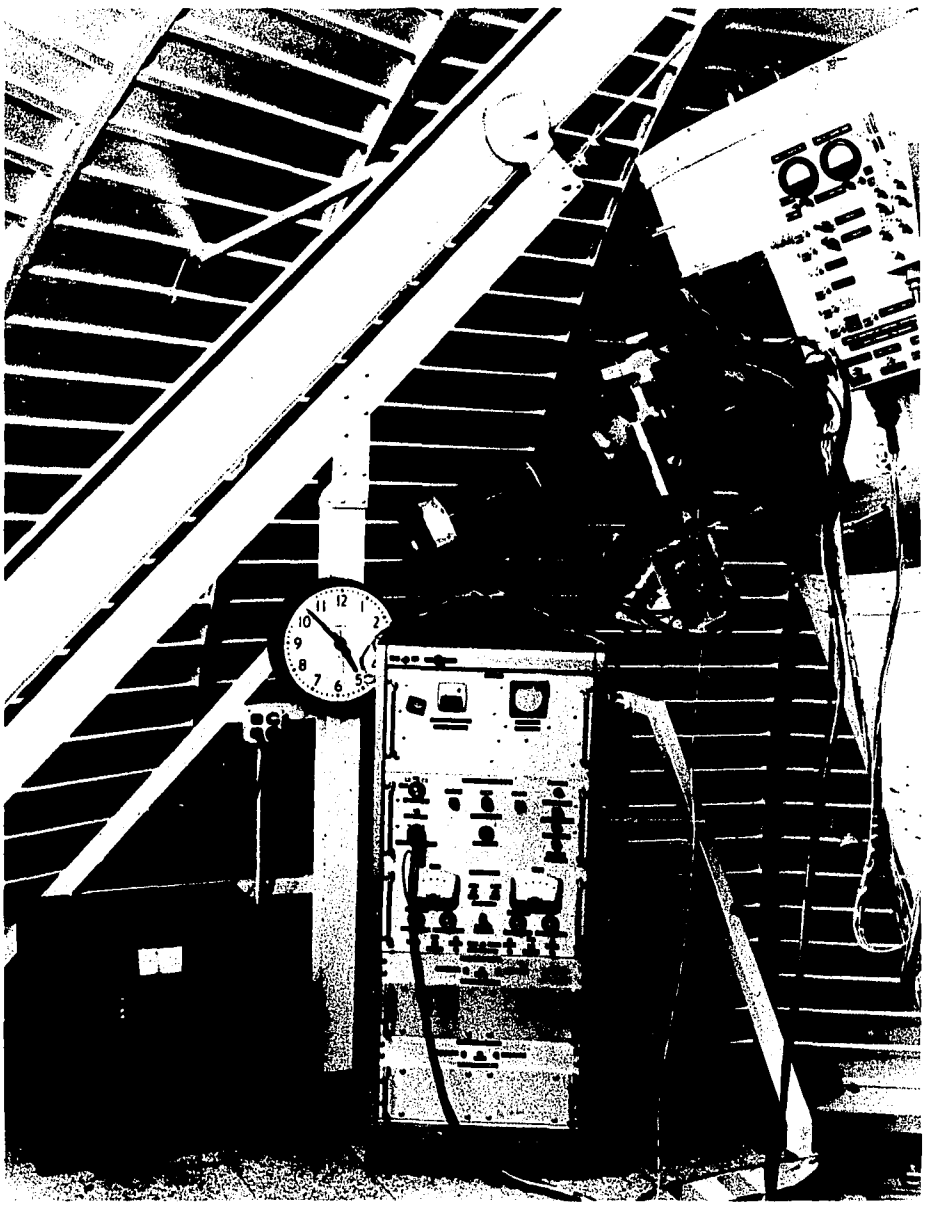

Fig. 16. Carnegie Image Tube at the Telescope.

The image tube system is shown here mounted in the automatic guider assembly at the Newtonian port of the Steward Observatory 36-inch telescope. The image tube extends left from the plateholder, and its voltage divider is attached underneath. The automatic guider photomultiplier housing extends to the right, perpendicular to the image tube. On the observing platform are the high voltage power supply for the image tube (left) and the electronics rack for the automatic guider (right).

photocathode end is provided by a door in the wall of the double-slide plateholder.) An eyepiece is installed at the relay lens output of the tube. The high voltage supply is turned on and the voltage is slowly brought to 20 kV. During this step the phosphor output is often checked for any unusual flashes or luminance by viewing with the eyepiece. Also, the voltage cables are checked for anomalous electrical discharges. Two hours warmup time is allowed with the high voltage applied in order for the system to stabilize. Then, the resolution target projector is turned on and the relay lens image is examined with the eyepiece. Optimum electronic focus of the tube is obtained by adjusting the high voltage supply while visually inspecting the tube output. The optimum voltage is normally around 21 kV. Finally, a focus plate of the resolution target may be made in order to check the focus of the relay lens. The image tube system is then ready for use.

Before observation begins all lights in the dome are turned off, the resolution target projector is removed from the image tube, and a calibration wedge projector is inserted in its place. The projector images a step wedge on the photocathode and permits exposing separate image tube plates for intensity calibration. The calibration plates are later developed together with the program plates.

Once the necessary calibration plates have been exposed, the wedge projector is removed and the telescope field is imaged onto the photocathode. (Care is taken to see that no bright star is in the field.) The appropriate filter is inserted in front of the image tube and the field is focused critically on the photocathode by visual inspection of

the relay lens image. A guide star is located for the automatic guider. Springs are inserted in the appropriate positions of the double-slide plateholder to counterbalance the weight of the image tube system. (This step, which must be done for each new field, is necessary only because the present double-slide plateholder is not designed to support the entire weight of the image tube system.) The eyepiece is removed and a plate is inserted in its place. The exposure is made by opening and closing the plate darkslide. A cover is then inserted in front of the image tube to protect the photocathode from stray illumination. The telescope is then moved to the next program field and the above procedure is repeated.

One may note from the above description that, once the Carnegie system is set up, the only practical difference between using it and an ordinary photographic plate is the added precaution of covering the photocathode when not on a program field and the precaution of avoiding bright stars.

However, there are some strange side effects caused by the image tube system on the Steward Observatory automatic guider that should be mentioned. When the guider is in the "stand-by" mode (no signal), the guider oscilloscope display often oscillates at a high frequency. This appears to be caused by radio frequencies in the image tube power supply being picked up by the guider display. Also, when the guider is in the "guide" or "find" mode, the oscilloscope display is rotated about 45°. This is caused by the action of the image tube focusing magnet on the scanning photomultiplier tube of the automatic guider. Though the

observer is initially surprised by these effects on the automatic guider, they have no detrimental effect on its performance.

Iris Photometry of Stellar Images

To investigate the stellar photometry capabilities of the Carnegie image tube, photographs were taken of a starfield for which well determined photoelectric magnitudes are available. Direct plates were also exposed to the same starfield. By appropriate selection of the exposure time the threshold magnitude was made to be nearly the same for the direct and image tube plates. A comparison may thus be made between the image tube and normal direct plates by carrying out iris photometry of the two sets of plates and by comparing the respective mean errors in the observed magnitudes of the standard stars.

The Observations

The starfield S.A. 57. The starfield chosen for observation was Selected Area 57, which has several favorable characteristics for the present study. First, good photoelectric magnitudes have been determined by Stebbins, Whitford, and Johnson (1950) to Pg = 17.46 in the International photographic system. Second, the number of stars with accurate magnitudes in this field is sufficient to yield significant comparative mean errors for the unaided and image tube plates. Third, because the distribution of stars over the magnitude interval of 12.5 to 17.5 is rather uniform, a well defined calibration curve of iris readings versus magnitude can be determined for each plate. Finally, the field covered by S.A. 57 is small enough (diameter about 15 minutes

of arc) that there should not be a large coma effect on the photographs taken with the Steward Observatory 36-inch Newtonian.

A print of one of the image tube plates of S.A. 57 appears in Fig. 17. The stars that have been used in the present iris photometry study are indentified by their Selected Area numbers. (See Tables 9 and 10 for photoelectric magnitudes and other data.)

Spectral response of photographs. The filters for the image tube and direct plate observations were selected so that the spectral responses were as close as practicable to the International photographic magnitude passband. This passband is not accurately defined, but it extends somewhat farther into the ultraviolet than the B passband of the UBV system. A comparison of the blue magitude spectral responses for the image tube, direct plate, and standard B of UBV is made in Fig. 18. The filter used with the image tube was a sandwich of a 5 mm thick Corning CS 5-61 blue filter and a 2 mm thick Corning CS 0-52 ultraviolet absorbing filter. The filter-plate combination used for the direct plate photographs was a 2 mm thick Schott GG13 filter plus a IIa-O emulsion.

The direct plates. Four direct IIa-O plates were exposed in rapid succession at the Newtonian focus to S.A. 57. The exposure time for each was 5 minutes. An examination of the processed plates revealed that they were slightly out of focus, which caused the images to be somewhat elongated, or astigmatic, because of the warped primary mirror of the 36-inch telescope. The faintest stars recorded on the plates were measured to have diameters of about 50 μm (actually

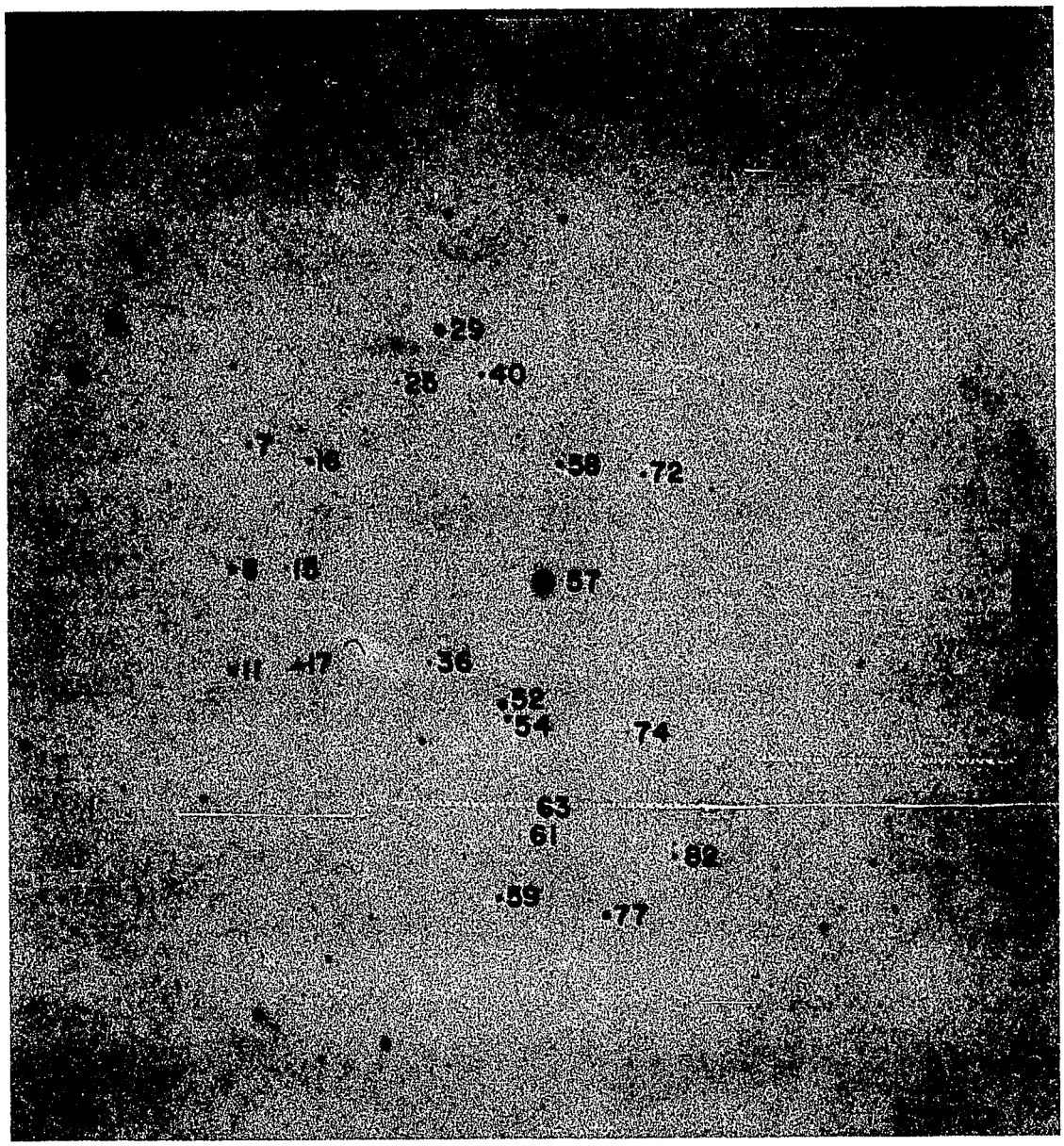

Fig. 17. 20^{S} Exposure of Selected Area 57 with Image Tube.

The faintest stars are weakly recorded on the original plate and are almost lost in this reproduction. The stars measured with an iris photometer are identified by their Selected Area identification number.

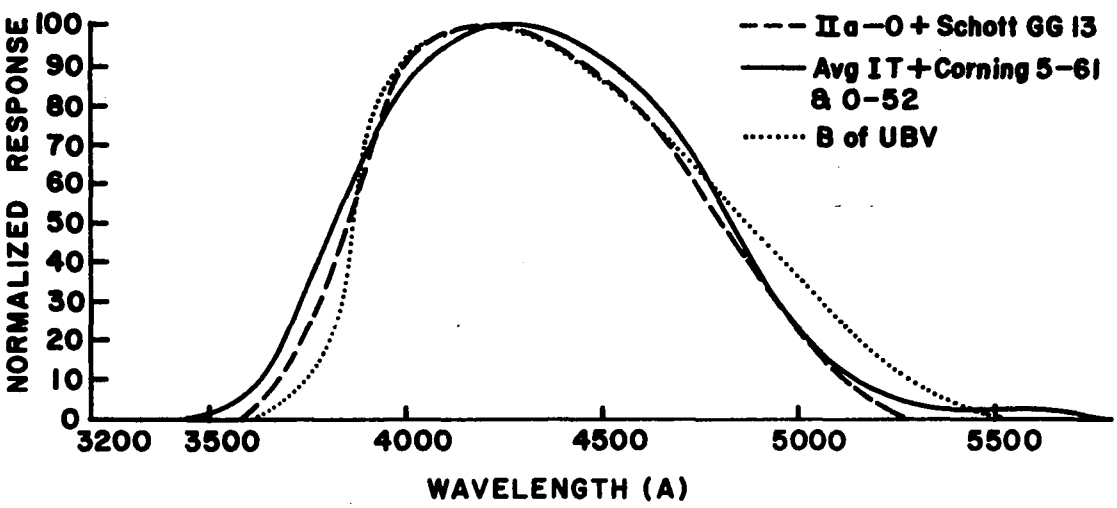

Fig. 18. Comparison of Blue Magnitude Passbands.

Shown are the blue magnitude color responses for the direct plate, image tube, and standard UBV system.

40 by 60 μm ellipses), which corresponds to 2.3 seconds of arc. (This image size represents unusually good seeing; in the author's experience, threshold star images recorded with the Steward Observatory 36-inch Newtonian during the past few years have generally been 5 seconds of arc in diameter.) The magnitude of the faintest stars on these plates is about 18.5. Thus, the plates are very suitably exposed for photometry of the desired magnitude sequence down to the faint end of magnitude 17.5.

The image tube plates. Several attempts were made to obtain direct and image tube photographs on the same night that were suitable for iris photometry. However, because of poor weather conditions and problems with the 36-inch telescope, this was not accomplished. Therefore, the image tube plates used in the present iris photometry study were not taken under the same observing conditions as the direct plates. The importance of this fact will be made clear in later sections which discuss the final iris photometry results.

Four image tube exposures, each of 20 seconds duration, were taken of S.A. 57. A IIa-O recording emulsion was used for these photographs. Because of poor seeing conditions and gusty winds, the images on the plates are rather spread out. The diameters of the threshold star images are about 140 μm, which corresponds to 6.5 seconds of arc. The average value of the threshold magnitude on these plates is around 17.8, but there is some variation from one plate to the next because of the varying image spread. The net result is that the image tube plates are effectively underexposed from 0.5 to 0.8 magnitude relative to the direct plate.

Iris Photometry Measurements

The calibration curves. The four direct and the four image tube plates were measured with the Cuffey iris photometer of Kitt Peak National Observatory, built by Astro Mechanics. Several precautions were taken in order to avoid systematic errors in the measuring procedure, and tests of repeatability indicated that the final iris measurements are reproducible to within ±0.005 magnitude. Figs. 19 and 20 show typical calibration curves obtained for a single direct and image tube plate, respectively. In these figures the iris readings of individual stars are plotted versus the Pg_{int} magnitudes of Stebbins, Whitford, and Johnson (1950). (Note that the authors have used the designation "Pg_p" to indicate that the magnitudes are photoelectrically determined.)

Check for color term and field radius term in errors. The error, δm, in a single iris photometer measurement is the difference between the known photoelectric magnitude and the magnitude predicted from the iris reading and the calibration curve. A check for a color term in the observed errors is presented in Fig. 21 for all four direct plates. Here, δm is plotted versus the photoelectrically determined color, C_p. A similar plot for the image tube plates is shown in Fig. 22. Within experimental accuracy, no color term appears to be affecting the photometry in either the direct or image tube measurements.

In Figs. 23 and 24 a check is made for a field radius effect on the observed magnitude errors. In these figures δm is plotted versus the star's distance from the center of the field. No systematic effect is observed for the image tube plates. For the direct plates, however,

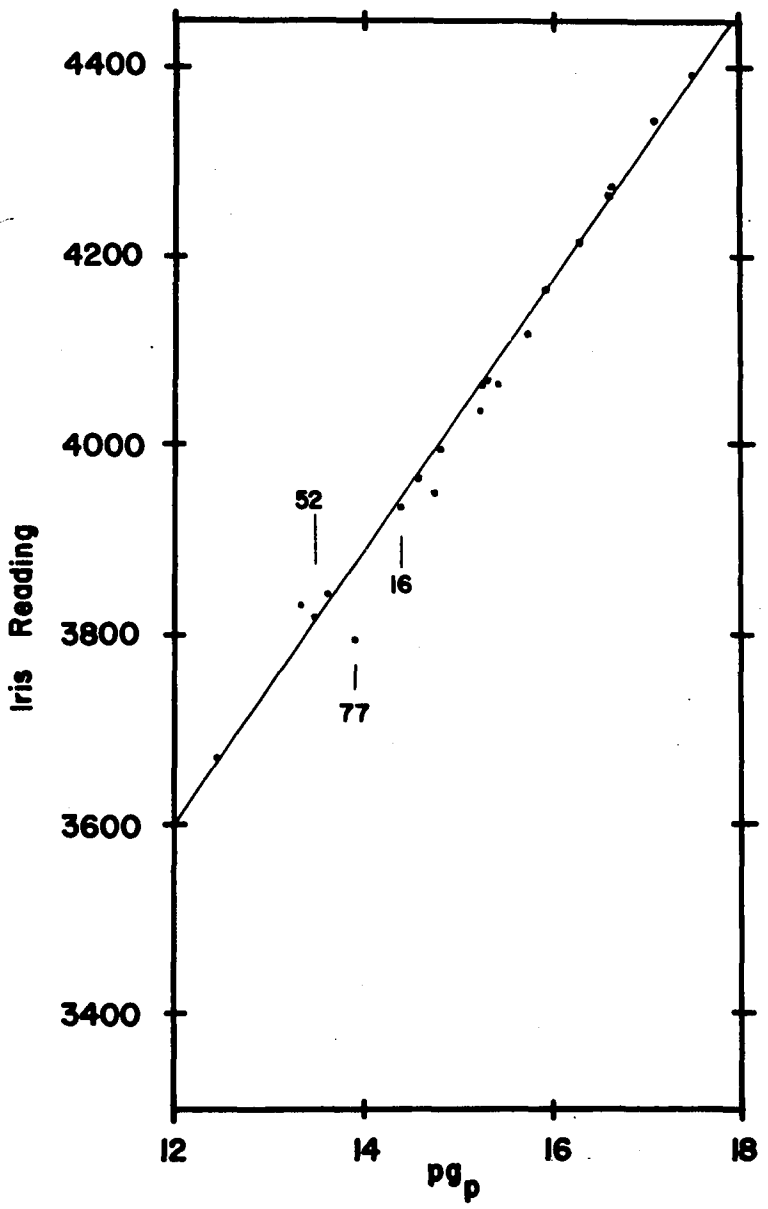

Fig. 19. Iris Photometry Calibration Curve, Direct Plate.

When all four plates are considered, the best fit to the data points is a straight line. Star 77 was found to be systematically deviant from the mean curve. Stars 52 and 16 were not. See text and Fig. 25 for details.

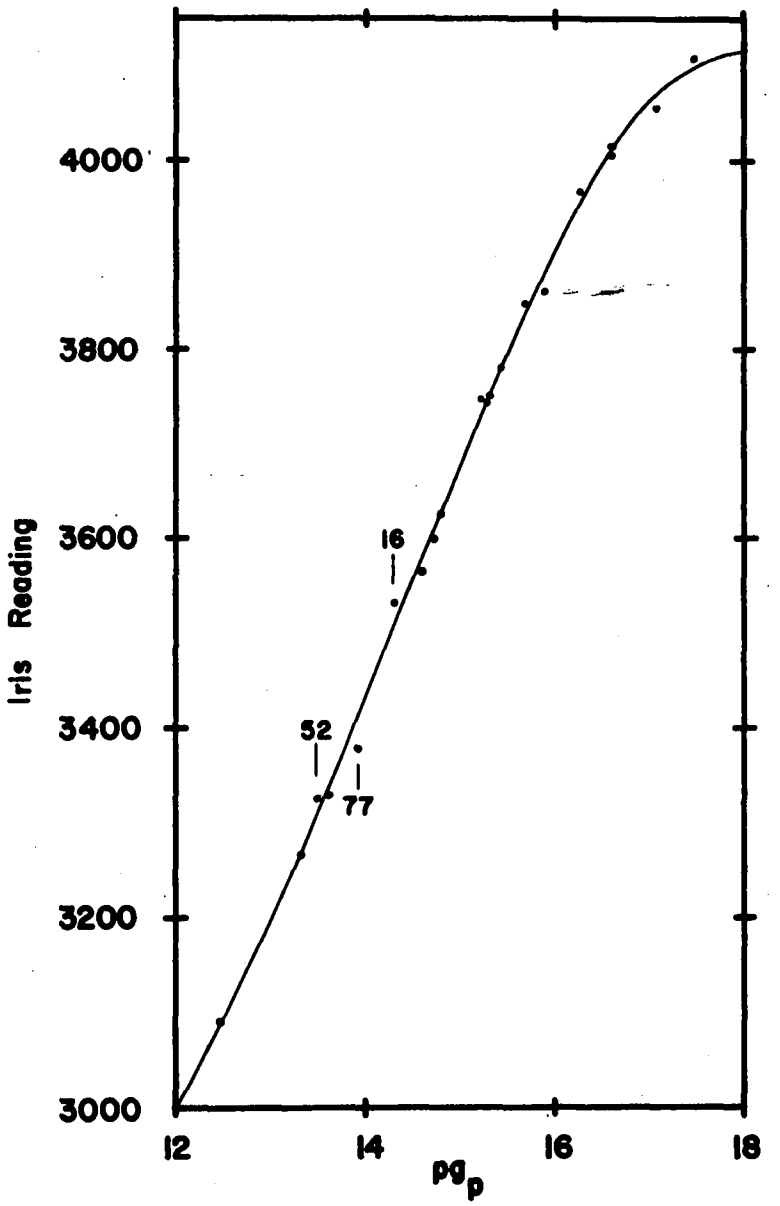

Fig. 20. Iris Photometry Calibration Curve, Image Tube Plate.

When all four plates are considered, the best fit to the data points is a straight line with curvature at both ends. The stars singled out in the direct plate data of Fig. 19 are also indicated here, although no systematic deviation was found for the image tube plates.

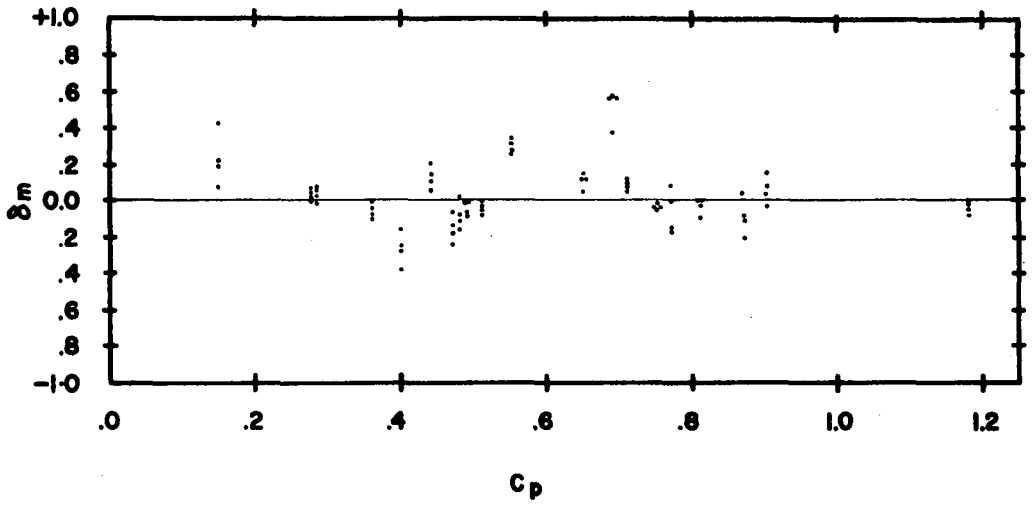

Fig. 21. δm vs. C_p for Direct Plates.

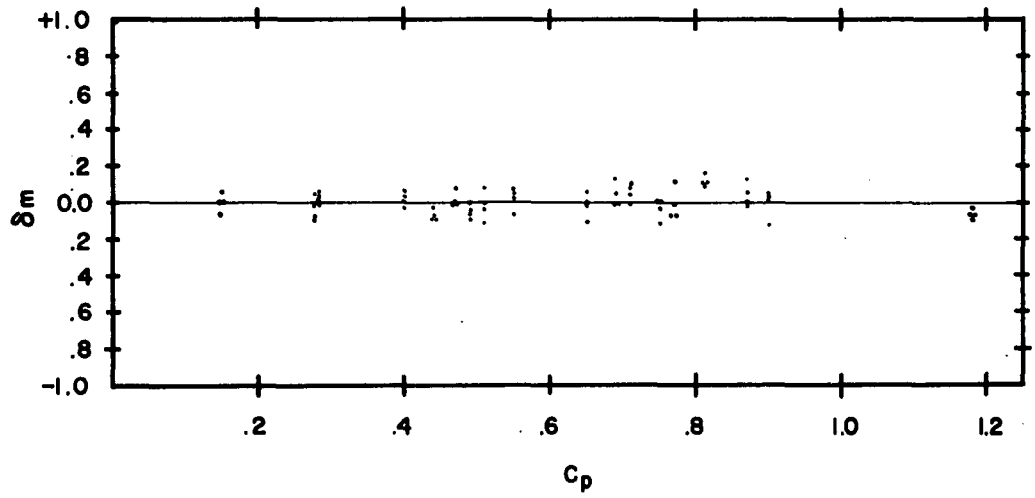

Fig. 22. δm vs. C_p for Image Tube Plates.

It is seen that within the accuracy of the observations there is no color dependence on the observed magnitude errors for either the direct or image tube plates.

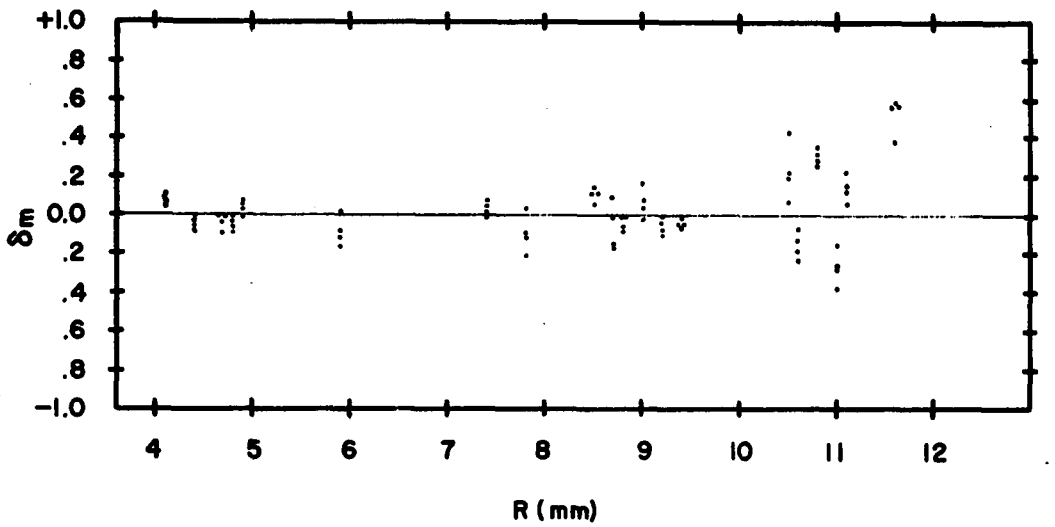

Fig. 23. δm vs. Radius for Direct Plates.

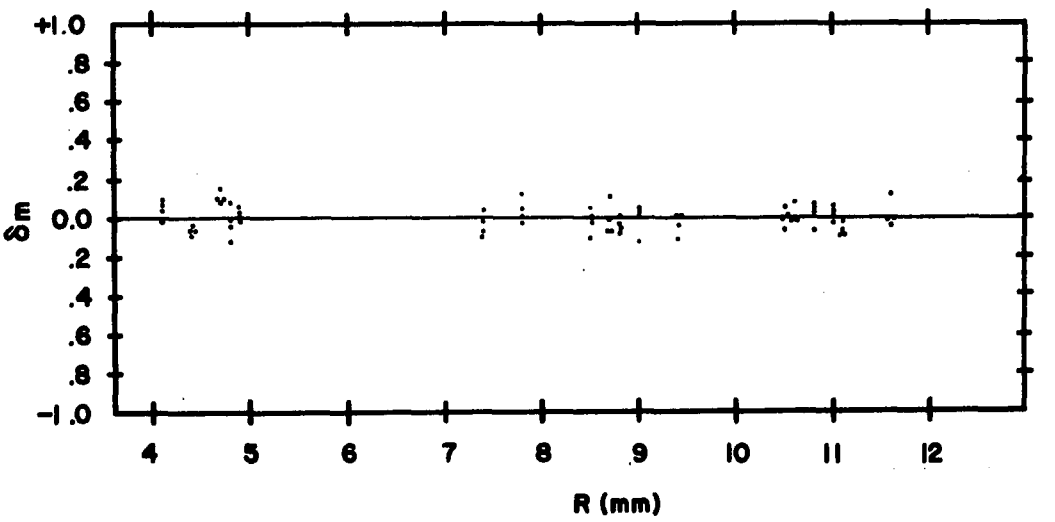

Fig. 24. δm vs. Radius for Image Tube Plates.

The general increase (both plus and minus) in the errors for the direct plate observations at the field edges is clearly demonstrated in the top figure. For the image tube plates, however, no systematic error is indicated as a function of field radius.

the size of the errors increases with field radius, although the sign of the errors (positive or negative) continues to be random. Because of the latter characteristic, no systematic corrections can be made for these errors.

The large errors for the off-axis stars on the direct plates have been found to be caused by optical aberrations of the 36-inch telescope. The reason that these errors are more significant on the direct plates than on the image tube plates may be explained as follows. The direct plates were taken under unusually good seeing conditions. The images are crisp and well defined and, as a result, the aberrations of the telescope are clearly recorded on the photographs. The image tube plates, on the other hand, were taken under poor seeing conditions. The star images are very spread out and, consequently, are hardly affected by the aberrations. On the image tube plates, the structure of the stellar images throughout the field is quite similar. An example of the differences that exist in the images of the direct and image tube records is given in Fig. 25, where individual star images from the respective plates have been photographed through a microscope.

Comparison of Mean Errors of Direct and Image Tube Plates

The data used in calculating the mean errors of the present iris photometry measurements are given in Tables 9 and 10. The columns of these tables are as follows: Column 1 gives the identification number of the stars used in S.A. 57. Column 2 gives the photoelectrically determined magnitudes of these stars, reduced to the standard International photographic magnitude, as measured by Stebbins, Whitford, and Johnson

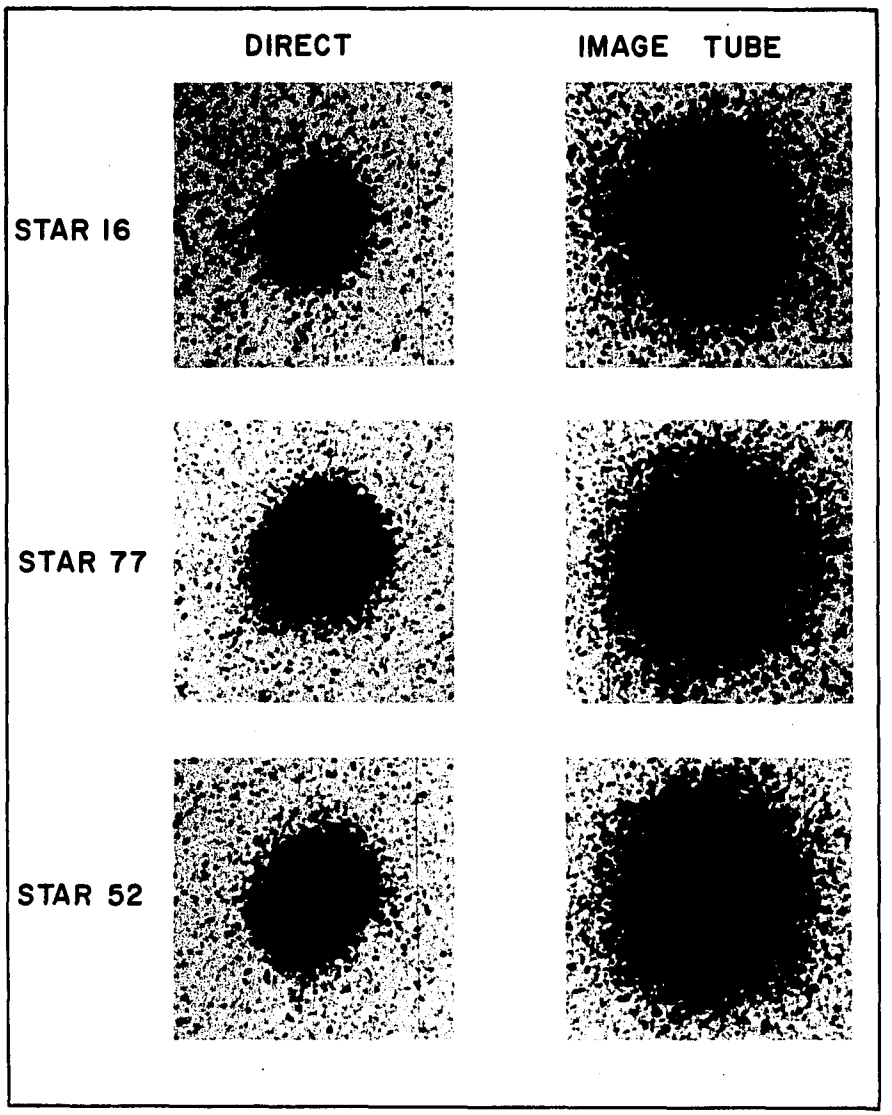

Fig. 25. Photomicrographs of Star Images.

This photograph reveals the cause for the large systematic errors in the iris photometry of the direct plates. In the direct plate images, stars 16 and 52 are slightly lined due to astigmatism, but show good iris photometry (Fig. 19). Star 77 has been spread out, due to coma, perpendicular to the astigmatism and therefore is anomalously large. This created an error of 0.57 magnitude in the iris photometry. The image tube plate, having large images due to poor seeing, shows good iris photometry for all images (Fig. 20).

Table 9

Direct Plate Iris Photometry Data

Star No.	Pg_p	C_p	R(mm)	$\delta m = Pg_p - m_{obs}$ Four separate plates				$\overline{\delta m}$	$\Delta m = \overline{\delta m} - \delta m$ Four separate plates			
57	9.04	+0.46	0.0	--	--	--	--	--	--	--	--	--
29	12.44	.75	9.4	-.02	-.05	-.06	-.05	-.046	-.03	.00	.01	.00
11	13.33	.40	11.0	-.26	-.38	-.16	-.28	-.271	-.01	.11	-.11	.01
52	13.48	1.18	4.4	-.01	-.08	-.02	-.05	-.040	-.03	.04	-.02	.01
8	13.60	.47	10.6	-.07	-.24	-.18	-.14	-.157	-.09	.08	.02	-.02
77	13.90	.69	11.6	.57	.56	.56	.37	.514	-.06	-.05	-.05	.14
16	14.38	.90	9.0	.07	-.03	.04	.15	.057	-.01	.09	.02	-.09
54	14.52	.51	4.8	.00	-.04	-.05	-.08	-.041	-.04	.00	.01	.04
59	14.72	.55	10.8	.31	.34	.27	.26	.295	-.01	-.04	.03	.04
58	14.78	.71	4.1	.05	.07	.08	.11	.078	.03	.01	.00	-.03
7	15.21	.44	11.1	.21	.05	.14	.12	.130	-.08	.08	-.01	.01
40	15.26	.28	7.4	.05	.00	.06	.01	.030	-.02	.03	-.03	.02
72	15.30	.28	4.9	.07	.06	.03	-.01	.038	-.03	-.02	.01	.05
82	15.42	.15	10.5	.21	(.42)[a]	.19	.07	.157	-.05	--	-.03	.09
25	15.69	.65	8.5	.11	.11	.05	.14	.102	-.01	-.01	.05	-.04
36	15.87	.81	4.7	-.03	-.09	.00	.00	-.030	.00	.06	-.03	-.03
15	16.24	.49	8.8	-.01	-.08	-.01	-.07	-.042	-.03	.04	-.03	.03
63	16.58	.87	7.8	-.09	.03	-.11	-.21	-.095	-.01	-.13	.01	.10
61	16.59	.77	8.7	-.01	.08	-.16	-.17	-.062	-.05	-.14	.10	.11
74	17.05	.48	5.9	-.11	.02	-.08	-.16	-.082	.03	-.10	.00	.08
17	17.46	.36	9.2	-.04	-.08	-.10	-.01	-.058	-.02	.02	.04	-.05
				$\sigma_m^* = \pm 0^m.081$					$\sigma_{\overline{\delta m}} = \pm 0^m.061$			
				$\sigma_m = \pm 0^m.181$								

a. Flaw on plate.

Table 10

Image Tube Iris Photometry Data

Star No.	Pg_p	C_p	R(mm)	$\delta m = Pg_p - m_{obs}$ Four separate plates				$\overline{\delta m}$	$\Delta m = \overline{\delta m} - \delta m$ Four separate plates			
57	9.04	+0.46	0.0	--	--	--	--	--	--	--	--	--
29	12.44	.75	9.4	-.04	.00	.00	-.12	-.040	.00	-.04	-.04	.08
11	13.33	.40	11.0	.00	.03	.05	-.03	.012	.01	-.02	-.04	.04
52	13.48	1.18	4.4	-.07	-.04	-.09	-.07	-.068	.00	-.03	.02	.00
8	13.60	.47	10.6	.01	.01	.08	.00	.025	.01	.01	-.06	.02
77	13.90	.69	11.6	.12	.04	-.01	-.01	.035	-.08	.00	.05	.05
16	14.38	.90	9.0	-.13	.03	.01	.02	-.018	.11	-.05	-.03	-.04
54	14.52	.51	4.8	.08	-.04	-.11	.00	-.018	-.10	.02	.09	-.02
59	14.72	.55	10.8	.03	.04	-.07	.05	.012	-.02	-.03	.08	-.04
58	14.78	.71	4.1	-.01	.07	.04	.09	.048	.06	-.02	.01	-.04
7	15.21	.44	11.1	-.08	-.09	-.03	-.09	-.075	.00	.01	-.05	.01
40	15.26	.28	7.4	-.02	-.08	.04	-.09	-.038	-.02	.04	-.08	.05
72	15.30	.28	4.9	-.01	.00	.05	.03	.018	.03	.02	-.03	-.01
82	15.42	.15	10.5	.00	.06	-.07	.00	-.002	.00	-.06	.07	.00
25	15.69	.65	8.5	-.02	-.11	.05	.00	-.020	.00	.09	-.07	-.02
36	15.87	.81	4.7	.10	.09	.15	.10	.110	.01	.02	-.04	.01
15	16.24	.49	8.8	-.05	-.08	.00	-.06	-.048	.00	.03	-.05	.01
63	16.58	.87	7.8	.02	.00	.05	.12	.048	.03	.05	.00	-.07
61	16.59	.77	8.7	-.01	.11	-.08	-.08	-.015	-.01	-.09	.06	.06
74	17.05	.48	5.9	--	--	--	--	--	--	--	--	--
17	17.46	.36	9.2	--	--	--	--	--	--	--	--	--
				$\sigma_m = \pm 0^m.063$					$\sigma_{\overline{\delta m}} = \pm 0^m.046$			

(1950). Column 3 lists the photographic color index on the International System determined photoelectrically by the same authors. Column 4 gives the distance, in millimeters, a star is from the central star as measured on the Steward Observatory plates. Column 5 lists the four values of δm obtained from the four plates, where δm is the difference between the known magnitude and that predicted from the iris reading and calibration curve. Column 6 gives $\overline{\delta m}$, the average of the four individual measurements of δm. Column 7 gives four values of Δm, where Δm is the difference between δm and $\overline{\delta m}$.

Note that the purpose of exposing four similar plates in the present investigation is to provide a large number of measurements such that a significant mean error is determined. Thus, in calculating the mean error values, the four plates have been considered as if they were observations of four different magnitude sequences, and not as four observations of the same sequence.

Mean error of a single magnitude observation. The mean error of a single magnitude observation, calculated from the δm values, is listed at the bottom of column 5 in Tables 9 and 10 for the direct and image tube plates, respectively. In the case of the direct plates, two values appear. For the larger value, all the observations were used. For the smaller value, the observations of the six stars that occur at a field radius of greater than 10 mm were removed from the calculations. This was done in order to reduce the effects of the off-axis aberrations on the mean error value. For the image tube plates, the data for the two faintest stars were removed from the calculations because the stars were too weakly exposed.

The value of the mean error calculated from all the direct plate observations is seen to be unusually large (±0.181 magnitude). Even when the stars clearly affected by off-axis aberrations are removed from the calculations, the mean error (±0.081 magnitude) is somewhat larger than that of normal photographic iris photometry. This rather poor accuracy of the direct plates, it has been concluded, is most likely caused by the unusual aberrations that occur throughout the entire field of the 36-inch telescope. Because the plates were taken under very good seeing conditions, the effects of the aberrations are particularly severe.

The mean error of the image tube observations (±0.063 magnitude) is a reasonably acceptable value for photographic iris photometry. It is understood, of course, that the telescope aberrations have not severely affected the image tube photometry because the plates were taken under poor seeing conditions. The important conclusion, however, is that the mean error is small enough to indicate that accurate iris photometry may be carried out with the Carnegie tube.

Internal mean error. An "internal mean error" may be calculated for both the direct and image tube set of plates by using the values of Δm, instead of δm, for the mean error calculation. The numerical result is, in effect, the mean error of a single determination of $\overline{\delta m}$ and, thus, it is designated in Tables 9 and 10 as $\sigma_{\overline{\delta m}}$. An important characteristic of the internal mean error is that it is independent of the sources of systematic error previously discussed. Because of this property, the internal mean error provides a useful check for the existence of systematic effects on the iris photometry measurements. (It is assumed, of course,

that the obvious systematic errors discovered in the earlier sections have already been removed from the measurements.)

If there were no systematic effects at all on the iris photometry magnitudes, the internal mean error, $\sigma_{\overline{\delta m}}$, would be the same as the mean error of a single magnitude observation, σ_m. For both the direct and image tube set of plates, however, $\sigma_{\overline{\delta m}}$ is somewhat smaller than σ_m. This indicates that there are some systematic errors in the photometry, although they are fairly small. The most likely sources for such errors are: (1) errors in the standard magnitudes (note that the mean error of the photoelectric magnitudes measured by Stebbins, Whitford, and Johnson is ±0.018 magnitude), (2) field and instrument errors that are not quite revealed by the present number of observations, and (3) color term errors that also are not revealed by the present data.

Effect of Carnegie Tube Mottle Pattern on Iris Photometry

The four plates listed in Table 10 were exposed so that they form two specific pairs. One pair was taken while the image tube was in one particular position angle. Then the image tube was rotated about its axis to a new position angle and the second pair of plates was exposed. In column 5 of Table 10, the plates that were taken at the same position angle are the first and third entries for one pair and the second and fourth entries for the other pair. This "pairing" of the image tube plates provides a method of determining the effects of the mottled sensitivity pattern on iris photometry.

Note that, for any two plates represented in column 5, a mean value of δm and a deviation from the mean may be calculated for each

observed star. By using all the stars, a standard deviation in δm may be determined. If only the "paired" plates (those taken at the same position angle) are used in calculating the standard deviation, then the resulting value represents mainly the intrinsic scatter in the photographic process. However, if only "nonpaired" plates (plates taken at different position angles) are used in calculating the standard deviation, then the standard deviation is additionally affected by the errors produced by the mottle pattern of the image tube.

The two standard deviations described above have been calculated from the "paired" and "nonpaired" Carnegie tube plates. The resulting values, ±0.038 and ±0.039 magnitude, respectively, are found to be the same within the accuracy of the experiment. From this result it is concluded that the systematic errors introduced by the Carnegie tube mottle pattern are essentially lost in the presence of the appreciably larger intrinsic scatter of the photographic iris photometry process. This conclusion agrees well with the predictions made in Chapter II based on the laboratory experiments.

It should be pointed out that, even if the mottle pattern did produce a recognizable error in iris photometry measurements, the significance of the effect could be greatly reduced by rotating the image tube between exposures of a given starfield.

Iris Photometry of Stellar Images: Concluding Remarks

It is concluded from the present study that the Carnegie image tube is clearly useful for quantitative stellar iris photometry and that stellar magnitudes can be determined with an accuracy similar to that of normal direct plate methods. It may thus be argued that the appropriate

figure of gain for the image tube over an unaided plate, in this particular application, is measured as the relative exposure time of the direct and image tube records. Note that the relative exposure time is essentially equal to the relative detective quantum efficiency, which has been given for various spectral regions in Table 8 of Chapter III.

One particular phenomenon of the Carnegie tube that has not been evaluated in the present iris photometry study is the effect of light-induced background on iris photometry. Several plates taken at the telescope, however, tend to confirm the laboratory prediction that a detectable error will occur in the iris photometry of the faintest stars if a bright star, more than 12 magnitudes brighter than the faintest stars, is in the field. It should be pointed out, of course, that the detrimental effects of bright objects can often be avoided by masking the objects from the photocathode.

Areas of research in which image tube photometry should find particular application are studies involving relatively small fields, such as star clusters and galaxies, where the limited field of the image tube is not a disadvantage. Variable star and blue object surveys are examples of this type of program. Another possibility that exists for image tube photometry, but that is not generally available to direct plate methods because of lack of sensitivity, is photometry of objects through narrow passband filters. Surveys for objects with peculiar spectral features may be able to be made in this way. For example, Wolf-Rayet stars may perhaps be distinguished from surrounding stars by taking paired exposures with filters centered on, and off, one of the broad emission bands, such as the 4686 A He II feature.

Sky-Limited Stellar Photography

In this section the performance of the Carnegie tube is compared to that of unaided plates in the application of sky-limited photography of stellar images. Both direct and image tube plates have been exposed in such a way that the photographic density of the sky background is at its optimum value, which assures that the faintest stars possible to detect have been recorded with the respective plates. (See Table 6 of Chapter II for optimum densities of the various emulsions.)

Globular Cluster M13

The observations. Sky-limited photographs of the globular cluster M13, taken at the 36-inch Newtonian focus, were made on the same night with both the image tube and a IIa-O direct plate. Blue magnitude pass-bands were provided for both systems by using the same filters as described in the iris photometry section. By appropriate selection of zenith distances, the difference in limiting magnitude for the several exposures due to the difference in night-sky radiation was less than 0.2 magnitude. The atmospheric conditions were very uniform throughout the night and the seeing was average.

For the image tube plates the nucleus of the cluster was masked off in order to avoid excessive light-induced background. Exposures were made with both IIa-O and baked IIIa-J recording emulsions. In addition to the optimum sky-limited exposures, two additional image tube photographs were made with IIa-O recording emulsions. One was exposed about 40 percent longer than the optimum exposure time in order to demonstrate the effect of overexposure. Another was exposed for the same

duration as the optimally exposed plate, only with the cluster nucleus unmasked. This was done in order to determine the significance of the light-induced background arising from the nucleus of the cluster.

Finally, an exposure of M13 was made with the image tube at the Cassegrain focus of the 36-inch reflector. (The Cassegrain focal length of the Steward Observatory telescope is three times the Newtonian focal length.) The photograph was taken on a different night than that of the direct and image tube plates described above, but the observing conditions were similar.

Comparison of the photographs. Prints representative of the plates taken in this study are shown in Figs. 26 through 29. The telescope focus (Newtonian or Cassegrain) and the respective exposure times are given in the captions of these figures. A comparison of the direct IIa-O plate (Fig. 26) and the image tube IIa-O plate (Fig. 27) reveals that the image tube record is adversely affected by the ripples and mottle pattern of the Carnegie tube. The nonuniformities of the image tube stand out even more vividly on the IIIa-J exposure (Fig. 28), although the star images are also brought out more clearly. The significance of the mottle pattern is considerably reduced when the image tube is used at a longer focal length, as is evidenced by the Cassegrain photograph in Fig. 29. In fact, the sky background in this image tube record is the least noisy of all the M13 exposures.

To the eye, the resolution of the most tightly grouped stars is slightly different on the four plates. Considering only the Newtonian photographs the resolution increases according to the following sequence:

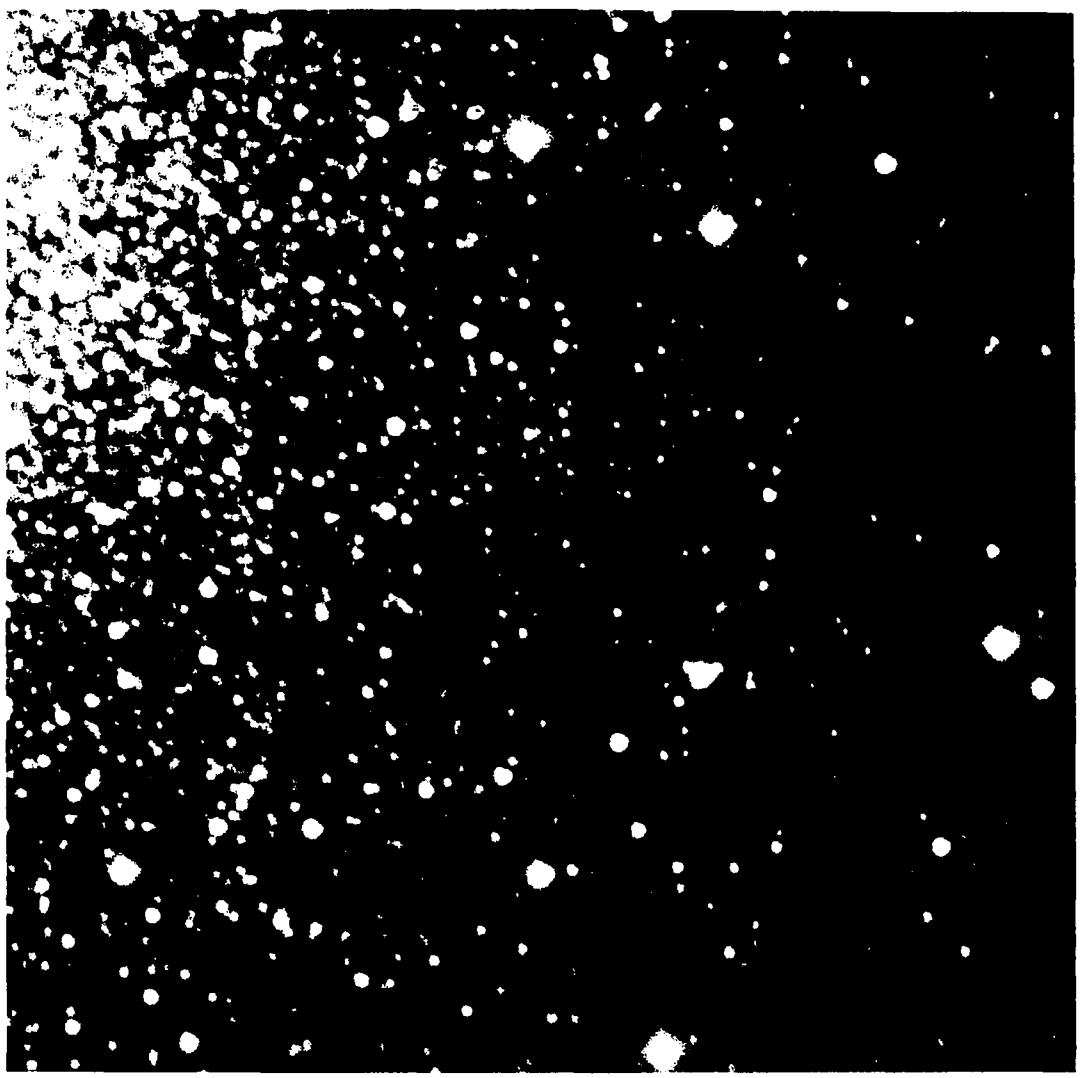

Fig. 26. Sky-Limited Photograph of Region in M13; Direct IIa-O Plate, 4^h30^m Exposure, Newtonian Focus.

A comparison of this photograph with the image tube photographs in Figs. 27 and 28 shows that the image tube records are adversely affected by the mottle pattern of the Carnegie tube. Fig. 29 shows that the significance of the mottle pattern is considerably reduced at the longer focal length of the Cassegrain focus. The limiting magnitudes of these plates are given in Figs. 30 and 31.

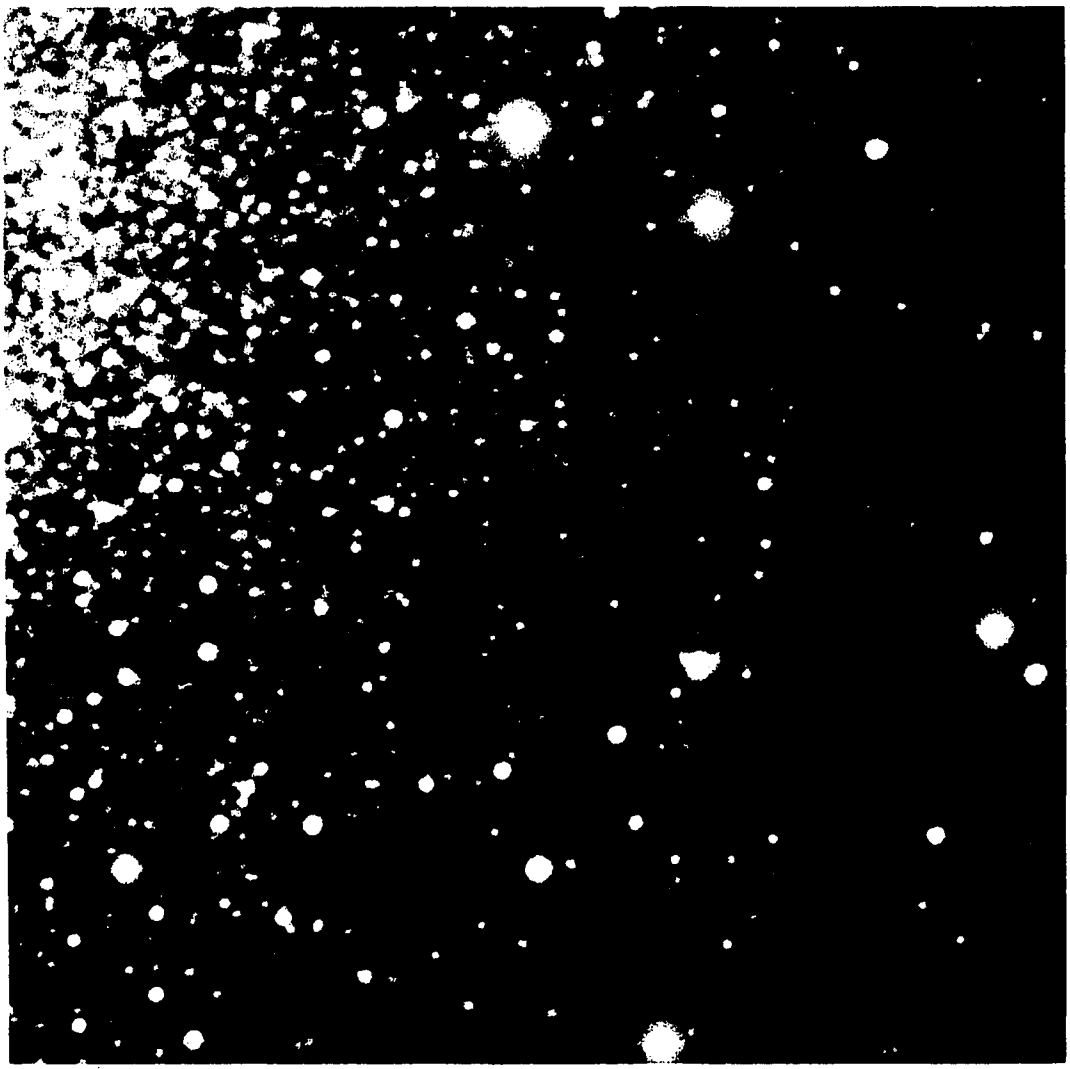

Fig. 27. Sky-Limited Photograph of Region in M13; Image Tube IIa-O Plate, $12^{m}30^{s}$ Exposure, Newtonian Focus.

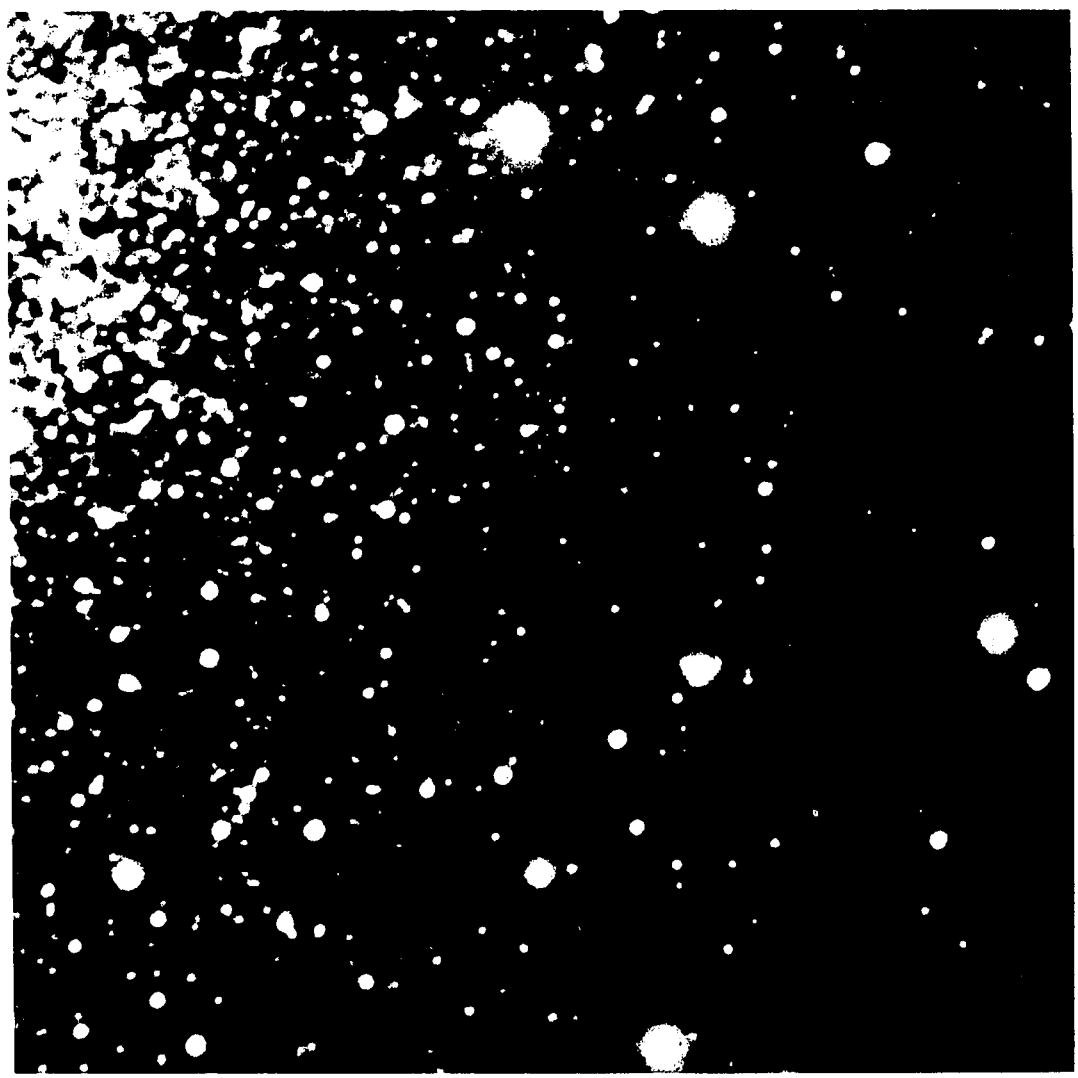

Fig. 28. Sky-Limited Photograph of Region in M13; Image Tube Baked IIIa-J Plate, 20^{m} Exposure, Newtonian Focus.

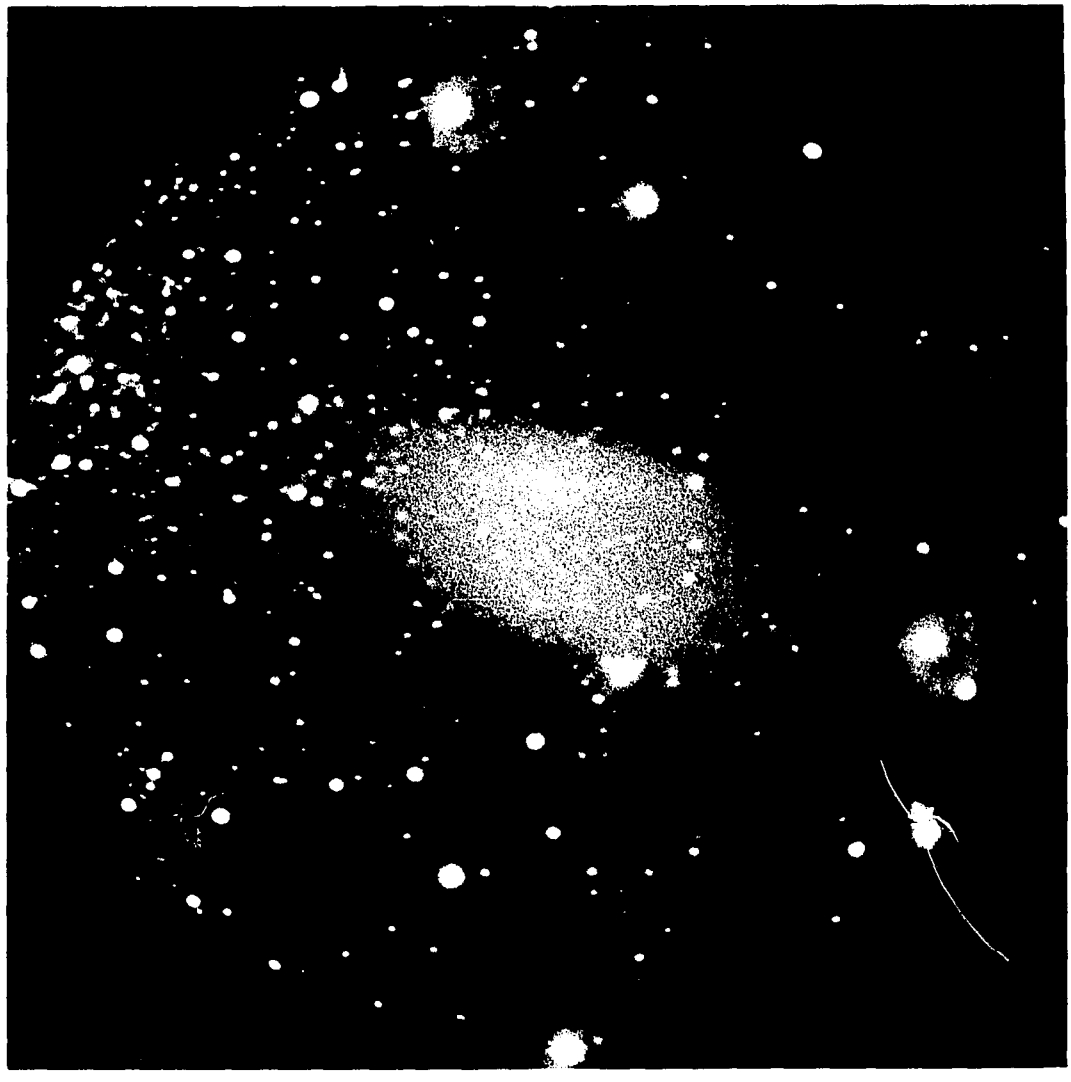

Fig. 29. Sky-Limited Photograph of Region in M13; Image Tube IIa-O Plate, 2^h30^m Exposure, Cassegrain Focus.

The bright fog in the center of the plate is due to light from the cluster nucleus being scattered into the focal plane because of inadequate sky baffling. The out-of-focus images around the bright stars are caused by reflections from the photocathode and filter.

image tube IIa-O plate, direct IIa-O plate, and image tube IIIa-J plate. The Cassegrain photograph, taken with the image tube and a IIa-O recording emulsion, shows the highest resolution of all the plates. This, of course, is due mostly to the greater image scale of the Cassegrain focus.

Limiting magnitude of the photographs. The magnitudes of the threshold star images on the several M13 photographs have been determined by comparing the present records with an identification chart and magnitude observations published by Baum, Hiltner, Johnson, and Sandage (1959). In order to make the limiting magnitude determination as accurate as possible, an average of 60 stars were checked for their presence or absence on each plate. Graphs were then made of the resulting data from each plate by plotting the percentage of stars detected versus magnitude. Fig. 30 gives a typical example of the data presented in this manner. The mean curve representing the data points is also indicated. A comparison of the sky-limited magnitudes of the direct plate and the various image tube plates is made in Fig. 31, where the mean curves of all the plates are shown. Fig. 31 also lists the exposure time of each of the plates.

It is seen by studying the results given in this figure that, when a direct IIa-O plate and an image tube IIa-O plate are exposed at the same telescope focus, the limiting magnitude of the image tube record is about 0.9 magnitude less than that of the direct plate. When a baked IIIa-J recording emulsion is used with the image tube, however, about 0.5 magnitude of the loss may be gained back. This 0.5 magnitude gain of the IIIa-J emulsion is in excellent agreement with that reported

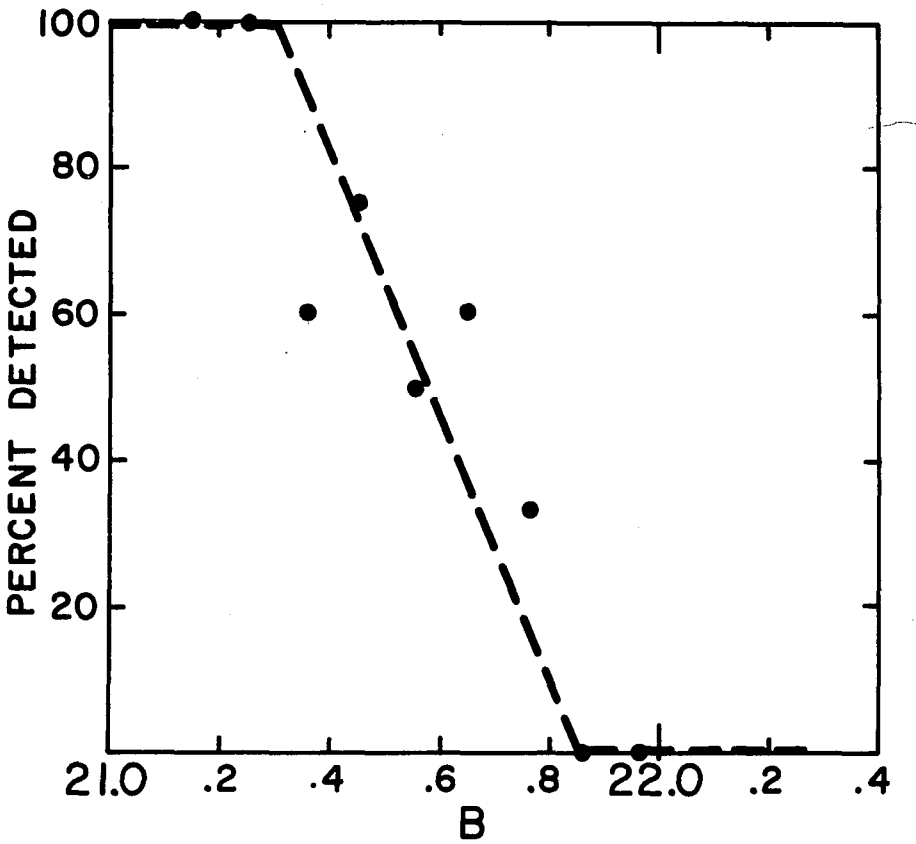

Fig. 30. Data Points and Mean Curve Showing Percent of Known Stars Detected for Sky-Limited Image Tube Cassegrain Plate.

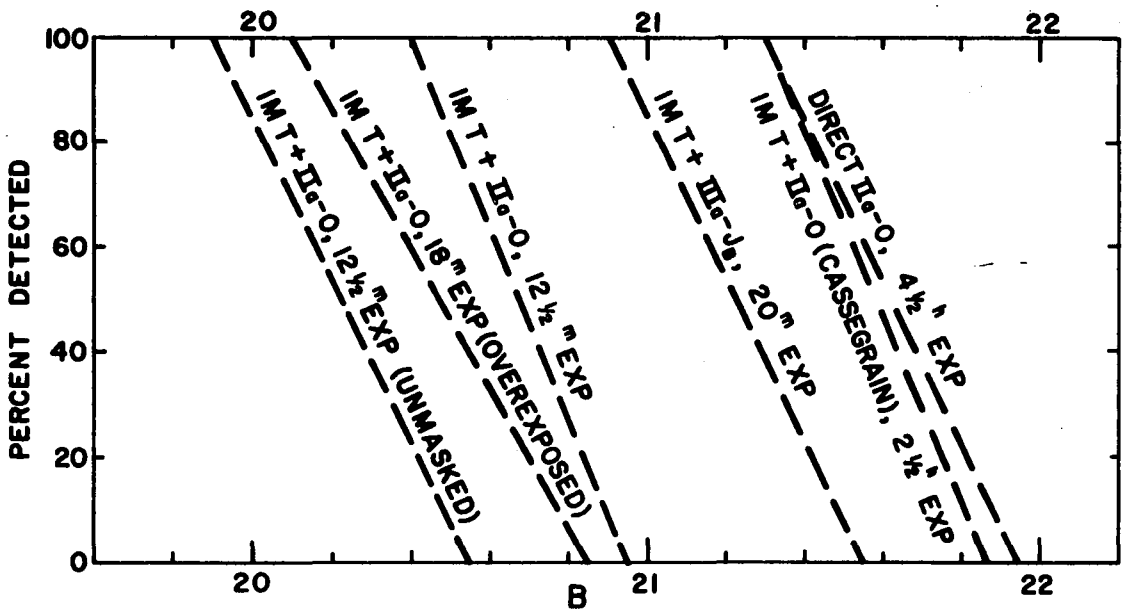

Fig. 31. Comparison of Sky-Limited Magnitudes for Image Tube and Direct Plates.

All of the above plates were exposed at the f/5 Newtonian focus, except for one image tube plate which was exposed at the f/15 Cassegrain focus. The loss of sky-limited capability is evident for the image tube plates exposed at the same focus as the direct plate. The effects of overexposure of an image tube (or direct plate) are demonstrated. For all but one of the image tube exposures the nucleus of the globular cluster was masked from the photocathode. The effect of the additional light-induced background created by the cluster nucleus is demonstrated by the unmasked plate.

by Marchant and Millikan (1965) in their paper discussing the theoretical basis for development of the new IIIa-J emulsion. The numerical results for both the IIa-O and baked IIIa-J emulsions are also in good agreement with the laboratory predictions of Chapter II.

The detrimental effect of the light-induced background caused by the cluster nucleus is clearly evident in Fig. 31, where the unmasked image tube record is shown to experience an additional 0.5 magnitude loss. Microphotometer measurements of this plate indicate that the background intensity was effectively increased 60 percent because of the light-induced background from the cluster nucleus. This, in turn, accounts for the loss in limiting magnitude (cf. Baum 1955).

The effect of increasing the exposure of a photographic emulsion beyond the optimum value is also evident in Fig. 31, where a 0.2 magnitude loss in limiting magnitude is shown for the overexposed image tube plate. A similar effect, of course, would occur for an unaided photograph.

Finally, it is noted that, when an image tube IIa-O plate is exposed at the Cassegrain focus, the limiting magnitude is nearly the same as that of a direct IIa-O plate exposed at the Newtonian focus. This is accomplished with a reduced exposure time of almost a factor of 2 compared to the direct plate. It should be pointed out that because the Cassegrain focus of the Steward Observatory 36-inch is not fully sky baffled, scattered light from the globular cluster nucleus and direct radiation from the night sky were incident on the image tube photocathode during the present exposure. Considering this fact, it is concluded that a Cassegrain image tube photograph would normally reach a fainter limiting

magnitude than a Newtonian direct plate. An argument can be made, in fact, that the limiting magnitude should be at least 0.3 magnitude fainter than that of the present record.

S.A. 47; Near-Infrared Photography

Two plates that were taken in order to evaluate the usefulness of the Carnegie tube in application to near-infrared photography are shown in Fig. 32. The upper photograph was taken through a blue filter (as previously described) and the lower photograph was taken through a Schott RG10 filter. The wavelength sensitivity of the latter filter-image tube combination is characterized by a peak near 7400 A and a halfwidth of about 700 A. A baked IIIa-J recording emulsion was used for the two exposures, and both plates were exposed to the sky limit.

The starfield recorded on these plates is Selected Area 47, a region that is obscured by dark interstellar clouds. The red and blue prints of the National Geographic Society-Palomar Observatory *Sky Atlas* show that the dustclouds in S.A. 47 are more transparent to red radiation than they are to blue radiation, as evidenced by the increased number of stars appearing on the red print. The infrared plate shown in Fig. 32 was taken in order to determine if the Carnegie tube could provide detection of reddened stars beyond those observed on the red Sky Survey photograph. A positive result would suggest that the image tube could be used to extend the infrared measurements of dark cloud obscuration.

A comparison of the plates in Fig. 32 with the Sky Survey photographs, however, shows that the limiting magnitude of the red Sky Survey photograph is about 0.2 magnitude fainter than that of the infrared image

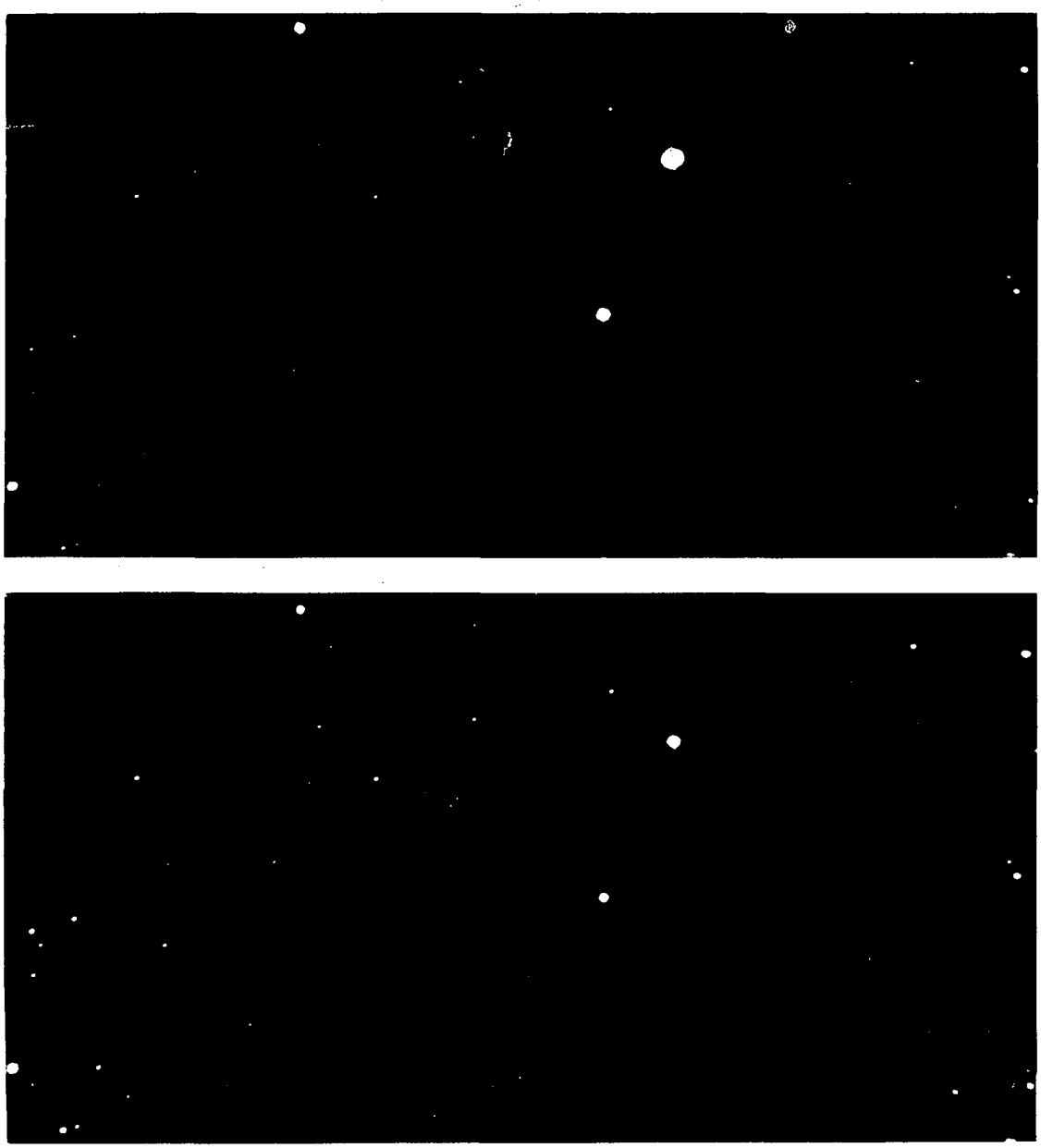

Fig. 32. Comparison of Sky-Limited 11^m Blue and 1^h30^m Near-Infrared Photographs of Selected Area 47.

The increased transparency in the near-infrared of the dark cloud in this area is evidenced by the additional stars appearing on the infrared (lower) plate.

tube plate. The limiting magnitude of the respective blue photographs, on the other hand, is essentially the same.

It is concluded from the above results that the Carnegie tube cannot significantly extend the application of direct photography into the infrared. (This conclusion, however, does not necessarily apply to image tubes with an S-1, infrared sensitive photocathode.) Also, the present photographs serve to point out that the Carnegie tube experiences an additional loss in limiting magnitude, compared to that experienced in the blue spectral region, when it is used in the near infrared. This small effect may be explained as a result of the color dependence of the light-induced background of the Carnegie tube.

Sky-Limited Stellar Photography: Concluding Remarks

One significant conclusion obtained from the present study is that, in order to record the same sky-limited magnitude on a Carnegie tube plate and a direct plate, the image tube record must be made with a longer focal length telescope. The reduction of exposure time permitted by the image tube under this condition is estimated to be about 2 or 3. For certain areas of research this relative exposure time may often be the significant comparative figure of merit of the image tube and an unaided plate. However, in applications where the greater scale of the image tube photograph is important, the figure of merit of the image tube may be better than that calculated from only the exposure time ratio. An example of such an application is the photometry of faint stars in the crowded field of a globular cluster.

When an image tube plate and a direct plate are exposed at the same telescope focus, it has been demonstrated that the Carnegie tube cannot reach as faint a limiting magnitude as the direct plate. This fact may be important in certain astronomical investigations. However, the Carnegie tube can still provide useful observations of relatively faint stars and can do so in less exposure time than is required by a direct plate. To reach a specified faint threshold magnitude, the relative exposure time may be estimated to be typically around 5, although the exact figure will depend on how close to the sky limit the image tube plate has been exposed.

It should be pointed out that the results of the present study cannot be accurately predicted from the detective quantum efficiency concept. Additional characteristics of the image tube besides those considered in the calculation of the detective quantum efficiency are important in sky-limited stellar photography. Two particularly important phenomena in the Carnegie tube are the light-induced background and the mottle pattern. The light-induced background arising from the night-sky radiation alone has been calculated to produce a 0.3 magnitude reduction in the limiting magnitude of a Carnegie tube record. The mottle pattern, as evidenced by the present starfield photographs, also reduces the limiting magnitude by a significant amount. Although the detective quantum efficiency takes into account the rms noise produced by the mottle pattern, the effect of the mottle pattern on the detectability of faint star images appears to be significantly larger than the rms value.

Photography of Extended Objects

The performance of the Carnegie tube in recording extended objects and a comparison to normal photographic techniques are reported in this section. The results will clearly point out that additional problems besides those encountered in recording stellar images can often be important in extended object photography.

Spiral Galaxy M51

For the present study, photographs of the spiral galaxy M51 were taken at the Newtonian focus on a direct IIa-O plate and an image tube IIa-O plate. The exposures were selected so that the sky background densities were as identical as possible. The background densities were also fairly high, though not at the sky-limited value. In addition to these plates, a baked IIIa-J recording emulsion was used with the image tube to make a sky-limited photograph. Finally, an exposure was made with the image tube at the Cassegrain focus so that the sky density matched that of the direct and image tube Newtonian IIa-O plates. The recording emulsion used here was again a IIa-O. Blue passband filters were used for all the exposures. Prints of the four plates are presented in Figs. 33 through 36 and the exposure times are given in the captions.

Comparison of the direct and image tube IIa-O plates taken at the Newtonian focus (Figs. 33 and 34, respectively) shows that the direct plate is somewhat better in several respects. The very tenuous luminosity surrounding the outer spiral arms and the satellite of M51 is reasonably well detected on the direct plate but is almost lost on the image tube record. Comparing the rendition of the spiral arms, the direct

Fig. 33. Photograph of M51; Direct IIa-O Plate, 1^h30^m Exposure, Newtonian Focus.

This direct plate and the two image tube plates of Figs. 34 and 35 were exposed to the same sky density. Comparing the unaided and image tube exposures obtained at the Newtonian focus, the noise produced by the image tube mottle pattern is seen to lower the detection of the low contrast features of extended objects. However, it is seen in Fig. 35 that an image tube photograph exposed at the Cassegrain focus is not severely affected by the mottle pattern and is generally superior to an unaided photograph obtained at the Newtonian focus. The sky-limited image tube photograph in Fig. 36 shows the faintest luminosity of the object more clearly than any of the other plates. The baked IIIa-J record also reveals the sensitivity ripples of the image tube.

Fig. 34. Photograph of M51; Image Tube IIa-O Plate, 3^m10^s Exposure, Newtonian Focus.

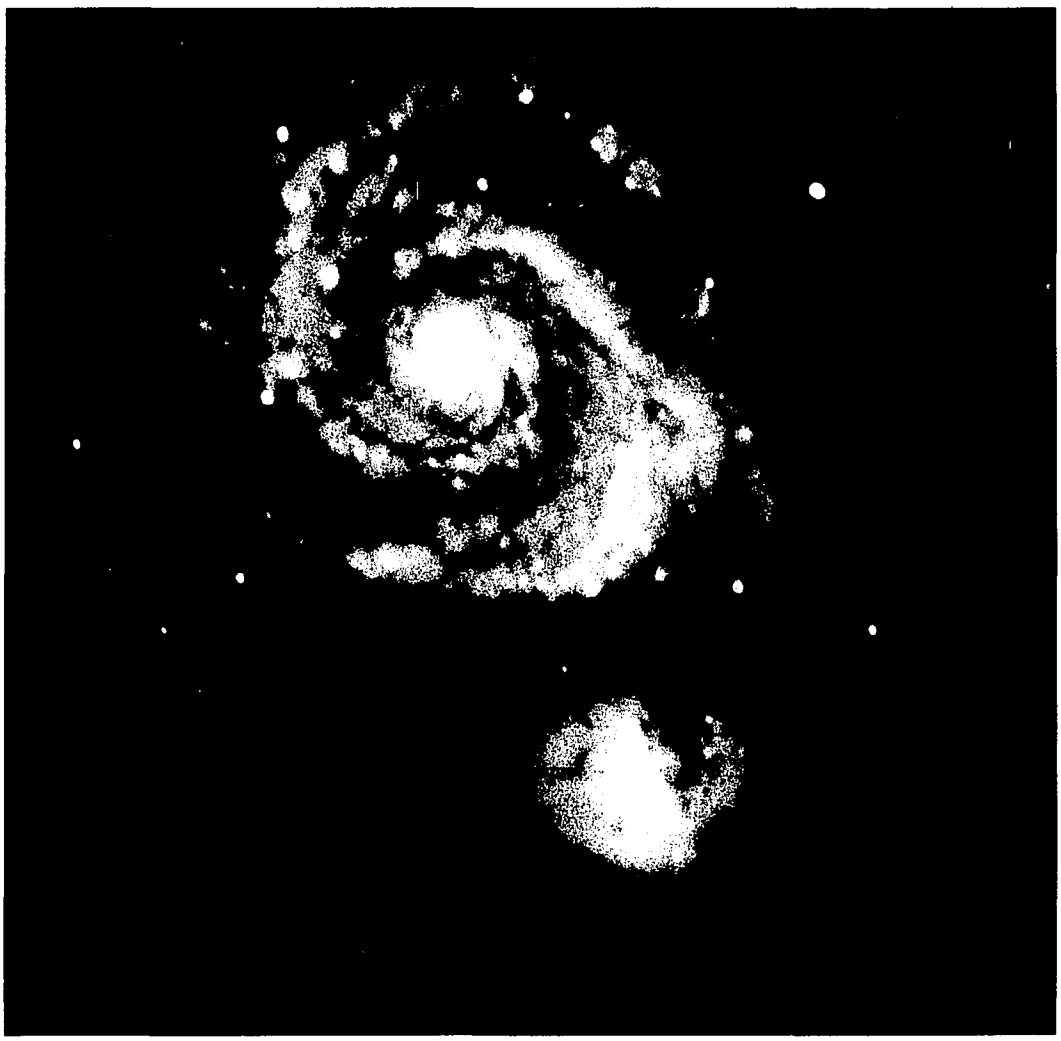

Fig. 35. Photograph of M51; Image Tube IIa-O Plate, 45^{m} Exposure, Cassegrain Focus.

Fig. 36. Photograph of M51 (Sky-Limited); Image Tube Baked IIIa-J Plate, 13^m Exposure, Newtonian Focus.

plate more clearly delineates the boundaries of the bright knots of stars and gas and the dark dust lanes. It is interesting to note that, although the fine detail within the galaxy is brought out more clearly on the direct plate, the field-star images are quite similar in size. (Slight differences in guiding and focus are apparent on the present photographs. These differences, however, are considered negligible in comparison to the effects discussed here.)

From the study of the Newtonian photographs, it is evident that the lowered definition of the image tube plate is primarily caused by the mottle pattern of the Carnegie tube. The noise produced by this phenomenon essentially masks the small, low contrast features of the galaxy. For the faintest regions of the object, it may be argued that the light-induced background of the image tube is also reducing the detection.

A comparison of the image tube Cassegrain photograph (Fig. 35) with the Newtonian direct exposure shows that the image tube record is, in most respects, slightly better than the direct plate. It should be pointed out, however, that the present Cassegrain image tube plate does not provide increased detection of the faintest luminosity of the galaxy. The most likely explanation for this is that there was a reduction in contrast between the sky background and the galaxy because of incomplete sky baffling of the Cassegrain focus, as mentioned earlier in the description of the M13 photographs.

Considering the sky-limited image tube IIIa-J exposure, it is seen that the very faintest regions of the galaxy are more clearly recorded on this plate than on any of the non-sky-limited exposures.

However, the nonuniformities of the image tube are very obvious on this photograph. A sky-limited direct plate would of course be superior to this plate. However, the exposure time for a sky-limited direct IIa-O photograph would be 4½ hours instead of the 13 minutes required for this image tube IIIa-J plate.[1]

Spiral Galaxy M81

Photographs of another spiral galaxy, M81, serve to point out additional problems that can be encountered with the Carnegie tube. A direct plate record is given in Fig. 37 and an image tube record is shown in Fig. 38. Comparison of these photographs shows that some of the bright and dark rift structure visible on the image tube record is not real in the galaxy but is caused by ripples in the image tube sensitivity pattern (examples are indicated by solid arrows). Because the image tube defects effectively mimic the structure of the galaxy, it is difficult to separate the real features from those produced by the image tube. (Note that the two parallel dust lanes to the right of the nucleus that cross down through the spiral arms are real. They are revealed more clearly on the image tube photograph because the Carnegie tube record is effectively exposed to a fainter limit than the direct plate.)

Another fault visible on the image tube photograph is a faint linelike extension of light that is associated with each of the three

---

1. Note that there is a variation of the exposure times reported for sky-limited baked IIIa-J emulsions in the different discussions of this chapter. The reason for this is that the response of the plates to the somewhat excessive baking process is not always the same. Therefore, exposure corrections for individual baked plates have been made.

Fig. 37. IIa-O Unaided Photograph of M81; 1^h15^m Exposure, Newtonian Focus.

A comparison of this unaided photograph with the image tube photograph of Fig. 38 shows that the mottle pattern of the image tube is suppressing the fine detail of the galaxy. In addition, certain image tube defects (indicated by arrows in Fig. 38) are found to effectively mimic the structure of the galaxy, making it difficult to separate real features of the galaxy from the defects.

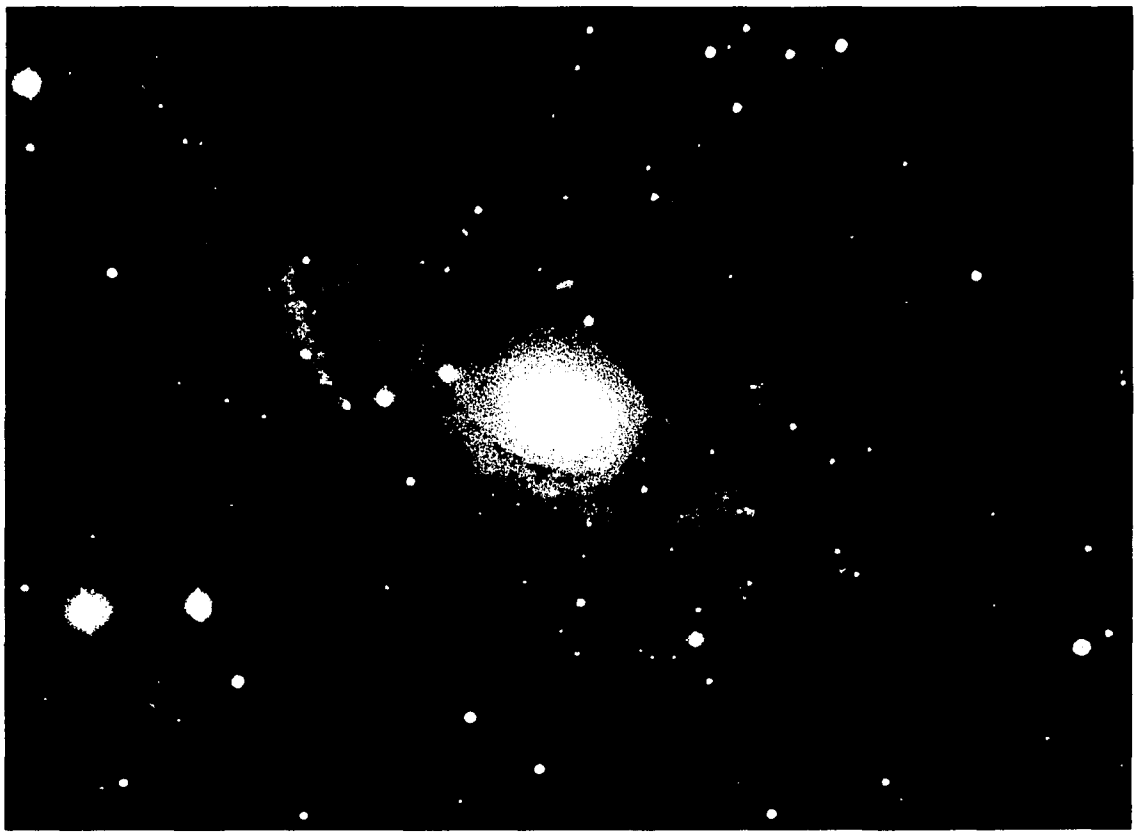

Fig. 38. IIa-O Image Tube Photograph of M81; 6^m Exposure, Newtonian Focus.

bright star images on the left side of the field (indicated by dashed arrows). This phenomenon creates the false impression in the present photograph that one of the spiral arms of M81 (upper left) is unusually extended. The same phenomenon strongly gives the impression that a nebula is associated with the bright star in the blue photograph of S.A. 47, given in Fig. 32.

Planetary Nebula M57

It has been pointed out in Figs. 29 and 35 that an image tube record exposed to a certain density at the Cassegrain focus is generally superior to an unaided photograph exposed to the same density at the Newtonian focus. Two exposures that allow a quantitative test of this property are reproduced in Fig. 39. The object shown here is the planetary nebula M57 (Ring Nebula). Microphotometer traces of the respective plates are shown under the two prints. The area of the microphotometer slit for the Cassegrain plate was 9 times that of the Newtonian plate (to cover equal areas of the original object) and was smaller than the size of a stellar image.

Visual inspection of the photographs shows that the image tube record is less noisy and outlines detail more clearly than the unaided plate. By applying the relative detective quantum efficiency of Chapter III, it may be predicted that the square of the signal-to-noise ratio of the present image tube record is about 10 times that of the unaided photograph. This agrees rather well with the microphotometer traces. The reason that the detective quantum efficiency concept can be applied with reasonable success to the present photographs is that there is not a

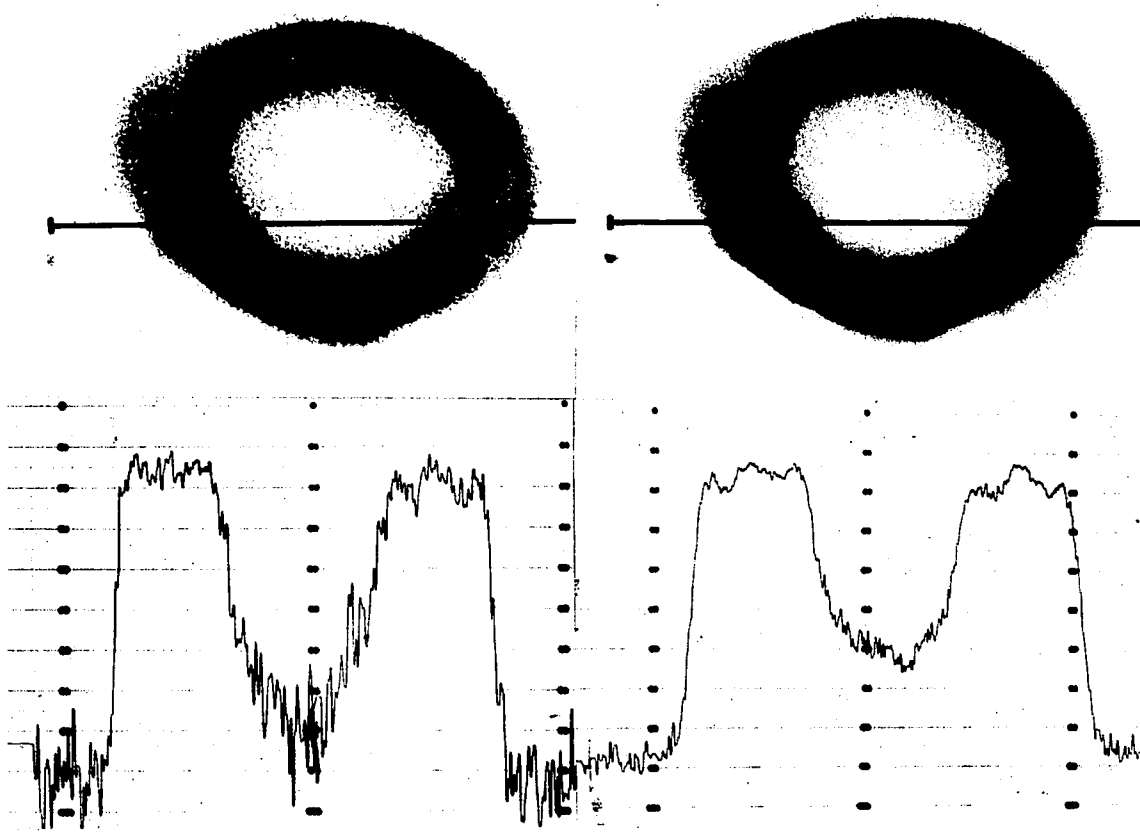

Fig. 39. Comparison of Unaided Newtonian and Image Tube Cassegrain Hα Photographs of M57.

The left image was recorded at the Newtonian f/5 focus in 10^m with an unaided 103a-E emulsion. That to the right was recorded at the Cassegrain f/15 focus in 12^m with the image tube, using a IIa-O recording emulsion. A 50 A halfwidth interference filter was used. The increased photometric accuracy of the image tube photograph is obvious in both the prints and in the microphotometer traces of the original plates.

strong light-induced background (because the sky background and other sources of light are very weak in comparison to the nebula) and that the particularly strong, subjective effects of the image tube mottle pattern have been reduced by virtue of the long focal length of the telescope.

Photography of Extended Objects: Concluding Remarks

Many of the results of this study are similar to those found in the study of sky-limited stellar photography and need not be repeated. The most significant additional conclusion is that the mottle pattern and the discrete patches and ripples of the image tube take on increased significance in extended object photography. Fortunately, it has also been demonstrated that these effects can be reduced by using sufficiently long focal length telescopes.

The practical figure of gain for the image tube compared to unaided photography has been shown to be, in certain applications, the relative detective quantum efficiency. Gains as high as 10 to 30 may therefore occasionally be achieved. However, in many cases of extended object photography (as well as sky-limited stellar photography), the adverse effects of the image tube serve to lower the relative gain. In these cases the gain may more typically be 2 to 5.

Interference Filter Photography

An application for which the Carnegie image tube has particular promise is the photography of astronomical sources through narrowband interference filters. The results of some preliminary tests of this

application are given in the following pages. All photographs in this section, with the exception of Fig. 40, were obtained with the Carnegie image tube.

The Nebula Sharpless 224

A phenomenon that is characteristic of several supernova remnants is the peculiar filamentary structure of the associated nebulosity. Van den Bergh (1960) has searched for nebulae that exhibit this type of structure on the red prints of the Palomar Sky Survey and has identified several optical H II regions as possible supernova remnants. One such region is Sharpless 224 (Sharpless 1959), a print of which is given in Fig. 40. This figure is an enlargement obtained from the red transparency of the Palomar Sky Survey.

Fig. 41 shows a photograph of Sharpless 224 taken through an interference filter with the Carnegie tube. The filter has a halfwidth of 50 A and its transmission is centered at 6563 A (wavelength ~~of~~ Hα emission line). Comparison of the image tube photograph with that of the Palomar Sky Survey shows that the entire nebula is brought out more clearly on the image tube record. Particularly significant is the degree to which the delicate filamentary structure is revealed on the image tube plate. This tends to strengthen the suggestion made by van den Bergh that Sharpless 224 is a supernova remnant.

It should be noted that the superiority of the image tube photograph is due to the narrow passband of the interference filter. The star images, formed by continuum radiation, are suppressed relative to the nebular image, formed by emission line radiation. In the same manner,

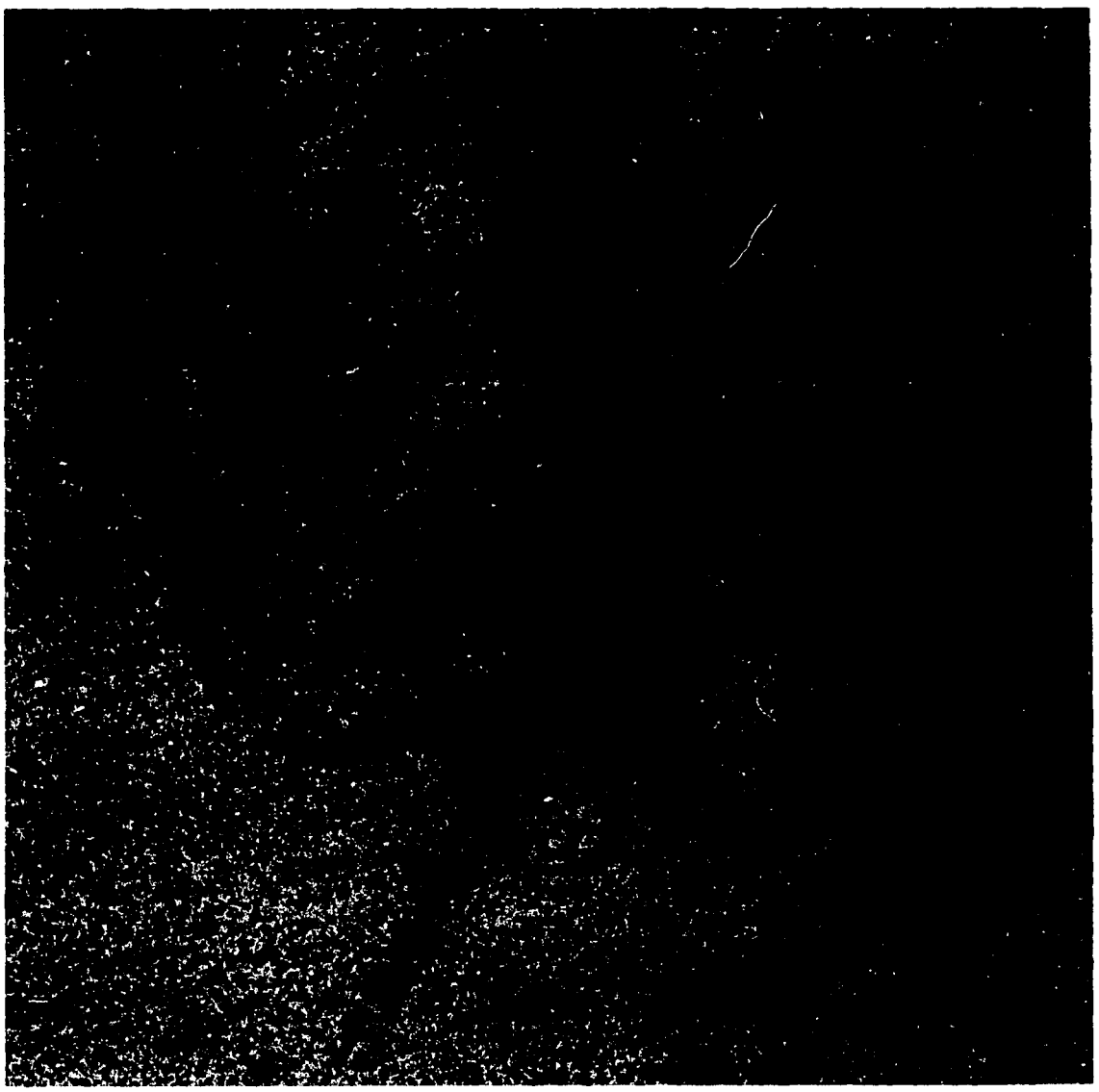

Fig. 40. Print from Red Sky Survey Plate of Sharpless 224; 40^m Exposure, Palomar 48-Inch f/2.4 Schmidt.

A comparison of this photograph with the image tube interference filter photograph of Fig. 41 shows that the filamentary character of the nebula is brought out more clearly on the image tube record. The photograph in Fig. 42, which was exposed to continuum radiation near Hα, shows that essentially no radiation from Sharpless 224 is reflected starlight.

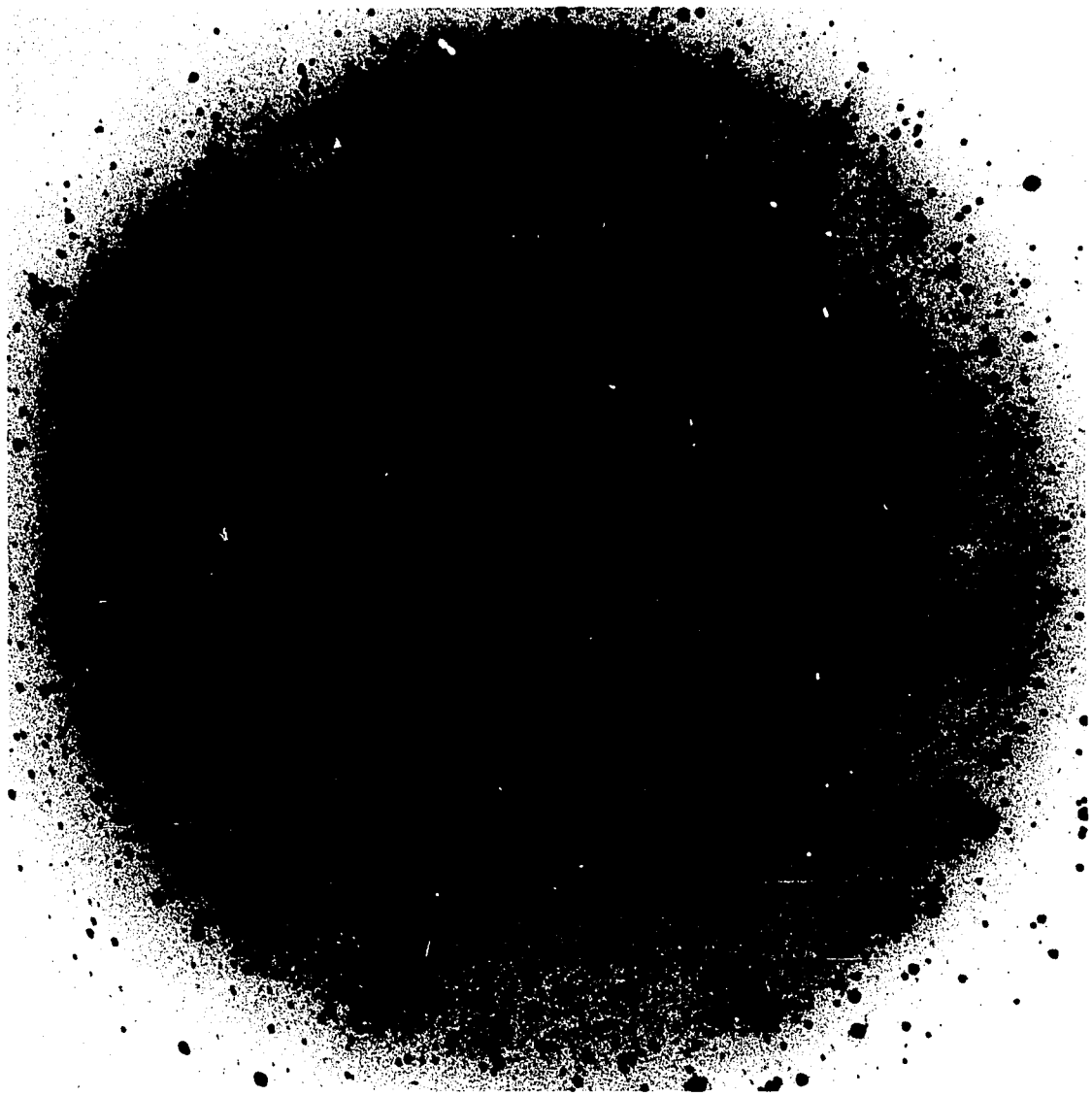

Fig. 41. 6563 A (Hα Emission) Interference Filter Photograph of Sharpless 224; 2^h30^m Exposure, 36-Inch f/5 Newtonian.

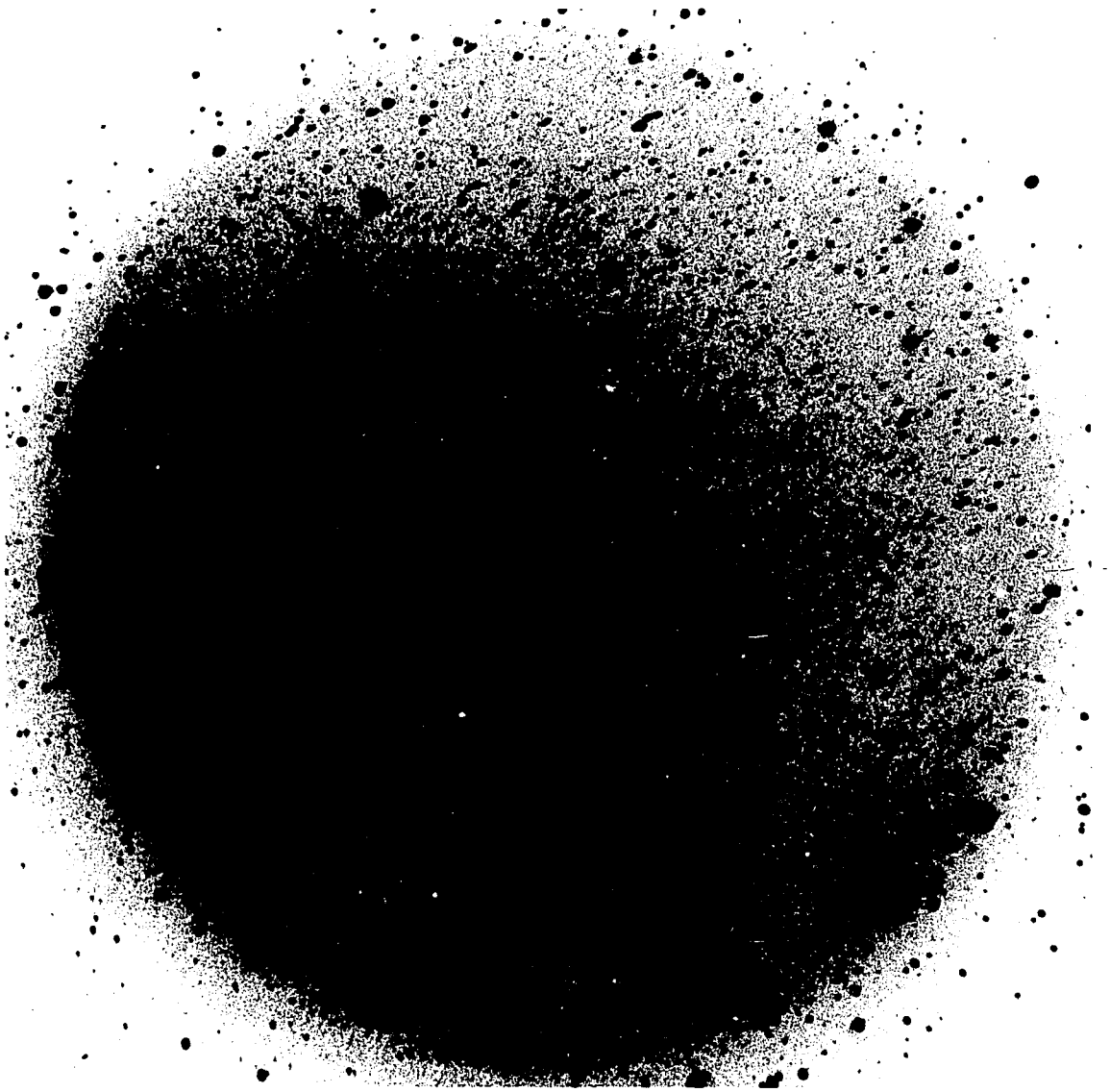

Fig. 42. 6490 A (Continuum) Interference Filter Photograph of Sharpless 224; 2^h30^m Exposure, 36-Inch f/5 Newtonian.

the background produced by the continuum radiation of the night sky is also suppressed. (The latter effect is not apparent on the prints shown here because the illustrations have been printed to the same sky density for comparison purposes.)

The existance of several bright red stars in the immediate vicinity of Sharpless 224 had suggested that a significant proportion of the radiation from this nebula might be reflected starlight. In order to test for this possibility, a photograph was taken through an interference filter that transmits only continuum radiation. (The filter passband is centered at 6490 A and the halfwidth is again 50 A.) The photograph, which is reproduced in Fig. 42, fails to show even a trace of the nebula. Clearly, very little of the radiation from Sharpless 224 is reflected starlight.

Observations of Planetary Nebulae

With the aid of very narrowband interference filters it is possible to photograph planetary nebulae in the light of single emission lines. An important characteristic of this method of studying planetary nebulae is that certain spectral features can be directly correlated with the morphological characteristics of the nebulae. Such correlations are significant aids to the study of the ionization, temperature, and pressure structure of these objects.

The manufacture of the filters required for this application is extremely difficult and, for this reason, the desired filters have not presently been obtained. Nevertheless, using filters that have broader passbands than are ultimately required (and that therefore generally

transmit spectral lines in addition to the one of interest), several photographs have been taken that indicate the promise of this technique in studying planetary nebulae. The photographs are shown in Figs. 43, 44, and 45 and the captions point out some of the more interesting features of the planetaries observed. Unless otherwise specified, the photographs were obtained at the 36-inch f/15 Cassegrain focus.

Diffuse Nebula Near BD $+8^{\circ}$ 933

Interference filters, in conjunction with the Carnegie tube, have been used to a significant advantage in studying the properties of a nebula that is associated with the star BD $+8^{\circ}$ 933. The filter-Carnegie tube combinations have allowed photographs to be taken in four relatively narrow regions of the visible spectrum. This, in turn, has permitted increased interpretation to be made of the nebular radiation. The four photographs are presented in Fig. 46. The central wavelength and the halfwidth of the respective filters are indicated in the four illustrations.

The unusual changes that occur in the four photographs of this nebula may be interpreted as follows. The light that is recorded on the 3700 A photograph, and also on the 4970 A photograph, is scattered continuum radiation from the star. This light outlines primarily the distribution of dust within the nebula. The light that is recorded on the 6563 A photograph is Hα emission, which outlines primarily the distribution of gas in the nebula.

Further, noting that the nebular continuum radiation is entirely absent on the 6490 A photograph (the faint light areas are image tube

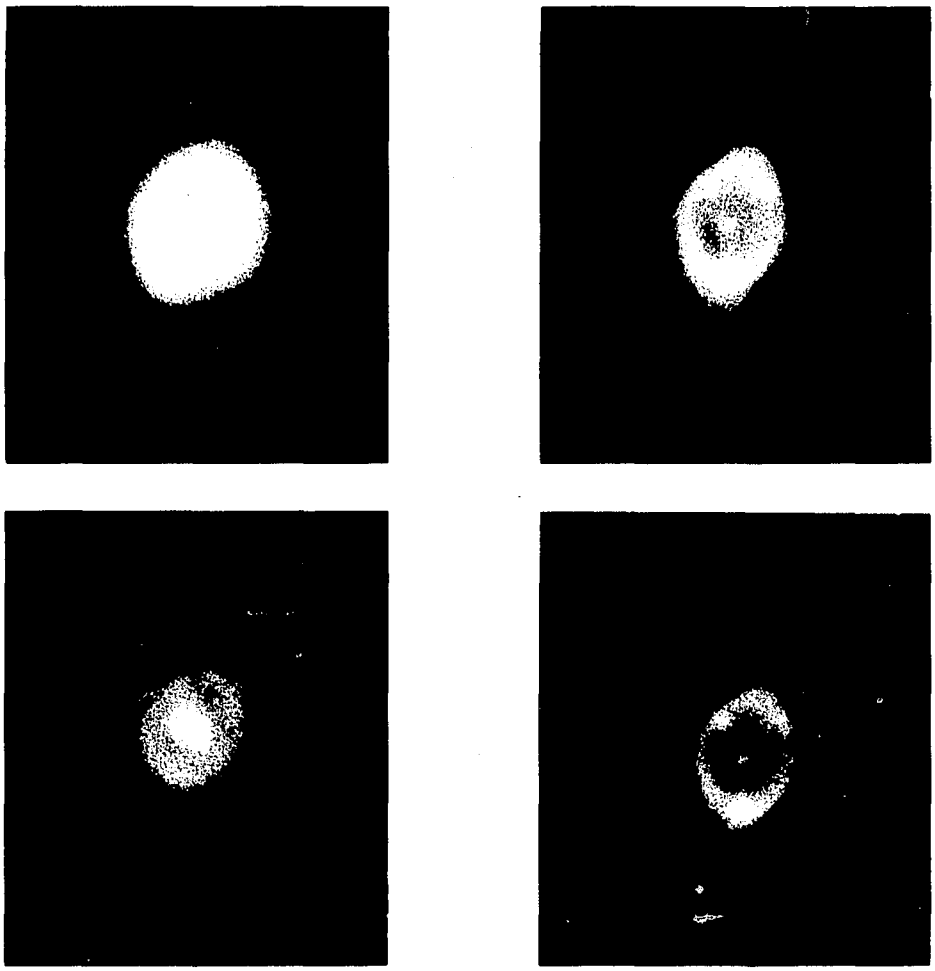

Fig. 43. NGC 3242 in Light of [Ne V] and Hα.

Two prints from each plate are reproduced here in order to show the structure of both the bright and faint portions of the nebula. Two primary shells in this planetary are seen. The unusual knots of luminosity that occur in the Hα photograph are nearly absent in the [Ne V] photograph. The distribution of Ne V in the inner shell is seen to be more centrally concentrated and more spherically symmetric than is the distribution of H I. In the outer shell H I appears to be concentrated in a plane that is perpendicular to the major axis of the inner shell. The distribution of Ne V in the outer shell is more uniform. Exposure times were 2^h30^m for [Ne V] and 3^m for Hα.

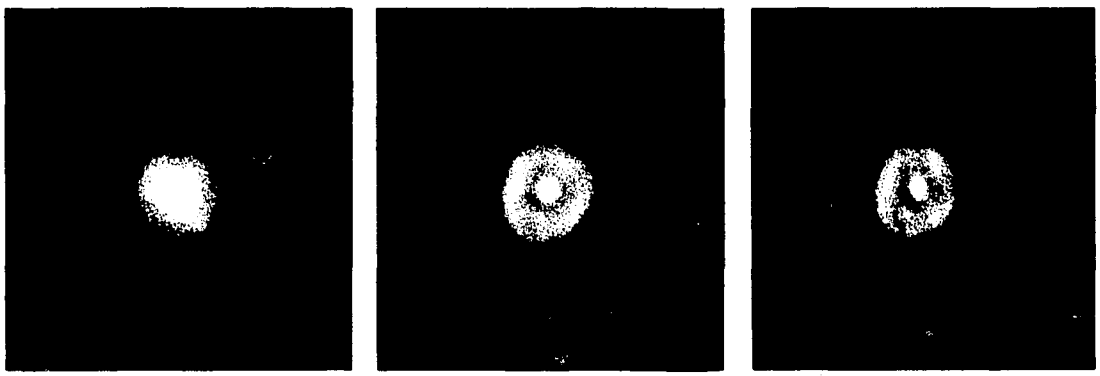

Fig. 44. NGC 2392 in Light of [Ne V], [O III], and Hα.

There is seen to be a considerable amount of structure in even the outer shell of this planetary. (The outer shell is underexposed in the [Ne V] record.) The inner shell is clearly more spherical and less structured in [Ne V] than in [O III] or Hα. (Note that a short duration guiding failure caused the streak shown in the [Ne V] photograph.) Exposure times were 1^h45^m for [Ne V], 10^m for [O III], and 10^m for Hα.

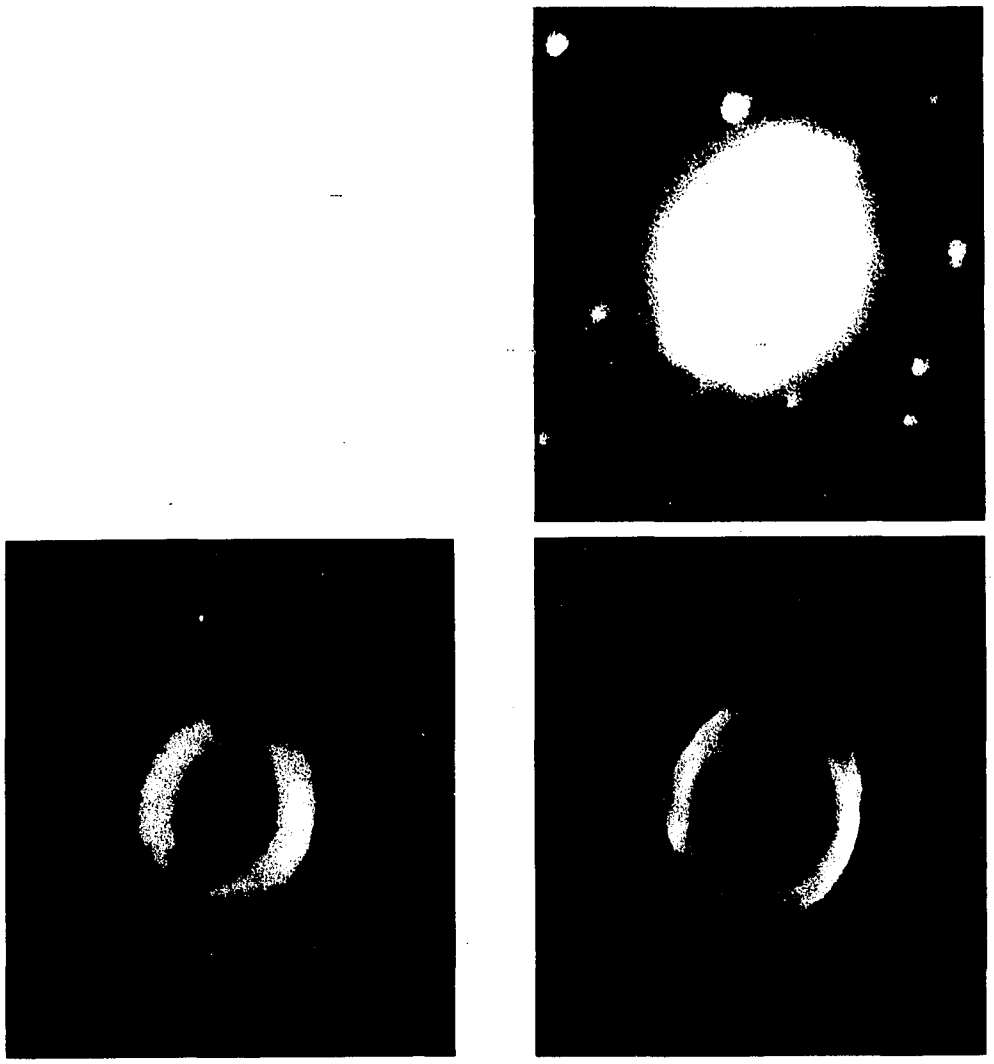

Fig. 45. M57 (Ring Nebula) in light of [O III] and Hα.

The difference in the distribution of O III and H I in the Ring Nebula is clearly indicated in the lower two photographs. The O III shell is closer to the center of the nebula and is less structured than the H I shell. An extremely faint outer shell, shown in the light of Hα in the upper photograph, is observed in [O III] as well. The upper photograph was obtained in a 1^h exposure at the Newtonian focus. For the lower records, obtained at the Cassegrain focus, the exposure times were 8^m for [O III] and 12^m for Hα.

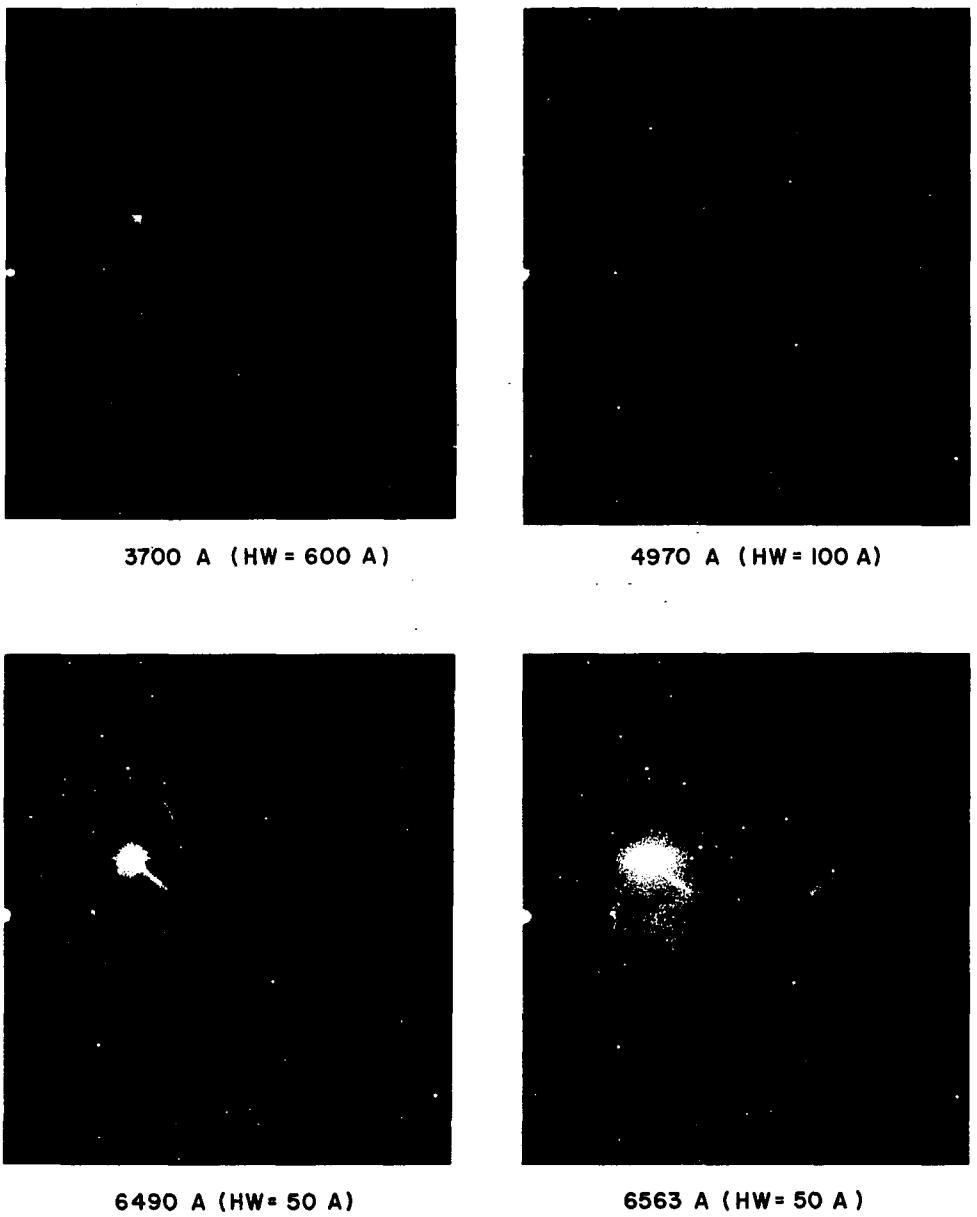

Fig. 46. Narrowband Photographs Showing Reflection-Emission Character of Diffuse Nebula Near BD $+8^{\circ}$ 933.

The central wavelength and halfwidth of the respective filters are indicated below the four photographs. The reflection component of the nebula, as recorded in the top two photographs, is shown to be unusually blue. The bright star was masked from the photocathode for the upper exposures. The bottom two photographs indicate that the red light from the nebula is produced by emission line radiation. (The two concentric rings on the lower photographs are properties of the interference filters.)

defects) and noting that it is exceedingly weakly recorded on the 4970 A photograph, the nebula is concluded to be unusually blue. Additional plates, taken in more passbands of this nebula, including plates for brightness measurements of the star, should allow a quantitative analysis to be made of the relative color distribution of the nebula and the star. An analysis such as this can supply significant data for determining the properties of the scattering particles within the nebula.

Hα Photography of Spiral Galaxy M81

Two photographs have been taken of the spiral galaxy M81, using respectively a broad passband blue filter and an Hα interference filter. The plates, which are shown in Fig. 47, demonstrate the capability of studying H II regions and general spiral structure of external galaxies with the Carnegie tube. Some of the more interesting features of M81 that are revealed by the two exposures are pointed out in the caption.

Crab Nebula Observations

Photographs of the Crab Nebula have been taken that very effectively separate the bright amorphous structure of the nebula (comprised of synchrotron continuum radiation) from the filamentary structure (comprised of emission line radiation). The photographs are reproduced in Fig. 48. The two illustrations that show only the continuum radiation were taken through a polaroid filter, the position angle of which was rotated through 90^{o} between the two exposures. A Wratten 90 filter was used to isolate the continuum radiation from that of the emission lines.

The polarization of the amorphous mass of the Crab Nebula is clearly indicated by the two polaroid photographs. These photographs

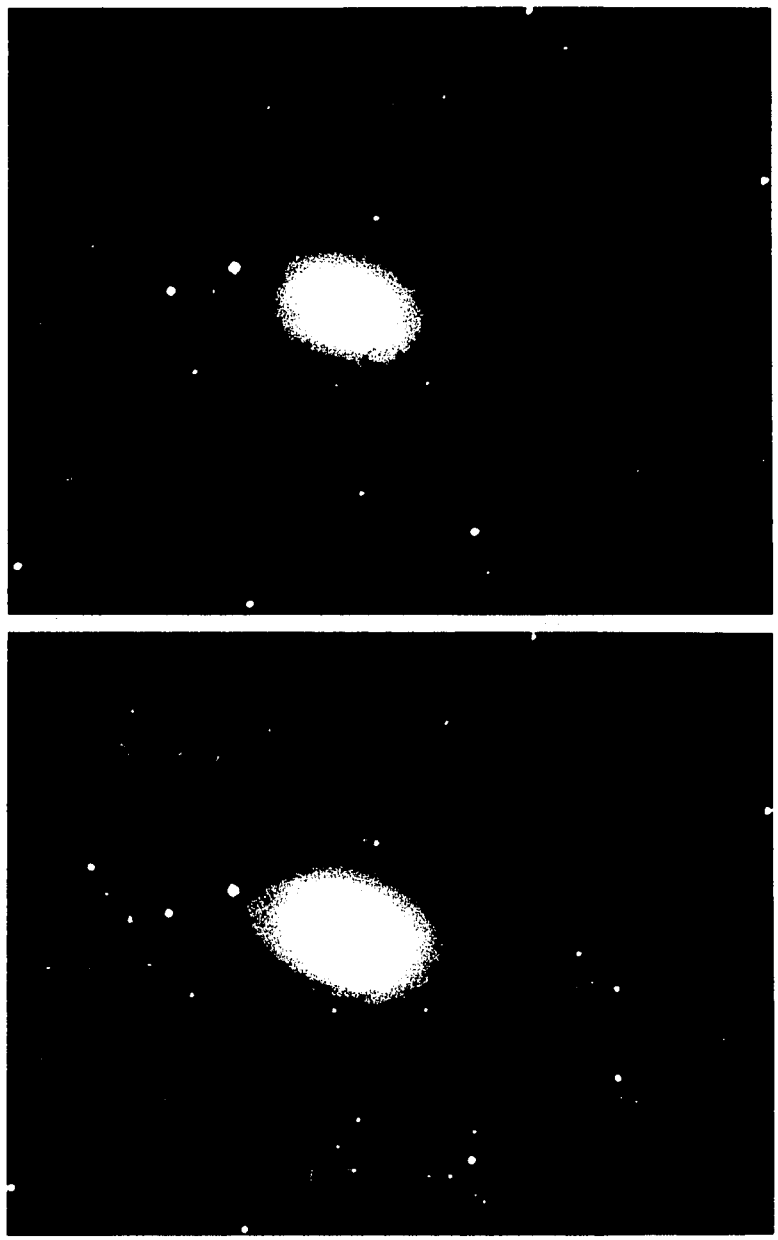

Fig. 47. Blue Magnitude and Hα Photographs of M81.

The upper photograph is a 2^m blue magnitude exposure; the lower is a 55^m Hα exposure. The spiral arms of this galaxy are more clearly outlined by the H II regions than by the blue stellar radiation. Note the several blue star associations that occur in the H II regions. The nucleus appears particularly bright on the Hα photograph because of a predominantly red continuum from the old generation stars.

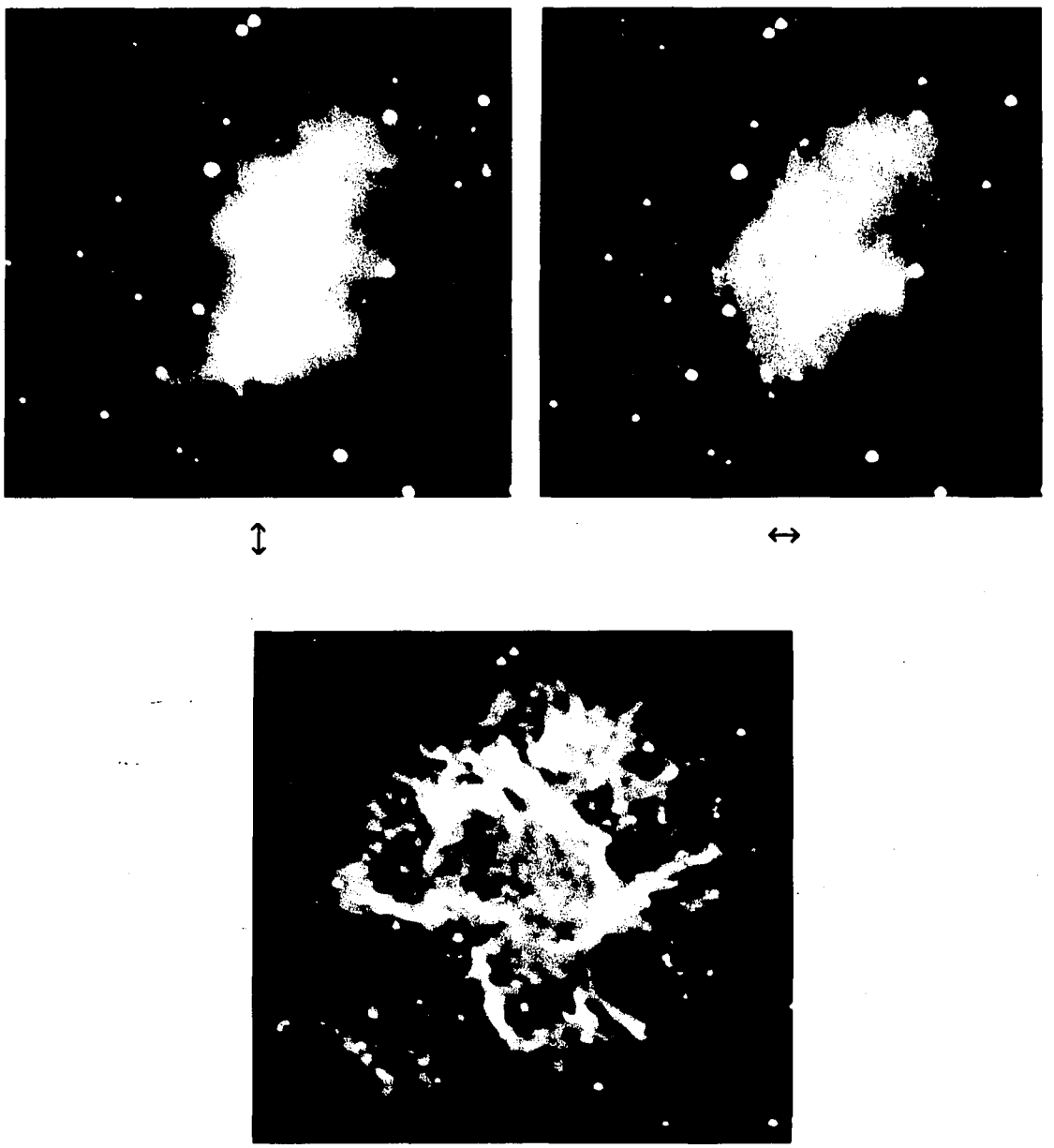

Fig. 48. Polaroid Continuum and Hα Emission Photographs of Crab Nebula.

The direction of the polaroid E vector transmission is indicated for the two polaroid photographs of the continuum component. The continuum radiation is seen to be effectively suppressed in the Hα interference filter photograph.

appear to be in good agreement with those taken by Baade (1956) with the 200-inch Palomar telescope.[1] However, it should be pointed out that, because the background on the present image tube photographs is roughly 25 percent scattered light and because the scattered component may be polarized in a very complex fashion, several precautions would be required in analyzing these records for polarization data.

The Hα interference filter photograph in Fig. 48 brings out the filamentary structure of the Crab Nebula very well. An application of the Carnegie tube that looks particularly promising with regard to the Crab Nebula is the determination of the relative intensities of several emission lines throughout the filaments by interference filter photography.

Interference Filter Photography: Concluding Remarks

Application of interference filter techniques to direct astronomical photography must be considered one of the most promising applications of the Carnegie image tube. Increased astrophysical interpretation of not only emission line objects, but contiuum radiation objects as well, has been shown to be possible through the use of interference filter photography. These techniques, it should be pointed out, are seldom possible with unaided photographic materials. For many objects, unaided emulsions are simply not sensitive enough to produce an acceptable record within practical exposure times.

---

1. The resolution and fine detail of Baade's plates are far superior to the present image tube plates. The reason for this is primarily the larger scale and the superior image characteristics of the 200-inch compared to the 36-inch. Also, the contrasty baked IIIa-J plates used here tend to wash out the detail in the highly exposed central portions of the nebula.

CHAPTER V

CONCLUSIONS OF INVESTIGATION

The Carnegie image tube has been shown to provide a significant gain over unaided photographic emulsions in applications to direct photography of astronomical sources. Based on the detective quantum efficiency, a figure of merit that is determinable from laboratory measurements, the gain over typical astronomical emulsions has been found to be in the range 10 to 20. This value applies to the Carnegie tube when a IIa-O emulsion is used to record the image tube output. When a baked IIIa-J emulsion is used as the recording medium,the detective quantum efficiency is increased but the baked IIIa-J record tends to be unreliable photometrically.

In several applications the relative detective quantum efficiency may be used to accurately predict the relative performance of an image tube and an unaided photographic emulsion. In many other applications, however, certain characteristics of the image tube seriously affect the quality of the final record. These characteristics, primarily, are low resolution, nonuniformities in sensitivity, and light-induced background.

The average resolution limit of a Carnegie tube record, about 25 lp/mm, is somewhat less than half that of common astronomical emulsions. Therefore, if the size of the seeing image produced by a given

telescope is smaller than a resolution element of the image tube, then an object that is recorded with the Carnegie tube will not be as well resolved as it would be on an unaided photograph. In many applications, however, the seeing image produced by the telescope is enough larger than a resolution element that the final resolution is determined mostly by seeing effects. Then the lower resolution limit of the image tube is of little consequence.

One of the most important nonuniformities in sensitivity of the Carnegie tube is produced by a general mottled, or granular, structure of the dynode and output phosphors of the image tube. Also, there are a number of discrete variations, forming patches and ripples, that are important in certain applications. The mottle pattern is characterized by alternate bright and dark elements that have a mean spatial period of 350 μm and that produce an rms variation in sensitivity of ±1.3 percent. The discrete patches and ripples are somewhat larger in size and amplitude.

The adverse effects of these nonuniformities are particularly strong when the Carnegie tube is used at a moderately short focal length telescope (e.g., the 36-inch f/5 Newtonian telescope of Steward Observatory) and when the night-sky radiation is strongly recorded. Under these conditions the plate density representing the sky background is clearly modulated by the mottle pattern, and the individual mottle elements tend to mimic the small, faint star images that are produced by the telescope. This phenomenon serves to lower the detection of the threshold star images. The effects of the image tube

nonuniformities are subjectively the most severe on photographs of extended objects. The noise produced by the mottle pattern reduces the detection of small, low contrast features of galaxies and nebulae and the patches, ripples, and mottle pattern of the image tube are sometimes confused with the real details of the object being photographed.

By using a telescope with a moderately long focal length (e.g., the 36-inch f/15 Cassegrain telescope) the size of the seeing image is then sufficiently large in comparison to the image tube defects that they are no longer confused with real features. Thus, the rather strong subjective effects of the nonuniformities are significantly reduced. The noise produced by the nonuniformities is then very similar to normal photographic granularity.

The light-induced background of the Carnegie tube is primarily due to the transmission of a portion of the incident radiation by the semi-transparent photocathode. The transmitted light is scattered throughout the first stage of the image tube and some of it is consequently returned to the photocathode. This gives rise to a general background emission.

The detrimental effects of the light-induced background can often be avoided by masking off the images of bright small-area objects, such as field stars, in front of the photocathode. In photographs that are exposed to near the sky limit, however, the night-sky radiation is generally the dominant source of light and this radiation cannot be masked from the photocathode. The light-induced background in this case contributes about 25 percent additional background to the final

record, although the exact amount depends upon the color of the incident radiation and upon the position within the field of the image tube. The additional noise produced by the light-induced background significantly reduces the signal-to-noise ratio of weak images and, of course, corrections for this background must be made to photometric data obtained from Carnegie tube records.

Because the magnification of the image tube changes as a function of radius, there is an apparent increase in sensitivity toward the edge of the field. At an 18 mm radius the sensitivity appears to be 30 percent greater than at the center. This effect must also be accounted for in making a photometric analysis of a Carnegie tube record.

It has been demonstrated that the iris photometry of Carnegie tube plates is essentially as accurate as that of unaided plates. The reduction in exposure time provided by the image tube is numerically equal to the relative detective quantum efficiency of the image tube and the respective photographic plate. These statements hold true as long as the exposures are not near the sky limit and provided that the images formed by the telescope are larger than the resolution limit of the image tube.

When sky-limited exposures are obtained at the same focal length telescope, the limiting magnitude on a Carnegie tube photograph is about 1 magnitude brighter than that on an unaided photograph. This loss in limiting magnitude is attributed primarily to the mottle pattern and the light-induced background of the Carnegie tube. In order to reach the same limiting magnitude with the Carnegie tube as is

possible to reach with an unaided plate the Carnegie tube must be used at a longer focal length telescope. The reduction in exposure time provided by the image tube is then only about 2 or 3. The effective gain of the image tube is generally somewhat higher than this, however, because of the higher scale of the image tube photograph. Most of the star images (or the details of an extended object) in the field have a higher signal-to-noise ratio on the image tube photograph. Only the threshold images, which are particularly affected by the non-uniformities of the image tube, have about equal signal-to-noise ratios on the two records.

The Carnegie image tube has been shown to be particularly effective in application to the photography of astronomical sources through narrowband interference filters. Direct plates are generally not sensitive enough to be in competition with the image tube in this specialized application. (A reducing camera can of course be used in conjunction with a direct plate,but then the final record is seriously affected because of the small image scale.) It has been shown that the detection of emission line objects can be significantly improved through the use of interference filters and the Carnegie tube. The filters effectively suppress the night-sky radiation and the local background of the source. It has also been demonstrated that the interpretation of continuum radiation objects can be significantly aided through the use of narrowband filter photographs.

On the basis of the present investigation a few general statements can be made in regard to using other image tubes for direct

astronomical photography. Because the principal nonuniformities of the Carnegie tube have been found to be caused by the phosphor screens, it may be expected that similar nonuniformities exist in the several other image tubes that use phosphor screens. The electronographic image tubes of course do not have phosphor screens and, therefore, they may be expected to have superior small-scale uniformity. The light-induced background due to light that is transmitted by the photocathode has been found to exist in other tubes. Fortunately, both the phosphor nonuniformities and the light-induced background can be somewhat controlled by specific manufacturing techniques. However, the researcher often requires more quantitative descriptions of these phenomena than are currently provided by manufacturers.

Geometrical distortion and large-scale nonuniformities in sensitivity are problems that certain other image tubes clearly possess. Again, more information than is presently available is needed to quantitatively compare these characteristics among the available image tubes. Resolution of the various tubes is a rather uncertain specification and there appears to be substantial variation even among samples of the same design from some manufacturers. The electronographic tubes, of course, have resolution superior to any other design of image intensifier presently available.

In direct photography of sources that have high contrast with respect to their surroundings the high gain tubes, such as the English Electric Valve and EMI tubes, may have considerable success. These tubes provide very high efficiencies in this specific application

because only a relatively small number of photoevents need be recorded in order to provide adequate recognition of a high contrast object. A useful application of these tubes might be the photography of emission objects through very narrowband interference filters.

In the photography of low contrast sources (e.g., faint stars against the sky background or low contrast details of galaxies) the high gain tubes generally saturate the photographic emulsion before a sufficient number of photoevents are recorded to permit discrimination of the source and its background. The electronographic tubes, on the other hand, are capable of storing a very large number of photoevents before saturation occurs and, therefore, these tubes can successfully record objects of very low contrast. Stars fainter than those possible to observe with direct plates have, in fact, recently been recorded with electronographic devices.

It is important to note that one particular image tube may often be superior to other available image tubes in a specific application. A substantial amount of evaluation is still required of these devices in the area of astronomical photography. In view of the promise shown by the Carnegie image tube and other image tubes, continued evaluation is of considerable interest to the astronomical community.

LIST OF REFERENCES

Ables, H. D., and Kron, G. E. 1967, *Pub. Astron. Soc. Pacific*, 79, 423.

Argyle, P. E. 1955, *J. Royal Astron. Soc. Canada*, 49, 19.

Baade, W. 1956, *Bul. Ast. Inst. Netherlands*, 12, 312 (No. 462).

Bakos, G. A., and Rymer, K. R. 1964, *Astron. J.*, 69, 531.

Baum, W. A. 1955, *Trans. Int. Astron. Union*, 9, 681.

Baum, W. A. 1962a, *Astronomical Techniques*, 1, Ed. by W. A. Hiltner (Chicago: University of Chicago Press).

Baum, W. A. 1962b, *Adv. El. and El. Phys.*, 16, 391.

Baum, W. A., Hall, J. S., Marton, L. L., and Tuve, M. A. 1955-1968, "Annual Reports of the Committee on Image Tubes for Telescopes", *Carnegie Institution Yearbook*, *55* through *67*.

Baum, W. A., Hiltner, W. A., Johnson, H. L., and Sandage, A. R. 1959, *Astrophys. J.*, 130, 749.

Beardsley, W. R., and Hansen, J. R. 1968, *Astron. J.*, 73, S4.

Bellier, M., Dupré, M. F., Wlérick, G., Rösch, J., and Arsac, J. 1963, *Mem. Soc. R. Liège*, 7, 522.

Bergh, S. van den 1960, *Z. Astrophys.*, 51, 15.

Bowen, I. S. 1967, *Ann. Rev. Astron. Astrophys.*, 5, 45.

Breckinridge, J. B., Kron, G. E., and Papiashvili, I. I. 1964, *Astron. J.*, 69, 534.

Butslov, M. M., Kopylov, I. M., Nikonov, V. B., Severnyi, A. B., and Chuvaev, K. K. 1962, *Soviet Astron. J.*, 6, 244.

Eastman Kodak 1967, *Kodak Plates and Films for Science and Industry*, Eastman Kodak Company.

Fellgett, P. B. 1953, *J. Opt. Soc. Am.*, 43, 271.

Fellgett, P. B. 1958a, *Monthly Notices R. A. S.*, 118, 224.

Fellgett, P. B. 1958b, *The Present and Future of the Telescope of Moderate Size*, 51, Ed. by F. B. Wood (Philadelphia: University of Pennsylvania Press).

Ford, W. K. 1967, Private communication, Carnegie Institution of Washington, Washington, D. C.

Ford, W. K. 1968, Private communication, Carnegie Institution of Washington, Washington, D. C.

Green, M. 1968a, *Sky and Telescope*, 35, 140.

Green, M. 1968b, *Astron. J.*, 73, S1.

Hiltner, W. A. 1958, *The Present and Future of the Telescope of Moderate Size*, 11, Ed. by F. B. Wood (Philadelphia: University of Pennsylvania Press).

Hiltner, W. A. 1962, *Astronomical Techniques*, 340, Ed. by W. A. Hiltner (Chicago: University of Chicago Press).

Hynek, J. A., Bakos, G., Dunlap, J., and Powers, W. 1966, *Adv. El. and El. Phys.*, 22B, 713.

Hynek, J. A., and Dunlap, J. R. 1964, *Sky and Telescope*, 28, 126.

Jones, R. C. 1958, *Phot. Sci. and Eng.*, 2, 57 (No. 2).

Jones, R. C. 1959, *Adv. El. and El. Phys.*, 11, 87.

Kron, G. E. 1967, Unpublished, Informal colloquium on image tubes, Kitt Peak National Observatory, Tucson, Arizona, October 11, 1967.

Kron, G. E., Breckinridge, J. B., and Papiashvili, I. I. 1965, *Pub. Astron. Soc. Pacific*, 77, 112.

Kron, G. E., and Mayall, N. U. 1960, *Astron. J.*, 65, 581.

Kron, G. E., and Papiashvili, I. I. 1967, *Pub. Astron. Soc. Pacific*, 79, 9.

Lallemand, A. 1936, *Compt. Rend. Acad. Sci.*, 203, 243.

Lallemand, A., Canavaggia, R., and Amiot, F. 1966, *Compt. Rend. Acad. Sci.*, 262, 838.

Laques, P. 1966, *Adv. El. and El. Phys.*, 22B, 755.

Latham, D. W. 1966, *Astron. J.*, 71, 168.

Livingston, W. C. 1962, *Adv. El. and El. Phys.*, 16, 431.

Livingston, W. C. 1967a, *Adv. El. and El. Phys.*, 23, 347.

Livingston, W. C. 1967b, Private communication, Kitt Peak National Observatory, Tucson, Arizona.

Lynds, C. R. 1968, Private communication, Kitt Peak National Observatory, Tucson, Arizona.

Marchant, J. C., and Millikan, A. G. 1965, *J. Opt. Soc. Am.*, 55, 907.

McGee, J. D. 1958, *The Present and Future of the Telescope of Moderate Size*, 31, Ed. by F. B. Wood (Philadelphia: University of Pennsylvania Press).

McGee, J. D. 1962, *Astronomical Techniques*, 302, Ed. by W. A. Hiltner (Chicago: University of Chicago Press).

Miller, W. C., Difley, J., Gilliam, L., Lutnes, J., and Hoag, A. 1966, "Photographic Plate Testing", summary of meeting at Mt. Wilson and Palomar Observatories, January 17 and 18, 1966.

Rösch, J., Wlérick, G., and Dupré, M. F. 1961, *Compt. Rend. Acad. Sci.*, 252, 509.

Rose, A. 1946, *J. Soc. Motion Picture Engrs.*, 47, 273.

Sharpless, S. 1959, *Astrophys. J. Suppl.*, 4, 257.

Soule, H. V. 1968, *Electro-Optical Photography at Low Illumination Levels* (New York: John Wiley and Sons, Inc.).

Stebbins, J., Whitford, A. E., and Johnson, H. L. 1950, *Astrophys. J.*, 112, 469.

Tuve, M. A., Ford, W. K., Jr., Hall, J. S., and Baum, W. A. 1958, *Pub. Astron. Soc. Pacific*, 70, 592.

Walker, M. F., and Kron, G. E. 1967, *Pub. Astron. Soc. Pacific*, 79, 551.

Webb, J. H. 1948, *J. Opt. Soc. Am.*, 38, 312.

Wlérick, G., and Grosse, A. 1966, *Adv. El. and El. Phys.*, 22A, 465.

Zweig, H. J., Higgins, G. C., and MacAdam, D. L. 1958, *J. Opt. Soc. Am.*, 48, 926.